



University of
Stavanger

Faculty of Science and Technology

MASTER'S THESIS

Study program/ Specialization:

Petroleum Engineering / Drilling Technology

Spring semester, 2014

Open

Writer:

Erling Strand

.....
(Writer's signature)

Faculty supervisors:

Mesfin Belayneh
Kjell Kåre Fjelde

Thesis title:

Hydraulic Calculations Using Discovery Web for Visualization

Credits (ECTS): 30

Key words:

Integrated Operations
Well Control
Real-time monitoring
Discovery Web
Rheology and Hydraulics
Drilling Scenario Simulations

Pages: 82

+ enclosure: 18

Stavanger, 12.06.2012

Abstract

Advanced real-time monitoring systems are useful tools for safe and cost effective well operation practices. As one moves into deeper water, higher pressure and higher temperature, the drilling operations only becomes more challenging. Since the operational drilling window is getting narrower, implementation of good IO technology (i.e. real-time data, technology and people) are necessary to increase safe operations, increase productivity, enhance HSE and reduce NPT.

This thesis is divided into a theoretical and a simulation part. The theoretical part presents major downhole drilling problems related to hydraulics, prevention and remedial actions. The theoretical part emphasizes on describing different rheological models for hydraulic calculations. The simulation part presents the real-time monitoring system Discovery Web application developed by Kongsberg Oil & Gas Technologies. In the simulation part, the rheology models are used for hydraulic calculation in different drilling scenarios. Pressure at different locations in the well (Pump pressure (bar), BHP (bar) and ECD (sg)) has been calculated. Different events and unwanted situations are considered and different visualization views have been provided to demonstrate how different well parameters will develop. The input parameters to the models have typically been ROP, flow rate, rheology data and mud density.

In order to illustrate the applicability of the implemented models, a case study is presented while drilling a vertical well from 4000m. The following drilling scenarios have been simulated and the results are briefly discussed. These are:

- Connection scenario
- Kick scenario during drilling
- Kick scenario during connection
- Pack-off scenario and sensitivity of pack-off
- Lost circulation scenario
- ROP vs cutting concentration scenario
- Hydraulics and rheology model comparison scenario
- Washout scenario

By building a monitoring panel in Discovery Web, based on the proper rheological models and hydraulic calculations, this thesis have been used to show how models and simulations can be combined in Discovery Web. The experience has been that it was easy to implement the model using Discovery Web Formulas. Another strength of the software is that it is very easy to visualize and import data from real wells in this application. Hence, it is a very good tool for comparing models with real data. This real-time data handling capability and visualization flexibility is considered as one of the major strengths. It has also been shown how to embed events into the models, which later can be used as a basis for developing training scenarios and demonstrations in teaching. The results show how the models implemented can be the first step in introducing models in combination with real-time data for monitoring and handling drilling problems using this application.

Acknowledgement

This thesis was written for the Department of Petroleum Engineering at the University of Stavanger in collaboration with Kongsberg Oil & Gas Technologies.

I would like to use this opportunity to thank the several people that have helped me in the work with this thesis. I would first like to express my appreciation to the Discovery Web team for allowing me to take on this assignment as well as the material and intellectual support that they have contributed in this process.

My deepest gratitude goes to my Discovery Web mentor Jan Kåre Igland whom have supported and educated me in drilling applications. His engagement in discussions and tutoring skills has been a most valuable asset in this process.

Finally, I would like to thank my advisors at the University of Stavanger Mesfin Agonafir Belayneh and Kjell Kåre Fjelde. They have provided excellent academic guidance and advisory through the process. Their engagement in discussions and knowledge within Drilling Technology has been a major motivation staying on the right track while working on this thesis.

Table of Contents

Abstract	2
Acknowledgement	3
Table of Contents	4
Table of Figures	5
Abbreviations	6
Nomenclature	7
1. Introduction	9
1.1 Background	9
1.2 Problem formulation	11
1.3 Objective of the thesis	13
2. Hydraulic Models	14
2.1 Rheology	14
2.1.1 Newtonian fluids	15
2.1.2 Non-Newtonian fluids	15
2.1.3 Comparison and error calculation of rheology prediction	20
2.2 Hydraulics	21
2.2.1 Pressure losses	21
2.2.2 Bit pressure losses	23
2.2.3 Cuttings concentration	23
2.3 Modeling in Discovery Web	25
2.3.1 Bingham frictional model	25
2.3.2 Herschel-Bulkley frictional model	27
2.3.3 Robertson-Stiff frictional model	29
3. Drilling Parameters, Problem Detection and Remedial Action	31
3.1 Drilling parameters	31
3.2 Typical equipment and wellbore problems	34
3.3 Stuck pipe	38
3.4 Lost circulation	45
4. Examples of other Software Tools	48
4.1 Sekal DrillScene	48
4.2 eDrilling Solutions	49
4.3 DrillBench	51
5. Architecture of Discovery Web	53
6. Discovery Web Real-time ECD Control Design	57
6.1 Simulation based on our built data	57
6.1.1 Connection scenario	58
6.1.2 Kick scenario during drilling	59
6.1.3 Kick scenario during connection	60
6.1.4 Pack-off scenario and sensitivity of pack-off	61
6.1.5 Lost circulation scenario	65
6.1.6 ROP vs. Cuttings concentration scenario	69
6.1.7 Comparison of different rheology models for hydraulic calculations	70
6.1.8 Washout scenario	71
6.2 Simulation based on real well based data	73
7. Summary and Discussion	74
8. Conclusion	77
9. Future Work	78
References	80
Appendix A	83
Appendix B	84
Appendix C	87

Table of Figures

Figure 1 - Pore pressure diagram illustrating the drilling window.	10
Figure 2 - Bingham-plastic model.	16
Figure 3 - Herschel-Bulkley fluid rheogram.	17
Figure 4 - Robertson-Stiff fluid rheogram.	19
Figure 5 - Comparison of rheology prediction.	20
Figure 6 - Pressure drops during circulation.	22
Figure 7 - Illustration of drill collar without centralizer sticking in a well [26].	42
Figure 8 - Well path for stuck point derivations.	43
Figure 9 - Illustration showing total loss of circulation.	45
Figure 10 - DrillScene: Drilling through a depleted region. Time frame is 2 minutes [31]. ...	48
Figure 11 - DrillScene: MPD solution based on back-pressure [30].	49
Figure 12 - eDrilling: Pump rate [32].	50
Figure 13 - eDrilling: Calculated bottomhole ECD [32].	50
Figure 14 - DrillBench: Kick during connection [34].	51
Figure 15 - SiteCom setup [35].	53
Figure 16 - Workflows of SiteCom [35].	54
Figure 17 - Basic drilling console - DrillingTime Playback UiS [37].	55
Figure 18 - Calculation model Discovery Web Formula and Arithmetic Smart Agent [37]...	55
Figure 19 - Discovery Web Formula [37].	56
Figure 20 - Well schematics based on our built data.	57
Figure 21 - Connection scenario.	58
Figure 22 - Kick scenario during drilling.	59
Figure 23 - Kick scenario during connection.	60
Figure 24 - Illustration of pack-off scenario.	61
Figure 25 - Pack-off scenario 1 (10% reduction in annulus diameter).	62
Figure 26 - Pack-off scenario 2 (16% reduction in annulus diameter)	63
Figure 27 - Pack-off scenario 3 (20% reduction in annulus diameter).	64
Figure 28 - Illustration of total loss of circulation at 9 5/8" casing shoe.	65
Figure 29 - Lost circulation scenario 1 (Partial loss at 9 5/8" casing shoe).	66
Figure 30 - Lost circulation scenario 2 (Total loss at 9 5/8" casing shoe).	67
Figure 31 - Lost circulation scenario 3 (Total loss at 4120 m).	68
Figure 32 - ROP vs. Cuttings concentration scenario.	69
Figure 33 - Comparison of different rheology models for hydraulic calculations.	70
Figure 34 - Illustration of washout scenario in drillpipe (Intellipipe).	71
Figure 35 - Washout scenario in Intellipipe.	72
Figure 36 - Temperature effect on density [39].	78

Abbreviations

(B)	-	Bingham
(H-B)	-	Herschel-Bulkley
(R-S)	-	Robertson-Stiff
AV	-	Apparent Viscosity
BHA	-	Bottom Hole Assembly
BHP	-	Bottom Hole Pressure
CTFV	-	Critical Transport Fluid Velocity
CTV	-	average Cuttings Travel Velocity
D&E	-	Drilling and Evaluation
DDM	-	Derrick Drilling Machine
E&P	-	Exploration & Production
ECD	-	Equivalent Circulating Density
ERD	-	Extended Reach Drilling
FIT	-	Formation Integrity Test
FLOWIN	-	Flow Rate In
FLOWOUT	-	Flow Rate Out
FRT	-	Free Rotating Torque
HPHT	-	High Pressure High Temperature
HWDP	-	Heavy Weight Drill Pipe
IO	-	Integrated Operations
IRIS	-	International Research Institute of Stavanger
KOG	-	Kongsberg Oil & Gas
LC	-	Lost Circulation
LCM	-	Loss Circulation Material
LOT	-	Leak-Off Test
LPM	-	Liter Per Minute
LWD	-	Logging While Drilling
MPD	-	Managed Pressure Drilling
MWD	-	Measurement While Drilling
MWIN	-	Mud Weight In
MWOUT	-	Mud Weight Out
NCS	-	Norwegian Continental Shelf
NPT	-	Non-Productive Time
OBM	-	Oil Based Mud Systems
OH	-	Open Hole
OPC	-	Standardized Alarm System
PDC	-	Polycrystalline Diamond Compact
POOH	-	Pull Out Of Hole
PUW	-	Pick-Up Weight
PV	-	Plastic Viscosity
PVT	-	Pressure Volume Temperature
RIH	-	Run In Hole
ROP	-	Rate Of Penetration
RPM	-	Revolutions Per Minute
SCFF	-	Subcritical Fluid Flow
SOW	-	Slack-off Weight
SPP	-	Stand Pipe Pressure
TD	-	Target Depth
TOC	-	Top of Cement
UBO	-	Underbalanced Operations
WOB	-	Weight On Bit
YP	-	Yield Point

Nomenclature

a	-	Frictional fractions parameters, dimensionless
A	-	Pipe Area, m ²
A	-	R-S model parameter similar to K , lbf. sec ^B /100 ft ² or dyne. sec ^B /100 cm ²
A_1	-	Area of drill pipe 1, m ²
A_2	-	Area of drill pipe 2, m ²
A_n	-	Total nozzle area, m ²
b	-	Frictional fractions parameters, dimensionless
B	-	Robertson-Stiff model parameter similar to n , dimensionless
C	-	Orifice coefficient (C: 0.80 for non-jet bit, C: 0.95 for jet bit), dimensionless
C	-	Robertson-Stiff model correction factor, 1/sec ^B
C_a	-	Herschel-Bulkley model parameter, dimensionless
C_c	-	Herschel-Bulkley model parameter, dimensionless
d	-	Density, sg or ppg
d	-	Diameter of pipe, in or m
d_H	-	Hydraulic diameter, in or m
D_{hole}	-	Diameter between annulus and pipe, in or m
D_1	-	Outside pipe diameter, in or m
D_2	-	Inside casing diameter, in or m
D_N	-	Nozzle diameter, in
D_p	-	Inside pipe diameter, in or m
E	-	Young's E-Modulus, Pa
ECD	-	Equivalent Circulating density, sg
F	-	Force, Pa
f_f	-	Fanning friction factor, dimensionless
f	-	Friction factor, dimensionless
f_a	-	Friction factor to the annulus, dimensionless
f_p	-	Friction factor to the pipe, dimensionless
g	-	Gravity, m/s ²
h	-	Height, m
K	-	Consistence index, lbf. sec ⁿ /100 ft ² or dyne. sec ⁿ /100 cm ²
k	-	Surface roughness, m
L	-	Length, ft
L_{DC}	-	Drill collar length, ft or m
n	-	Flow behavior index, dimensionless
N_{Re}	-	Reynolds number, dimensionless
$N_{Re Cr}$	-	Critical value of Reynolds number, dimensionless
P	-	Pressure, psi
P_p	-	Pump pressure, psi or bar
Q	-	Flow rate, gallon/min or lpm
R	-	Build or sail section radius, m
R_p	-	Length of b in Figure 7, m
R_w	-	Well radius, m
ROP	-	Rate of Penetration, m/h
s	-	Source (phase transfer between phases)
t	-	Time, s or hr
u	-	Fluid velocity, m/s or ft/s
v_a	-	Annular average velocity, ft/sec

V_{avg}	-	Average velocity, ft/sec or m/s
V_{Cr}	-	Critical velocity, ft/sec or m/s
v_p	-	Pipe average velocity, ft/sec
w	-	Weight of pipe, kg/m
x_{int}	-	Factor for interpolation, dimensionless
y	-	Herschel & Bulkley model parameter, dimensionless
z	-	Herschel & Bulkley model parameter, dimensionless
α	-	Angle, degree
β	-	Buoyancy, dimensionless
ε	-	Surface roughness coefficient, dimensionless
ρ	-	Density, lbm/gal, sg
ϕ	-	Porosity, percent
γ	-	Shear rate, 1/sec
γ^*	-	Shear rate value corresponding to geometric mean of the shear stress, τ^* , 1/sec
γ_{max}	-	Maximum shear stress value of data, 1/sec
γ_{min}	-	Minimum shear stress value of data, 1/sec
θ_3	-	Reading from rheometer at 3RPM
θ_6	-	Reading from rheometer at 6RPM
θ_{100}	-	Reading from rheometer at 100RPM
θ_{200}	-	Reading from rheometer at 200RPM
θ_{300}	-	Reading from rheometer at 300RPM
θ_{600}	-	Reading from rheometer at 600RPM
μ	-	Viscosity, cP
μ_p	-	Plastic viscosity, cP
τ	-	Shear stress, lbf/100 ft ²
τ^*	-	Shear stress value corresponding to the geometric mean of the shear rate, γ^*
τ_{calc}	-	Calculated shear stress, lbf/100 ft ²
τ_{max}	-	Maximum shear stress value of data, lbf/100 ft ²
τ_{meas}	-	Measured shear stress, lbf/100 ft ²
τ_{min}	-	Minimum shear stress value of data, lbf/100 ft ²
τ_o	-	Yield stress, lbf/100 ft ²
τ_y	-	Yield point, lbf/100 ft ²
$\%C$	-	Cuttings concentration, percent
∂	-	Partial derivative, dimensionless
Δ	-	Gradient
ΔL	-	Segment length, m
ΔP	-	Pressure, kPa or bar
ΔP_F	-	Frictional pressure drop, bar
ΔP_{FA}	-	Annulus pressure drop, bar
ΔP_{FB}	-	Drill bit pressure drop, bar
ΔP_{FD}	-	Nozzle pressure drop, bar
ΔP_{FM}	-	Downhole mud motor pressure drop, bar
ΔP_{FT}	-	Total pressure drop, bar
$\left(\frac{dp}{dL}\right)$	-	Gradient pressure, psi/ft

1. Introduction

Presently the oil industry is showing advancement in technology and methods to solve operational problems that the conventional methods cannot handle. The industry is facing drilling challenges such as deep-water, depleted formations, high pressure and high temperature formations, gas hydrate formations and extended reach drilling environments. New technologies allow us to explore and to produce from more and more challenging oil fields.

Application of integrated operation (IO) practices is important for reaching these strategic goals. IO practices utilize appropriate technologies, competent people, real-time data (gathering and processing) that are crucial for proper decision-making. The overall advantage of IO is to reduce non-productive time (NPT), increase productivity, increase safe operations, and decrease the risk of HSE accidents.

This thesis presents the real-time data application tool Discovery Web, where the focus is on implementing rheological models for pressure calculations and demonstration, and visualization of different drilling scenarios.

1.1 Background

Exploration and production (E&P) comprises of all the activities that are involved within exploration, development and production of hydrocarbons. When drilling through different formations one may encounter undesired well instability problems, such as well fracturing and well collapse. Well fracturing is due to well pressure exceeding the formation fracture pressure. This may result in formation fracture and huge mud losses into the formation. Well collapse occurs when the well pressure is lower than the collapse pressure of the formation. The problem results in bridging and pack-off. If this happens, it may cause drillstring mechanical sticking, and increase well pressures. This will be reflected in an increase in pump pressure (SPP). In the worst-case scenario, the drillstring needs to be cut and a sidetrack procedure initiated. Also, when drilling through a reservoir, well pressure lower than the formation pressure, may cause undesired influx of formation fluid into the well. This as a result causes a kick and in the worst-case scenario it may cause a blowout. The Macondo project can be referred to as an example. The drilling problems are still challenging for the oil industry and are huge cost factors [1].

Wellbore condition evaluation is based on detailed process models that are capable of predicting not just only downhole hydraulics, but also thermal and mechanical effects during a drilling operation. Nevertheless, how advanced these models are, there will always be uncertainties in input parameters, modeled effects and outcome. Exploration in deep water, HPHT wells limits the drilling window even more. This makes it almost impossible to ensure precise predictions under any circumstances [2].

Figure 1 is a typical figure found in drilling programs, which shows the safe operational drilling window. During operation, it is important to maintain the well pressure within the allowable drilling window. In this project the behavior of ECD with respect to the flow behavior will be monitored in Discovery Web.

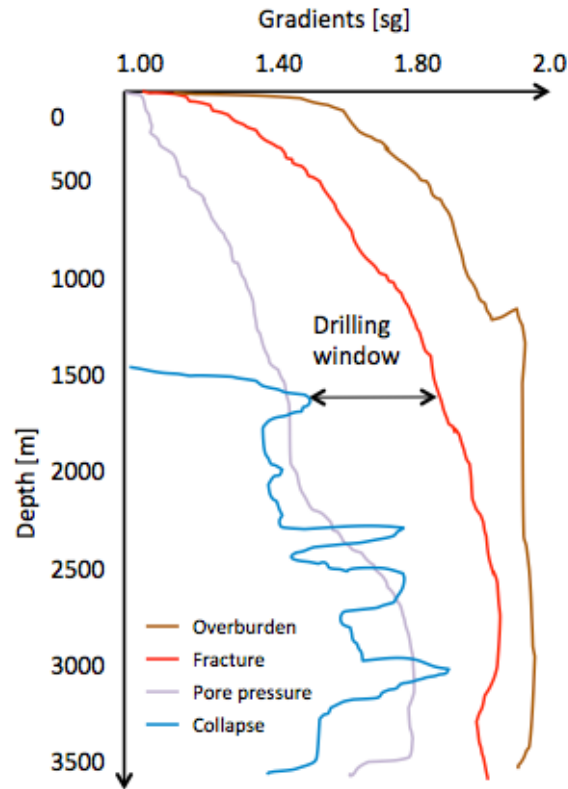


Figure 1 - Pore pressure diagram illustrating the drilling window.

The dynamic circulation pressure is determined by the static mud weight and the dynamic friction loss as given in Eq. 1:

$$ECD = \rho + \frac{\Delta P_f}{gh} \quad (1)$$

where ECD is equivalent circulation density, g is acceleration due to gravity, h is true vertical depth, ρ is static mud density and ΔP_f is friction loss. In some cases, there will also be a choke pressure like some of the managed pressure drilling (MPD) systems, as well as when circulating out a kick in a conventional well.

Drilling is the process that is used to connect the reservoir to surface, recovering potential hydrocarbons. During drilling, the drill bit intrudes several geological formations on its way down to target depth (TD). Knowledge about these formations is a key for drilling to the desired depth. By analyzing wireline logs, MWD, LWD, cores and cuttings, it is possible to determine the formations different properties. Wells are drilled using rotating bits and drilling fluid as circulation fluid. The drilling fluids have many functions, but the most important is to maintain the pressure in the borehole. Thus, maintaining the well pressure within the drilling window, avoiding fracture and collapse of formation. In addition one must also stay above pore pressure. Fluids are therefore a key element in the drilling process. It is therefore important to accurately predict the rheology and hydraulics at all times while drilling a well.

This thesis presents hydraulic calculations and visualization using Kongsberg Oil & Gas Technologies real-time monitoring program, Discovery Web. Discovery Web is a web-based browser that helps us reach out to all the involved by implementing a visualization and collaboration tool for multi disciplinary target groups [3].

1.2 Problem formulation

During drilling operations today, many operators are facing increased non-productive time (NPT). The NPT are due to drilling incidents (pack-off, kick, poor hole cleaning, excessive torque, fracture, collapse and lost circulation). If preventive measurements had been taken, many of these problems could have been avoided, or at least reduced the impacts affecting the drilling operations. There have been a few presented methodologies that are governing this proactive measurement [2]. Falconner presented in 1989 a work process that has the advantage of simplicity and does not require advanced computer systems for analyzing real-time data, but instead require special friction tests to be performed at regular intervals (for example between each connection). The method records pick-up weight (PUW), slack-off weight (SOW) and free rotation torque (FRT) while drilling, and comparing the measured data with simulations performed in advance based on torque and drag charts from the planned well path. If there are deviations from the pre-calculated data, the rate of penetration (ROP) may be reduced or hole cleaning procedures may be initiated to improve the downhole conditions [4]. Niedemayr developed another method in 2010, which performs automatic analysis of all bottom hook-loads and torque measurements. By using this system it is necessary to implement an external mechanical friction model to obtain the required torque and drag charts [2, 5].

The hydrodynamic force exerted on the inner and outer part of drilling string is caused by the rheology and circulation of drilling fluid, which again influences the drag force on the drillstring. This makes it necessary to perform friction tests with no circulation or low circulation rates to obtain comparable results. However, reduction of pump rate while taking PUW and SOW is not always the case, and essential data that could have been used to determine the downhole conditions are lost. Cayeux et al [6] developed in 2009 a continuous monitoring system using an embedded torque and drag model coupled with hydraulic calculations. By performing systematic analysis of all possible off-bottom weights and torque and with any flow rate, this model makes it possible to monitor friction in other conditions than drilling, like for instance running in hole (RIH), pulling out of hole (POOH) or back-reaming to casing shoe [2, 6]. The model was tested out on 5 fields and a total of 15 different wells. It warned in almost all cases about the evolution of poor downhole conditions prior to actual drilling incidents. It was only in a few specific instances that the monitoring system failed in showing advanced warning signs. Dependent on the different conditions from fast to slow changing conditions, the warning signs was visible between 30 minutes to 1 day before the actual incident, respectively [2].

Early symptom detection, armed with real-time calibrated process models, will help us to manipulate hydraulic parameters and avoid undesired events. By introducing the model to multiple drilling problem symptoms, the possibility for decreasing the NPT increases. The combined use of real-time data from Discovery Web and standard hydraulic calculations makes us able to regulate the ECD, by manipulation of rheology, geometry, flow rate, mud densities and ROP. Drilling is challenging when the window between the pore pressure and fracturing pressure becomes narrower. If the well pressure crosses the operational window, drilling problems such as kick, loss circulation or stuck pipe can occur.

The operational challenges include:

- Deep water:
 - Here the operational window is narrow. In addition, the formation can have higher temperature and pressure, which strongly affects the property of drilling fluids.
- Depleted reservoirs:
 - Here the formation pressure and the in-situ stresses of the formation are much lower than normal. Hole instability and formation damage may be a risk when drilling with a too high mud weight.
- Drilling in methane hydrate:
 - Drilling in gas hydrated formation leads to dissociation of gas out of hydrates. This as a result changes the properties of the drilling fluid and may cause a minor kick, which again may affect the drilling platform.
- Drilling extended reach horizontal wells:
 - In horizontal wells, the window between the fracture and collapse pressure are narrower. Horizontal wells may be exposed to well instability problems if one cannot properly manage the well pressure within the drilling window.

The overall problem occurs within these problematic areas and therefore increases the operational costs and creates impacts on health and environment. The oil and gas industry still continues to fight against borehole and string related issues. The well pressure with respect to the formation pressure and strength determines what kind of problems that can occur. In average, wellbore instability problems alone increased the total drilling budget by 10% [7].

Non-productive time (NPT) has usually a direct link to i.e. the time spent due to lost circulation, stuck pipe and tripping in and out. These problems cost operators a significant amount of money. There are also other forms of NPT that are invisible NPT. For example, the presence of vibration may cause a reduction in drilling rate. In addition, the vibration may also cause drill bit damage, which results in tripping in and out for changing the bit. Unwanted formation influx into the well is also a cost factor when having to circulate the kick out of the well. Optimization procedures do not only help reduce the visible NPT but it will also have a large impact on the invisible NPT as well. Studies from several drilling wells shows that NPT cost contributes to about 25-30% of the total drilling cost [8].

This thesis will analyze the mentioned problems based on literature review material and by building a monitoring panel in Discovery Web. This thesis therefore addresses issues such as:

1. How can integrated operations (real-time data) help reduce the possible problems, which indirectly reduces the NPT?
2. How sensitive the hydraulic parameters are with regard to the different types of events or unwanted problems that can occur?
3. Can Discovery Web be a useful tool in monitoring live wells?
4. Can Discovery Web be a useful tool for professionals and university level educational training?
5. Can real-time data contribute in improving drilling performances?

1.3 Objective of the thesis

The objective of this thesis is to show how models and simulations can be used in handling and monitoring possible problems that arises in operational challenging environments. This thesis provides the development of hydraulic visualization scenarios using Discovery Web; how we can use Discovery Web Formulas for calculating well pressures and how this could be visualized to demonstrate important pressure effects in the well.

- Provide an overview of the following:
 - Drilling parameters that are measured during drilling and what they represent.
 - Typical drilling problems that can occur.
 - Symptoms of the different drilling problems (trend changes in drilling parameters).
 - Examples where software tools have been used for well diagnostics and literature review.
- Describe the functionality of Discovery Web.
- Implement different rheology models in Discovery Web for hydraulic calculations.
- Develop hydraulic visualization views for different drilling scenarios using Discovery Web.
- Discuss the potential in using Discovery Web, how it can be used for engineering and education purposes, and potential recommendations for future work.

2. Hydraulic Models

2.1 Rheology

Rheology is a Greek word that comes from the words reo, meaning to float, and logy meaning science. Rheology deals with the study of deformation and flow of matter (mainly liquids and in some cases solids and soft solids). In short, the drilling fluid flow property is characterized by their rheological properties, which are a function of composition of the drilling fluid, temperature and pressure. Drilling fluid helps to remove cuttings from the wellbore by keeping the cuttings in suspension during drilling. Other characteristics are minimizing friction during pumping, minimizing impact on the formation as we drill and being able to separate the cuttings at surface. It is important analyze fluid flow velocity profiles, fluid viscosity, frictional pressure losses, ECD, and annular hole cleaning. It is the basis for all analyses of wellbore hydraulics [9, 10].

Flow properties for drilling mud is often characterized by the following rheology properties [9]:

- Plastic viscosity (PV)
This part of the flow resistance is caused by mechanical friction between the particles in the mud, between the particles and the liquid phase and the liquid elements themselves. Plastic viscosity depends on the liquid viscosity, and the particle concentration, size, and shape in the mud.
- Yield limit (YP)
Flow resistance transpires when attractive forces between the particles occur as a result of electrostatic forces. Yield limit will vary with the shear rate and decrease with increasing shear rate. The property is called shear thinning.
- Gel strength
Gel strength is related to the attractive forces between particles when the fluid is at rest, and is measured as a function of time. It expresses the liquid thixotropic properties, which means that shear stress is not fixed to a specific rate, but changes with shear time.
- Apparent viscosity (AV) and Funnel viscosity (“Marsh Funnel”)
Apparent viscosity and funnel viscosity will give an estimate of the total fluid viscosity. The combination of the three parameters mentioned above (PV, YP and gel strength) will affect the total viscosity. This measurement is only used as a control parameter for drilling fluids. To explain the cause of the change, the other rheological parameters need to be determined.

The fluids can be divided into two groups according to their rheological properties; these are Newtonian fluids and non-Newtonian fluids, respectively.

2.1.1 Newtonian fluids

Newtonian liquids have a viscosity, which is independent of shear rate. They are simple and clean liquids containing no particles larger than molecules. For instance liquids such as water, oil, and glycol behave as Newtonian fluids [9]. Given as Eq. 2 the shear stress is directly proportional to shear rate:

$$\tau = \mu \cdot \gamma \quad (2)$$

where τ is shear stress, μ is viscosity and γ is shear rate.

2.1.2 Non-Newtonian fluids.

Unlike the Newtonian fluids, the viscosity for non-Newtonian fluids depends on shear rate. These are divided into three main categories: Plastic liquids, pseudo plastic fluids and dilatant fluids. It follows that the assortment of drilling fluids will be either plastic or pseudo plastic fluids. In short, the main difference between plastic and pseudo plastic fluids are that plastic fluids have yield strength and a pseudo plastic does not. Still, both are simultaneously shear thinning, i.e. AV decreases with increasing shear rate. Two examples of plastic and pseudo plastic fluids; water with added bentonite, and water containing polymers [9]. The following rheology data set given in Table 1 is used as an example for how the different rheology parameters may be determined by using both graphics and equations. The fluid is made out of water, bentonite, polymer and barite [11]. The main goal will be to determine the rheological model that is best fitted to describe the given Fann data in Table 1.

RPM	Reading [°]
600	54.50
300	43.50
200	37.50
100	32.00
6	23.00
3	20.50

Table 1 - Fann data [11].

2.1.2.1 Bingham-Plastic model

The Bingham model best describes liquids that have a yield point, and includes suspension of solids. The model is widely used to describe the condition of drilling fluid. Nevertheless, it is not suitable for viscosity and pressure loss calculations. The model is based upon two measurements that are performed by a Fann viscometer, respectively at 600 and 300 rpm. It is from these measurements possible to calculate the different rheological properties. However, it does not represent the most accurate behavior of drilling fluid at the bit (very high shear rate) and in the annulus (very low shear rates).

To describe a fluid in the best possible way, good mathematical models needs to be developed; perhaps one of the most famous of these is the Bingham-plastic model. It follows from Figure 2 that the equation for shear stress (τ) is given by Eq. 3 [9]:

$$\tau = \tau_y + \mu_p \cdot \gamma \quad (3)$$

where the yield point, τ_y (YP) and plastic viscosity, μ_p (PV) can either be read from a graph similar to Figure 2 or calculated by using Eq. 4 and Eq. 5.

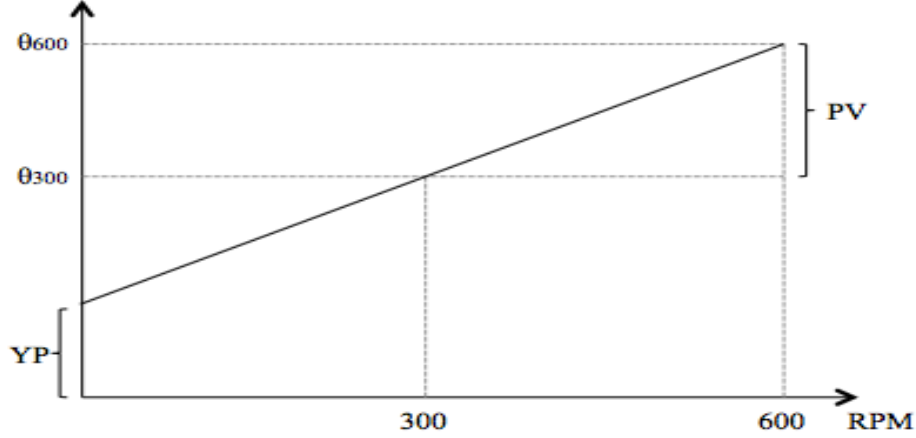


Figure 2 - Bingham-plastic model.

The slope of the curve in Figure 2 represents the plastic viscosity (μ_p).

$$\mu_p [cP] = \theta_{600} - \theta_{300} \quad (4)$$

Curve intersection with the shear stress y-axis gives the yield strength in Eq. 5.

$$\tau_y [lbs/100ft^2] = \theta_{300} - \mu_p = 2 \cdot \theta_{300} - \theta_{600} \quad (5)$$

Using Eq. 4 and Eq. 5 and values from Table 1 the parameters μ_p (PV) and τ_y (YP) can be determined.

$$\begin{aligned} \mu_p &= 54.50 - 43.50 = 11 \text{ cP} \\ \tau_y &= 43.50 - \mu_p = 32.50 \text{ lbf}/100 \text{ ft}^2 \end{aligned}$$

2.1.2.3 Herschel-Bulkley model

The Herschel-Bulkley model is a modified version of the power-law model and is the model that normally describes the measured data best. By defining a third parameter, yield stress (τ_0), it is possible to get better results at low shear rates. The model is defined by Eq. 6 [9, 12]:

$$\tau = \tau_0 + K(\gamma)^n \quad (6)$$

or

$$\log(\tau - \tau_0) = \log(K) + n \log(\gamma) \quad (7)$$

In comparison to Bingham, the model is using three parameters to describe the rheological behavior; therefore an initial calculation of τ_0 is required for calculation of the other parameters (Eq. 8).

$$\tau_0 = \frac{\tau^{*2} - \tau_{min} \cdot \tau_{max}}{2 \cdot \tau^* - \tau_{min} - \tau_{max}} \quad (8)$$

where τ^* is the shear stress value, corresponding to the geometric mean of the shear rate, γ^* and is calculated by interpolation.

$$\gamma^* = \sqrt{\gamma_{min} \cdot \gamma_{max}} \quad (9)$$

Using Eq. 8 and Eq. 9 and values from Table 1. The parameters τ^* , γ^* and τ_0 may be determined.

$$\begin{aligned} \gamma^* &= 72.25 \text{ sec}^{-1} \\ \tau^* &= 28.26 \text{ lbf}/100 \text{ ft}^2 \\ \tau_0 &= 20.14 \text{ lbf}/100 \text{ ft}^2 \end{aligned}$$

Figure 3 and Table 2 shows the final results. A trend line was obtained using regression techniques.

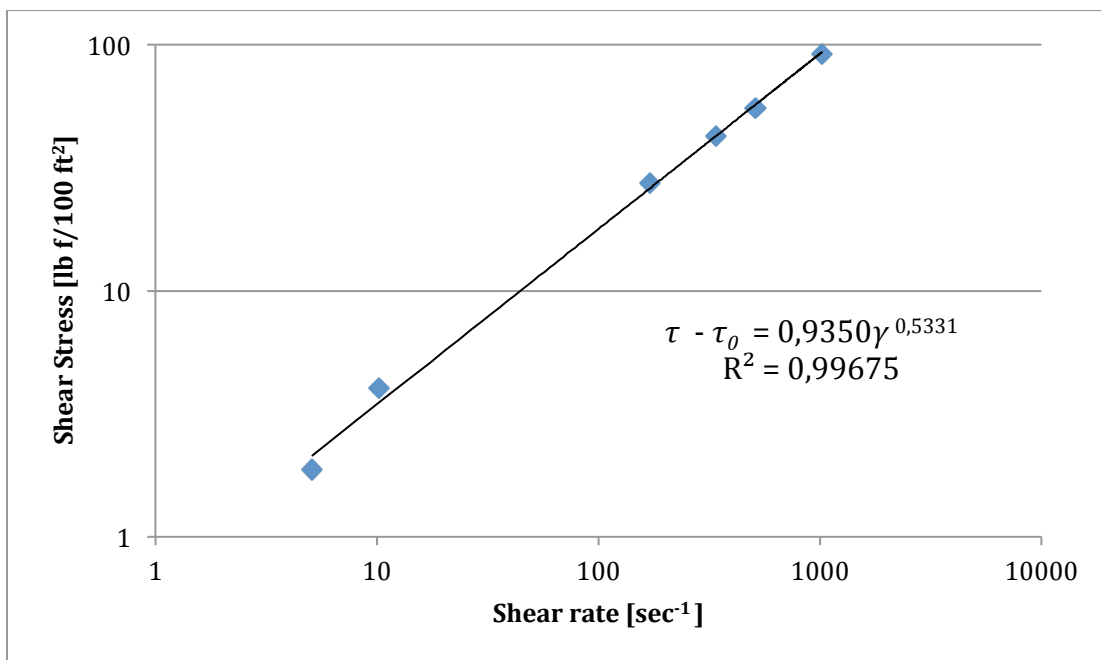


Figure 3 - Herschel-Bulkley fluid rheogram.

From Figure 3, the Herschel-Bulkley parameters are as follows:

$$\begin{aligned} n &= 0.5331 \\ K &= 0.9350 \text{ lbf}/100 \text{ ft}^2 \end{aligned}$$

γ [sec ⁻¹]	τ [lbf/100 ft ²]
1021,80	57,72
510,90	46,11
340,60	41,06
170,30	34,60
10,22	23,36
5,11	22,37

Table 2 - Shear stress calculated as function of Herschel-Bulkley parameters.

2.1.2.4 Robertson-Stiff model

Robertson-Stiff model was developed as a more general model to describe the rheology behavior of drilling fluids and cement slurries. The model is given by Eq. 10 [13]:

$$\tau = A(\gamma + C)^B \quad (10)$$

or

$$\log(\tau) = \log(A) + B \log(\gamma + C) \quad (11)$$

where A and B are model parameters similar to n and K in the Herschel-Bulkley model. Parameter C is the shear rate correction factor, so that the term $(\gamma + C)$ is considered the effective shear rate. Thus, τ is plotted against $(\gamma + C)$ on log-log coordinates, B is the slope and A is the intercept where $(\gamma + C) = 1$. Eq. 12 represents the yield stress for the Robertson-Stiff model.

$$\tau_0 = AC^B \quad (12)$$

$$C = \frac{\gamma_{min} \cdot \gamma_{max} - \gamma^{*2}}{2 \cdot \gamma^* - \gamma_{min} - \gamma_{max}} \quad (13)$$

where γ^* is the shear rate value corresponding to the geometric mean of the shear stress, τ^* , and is calculated by interpolation.

$$\tau^* = \sqrt{\tau_{min} \cdot \tau_{max}} \quad (14)$$

Again by using the data from Table 1, Eq. 13 and Eq. 14, the parameters τ^* , γ^* and C may be determined by calculations and interpolation.

$$\begin{aligned} \tau^* &= 35.66 \text{ lbf}/100 \text{ ft}^2 \\ \gamma^* &= 195.65 \text{ sec}^{-B} \\ C &= 52.01 \text{ sec}^{-B} \end{aligned}$$

Figure 4 and Table 3 shows the results. A trend line was obtained by using regression techniques.

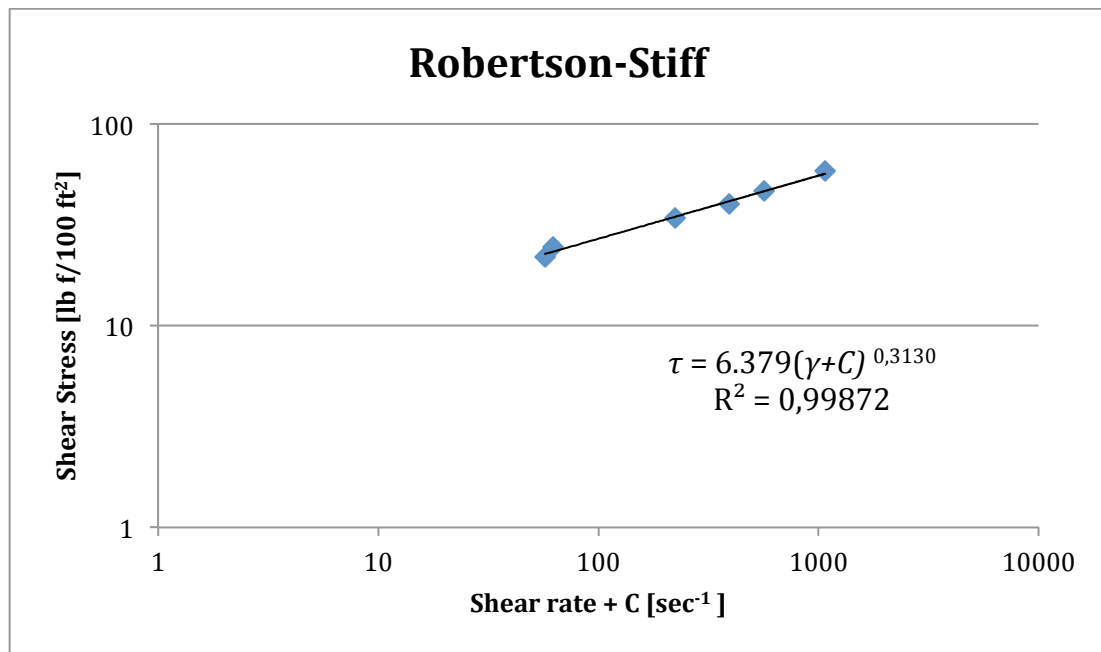


Figure 4 - Robertson-Stiff fluid rheogram.

From Figure 4 the Robertson- Stiff parameters are as follows:

$$A = 6.379 \text{ lbf} \cdot \text{sec}^B / 100 \text{ ft}^2$$

$$B = 0.3130$$

γ [sec ⁻¹]	τ [lbf/100 ft ²]
1021,80	56,70
510,90	46,32
340,60	41,38
170,30	34,63
10,22	23,25
5,11	22,63

Table 3 - Shear stress calculated as a function of Robertson-Stiff parameters.

2.1.3 Comparison and error calculation of rheology prediction

2.1.3.1 Comparison of the rheology prediction

An Excel sheet has been created to compare and evaluate the different rheology models against the experimental data set in Table 1. Figure 5 illustrates a comparison of shear stress and shear rate data for the given rheology models.

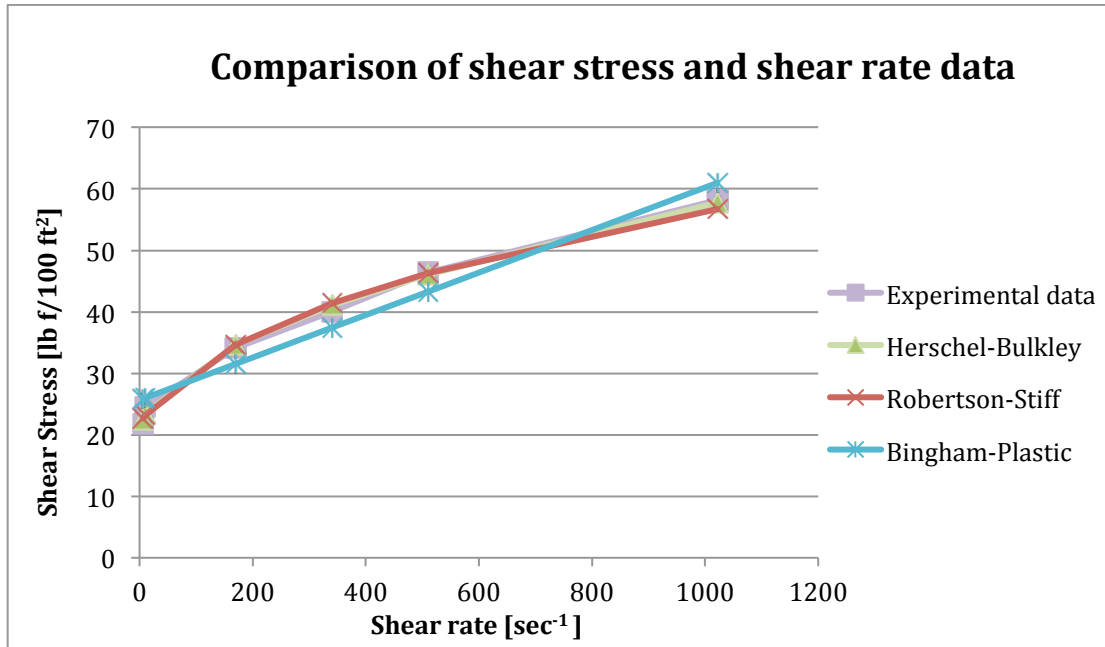


Figure 5 - Comparison of rheology prediction.

2.1.3.2 Error calculation of rheology prediction

By performing an error analysis, we can determine which model best represents the experimental data set in Table 1. Table 4 shows that the Herschel-Bulkley model gives the lowest error and has therefore been considered the best fit for the following simulations.

Rheology Model:	Error %
Bingham-Plastic Model	1,382
Herschel-Bulkley Model	0.344
Robertson-Stiff Model	0,452

Table 4 - Error analysis for rheology prediction.

2.2 Hydraulics

2.2.1 Pressure losses

While drilling a well it is important to always be aware of the pressure losses within the system, both at surface and downhole. The downhole static pressures can be calculated by using the pumped mud weight, while additional pressure losses caused by circulation can be calculated using the relationship between pump rates and drilling fluid rheological properties.

The downhole static pressure has however no influence on the pump pressure required to circulate drilling fluid. The mud pumps are located on the same deck as where the mud is circulated in return so that the drilling fluid is approximately in static equilibrium between the pump outlet and return flow from the wellhead (fixed platform) or on top of the standpipe manifold (semi-submersible rig). The frictional pressure drop and the nozzle pressure drop makes up most of the pump pressure, and it is therefore extremely important to calculate these before planning the drilling program. Yet, other pressure drops in the fluid flow should also be estimated [14].

The total pressure drop provided by the mud pumps is determined by:

- Drill pipe frictional pressure drop (ΔP_F)
 - Liquid rheology properties.
 - Lengths and inner diameters of the pipes and BHA components from the mud pumps to the drill bit.
 - Also note that some BHA components will have additional pressure losses due to motor and MWD. BHA components can also have a smaller diameter than regular drill pipe causing some additional pressure loss.
- Downhole mud motor pressure drop (ΔP_{FM})
 - Some of the pressure energy in the drilling mud is often used to operate downhole mud motors and sometimes turbines for rotating the drill bit or acquire energy for downhole measurement systems (MWD). The mud pumps, in form of higher pump pressure, must supply this energy.
- Nozzle pressure drop (ΔP_{FD})
 - A large portion of the dynamic pressure energy is transferred to velocity energy, which is used for flushing and partial breakage of the rock in the borehole.
- Drill bit pressure drop (ΔP_{FB})
 - Drill bit pressure drop is established when flow from the nozzles and the front of the drill bit passes the edge. This is different dependent on the drill bit type. For a roller cone there is ample space to flow around the cones, therefore this pressure drop is often negligible and can be set as equal to zero. However for a PDC drill bit, the bit body is seated firmly against the bottom of the borehole. This allows for a thin layer flow of drilling fluid and the frictional pressure drop can be significant.

- Annulus pressure drop (ΔP_{FA})
 - o The annulus can cause an additional pressure drop that represents lost energy, which must be taken from the pump pressure. When cuttings are mixed together with drilling mud, the average density is increased, and the static pressure in the annulus between the drill string and the borehole wall increases slightly due to this density increase.
 - o There will also be a large pressure loss around the BHA components due to the variation in annulus geometry. BHA components differ in outer diameter and may lead to a reduced flow area.

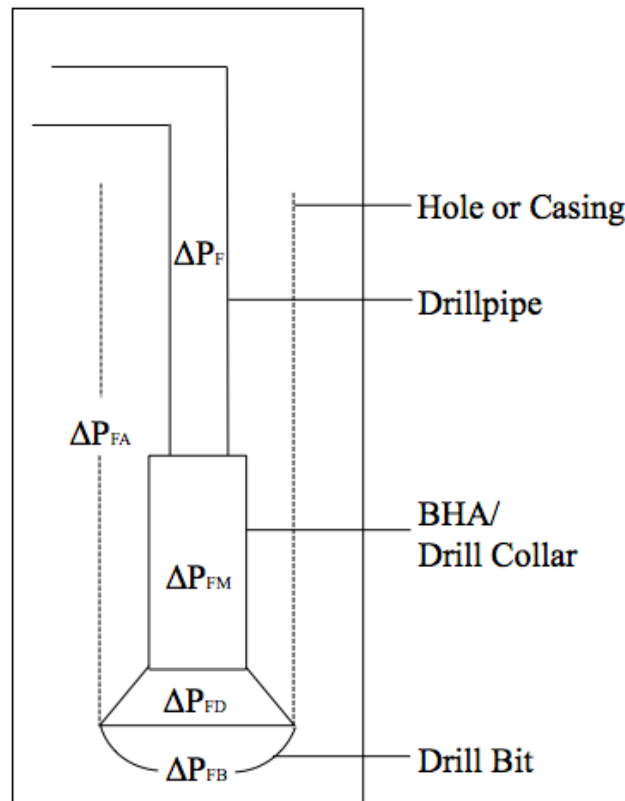


Figure 6 - Pressure drops during circulation.

The total pressure drop (ΔP_{FT}) illustrated in Figure 6 and shown in Eq. 15 is the sum of these individual contributions, and is equal the pump pressure (P_p), which must be supplied for by the mud pumps.

$$P_p = \Delta P_F + \Delta P_{FM} + \Delta P_{FD} + \Delta P_{FB} + \Delta P_{FA} = \Delta P_{FT} \quad (15)$$

Pump pressure is mainly determined by the frictional pressure losses. The mud density is a part of the frictional pressure loss calculation models and is influencing the pump pressure indirectly through the friction models. The hydrostatic component created by the cuttings will cause a different hydrostatic pressure in drillpipe versus annulus, which will be reflected in the pump pressure. Hence, the size of the hydrostatic pressure component is directly dependent on the depth and must be considered. When calculating the frictional pressure losses it might be efficient to subdivide the drillstring and annulus into shorter segments. This is because any change in flow regime, wellbore geometry or fluid properties will affect the frictional pressure loss.

The frictional pressure loss ΔP_f is calculated from Eq. 16:

$$\Delta P_f = \frac{2}{d_H} f_f \rho u^2 \Delta L \quad (16)$$

where d_H is hydraulic diameter, f_f is friction factor, ρ is fluid density, u is fluid velocity and ΔL is segment length [15]. It may be convenient to notice that that the friction will quadruple if the rate doubles.

From the following procedure it is possible to calculate the frictional pressure drop [13]:

1. Determine rheological properties and choose the best-fit rheological model.
2. Based on the chosen rheology model, calculate the Reynolds number.
3. By comparing the calculated Reynolds number, determine the following flow regime.
4. Calculate the fanning friction factor.
5. Use the correct formula to determine the pressure loss.

2.2.2 Bit pressure losses

As drilling fluid flows through nozzles, the pressure loss is based on change in kinetic energy. In oil field units, the pressure loss across the nozzle can be calculated from Eq. 19 [16]:

$$P = \frac{\rho Q^2}{2959.41 C^2 A_n^2} \quad (17)$$

where P [kPa] is pressure drop, ρ [kg/l] is specific gravity of drilling fluid, Q [l/min] is flow rate, A_n [in^2] is total nozzle area, and C is orifice coefficient (C : 0.80 for non-jet bit and C : 0.95 for jet bit).

2.2.3 Cuttings concentration

During drilling, a real-time analysis of downhole and surface measurements can give indications of poor hole cleaning. However, it is not always that intuitive to know how the cuttings are settling throughout the entire borehole section, this is because the transportation of cuttings and the formation of cuttings beds are largely influenced by a series of actions (i.e. reciprocation and circulation rate) performed during this operation. Larsen et al [17] have developed a model that is based on empirical correlations that enables a drilling engineer to select the proper hydraulics to ensure problem-free drilling in high angle wellbores (from 55 to 90° from vertical). The model predicts the required critical transport fluid velocity (CTFV), the average cuttings travel velocity (CTV) and the annular cuttings concentration under a given set of drilling conditions. Under development of this model, 7000 tests were simulated to show how CTFV and the Subcritical Fluid Flow (SCFF) would affect the annular cuttings concentration. CTFV is defined as the minimum fluid velocity required to maintain a continuously upward movement of the cuttings.

If cuttings start to accumulate in the wellbore, the annular fluid velocity is lower than the CTFV. SCFF is defined as any flow rate corresponding to an annular velocity below the CTFV. Following hydraulic drilling parameters were evaluated to investigate SCFF and CTFV: flow rate, inclination, mud density, mud rheology, cuttings size, drillpipe eccentricity and ROP. The predictions presented in Larsen et al can easily be read from charts, hand calculated, or programmed on a computer [17, 18].

By implementing a transient cuttings-transport model, it is possible to get an updated prognosis of the distribution of cuttings in suspension and in beds along the annulus, thus giving us a more correct measurement for the cuttings concentration. Cayeux et al [18] implemented a cuttings-transport model where the transport of cuttings is governed by the mass-conservation equation. This equation can be written as Eq. 20.

$$\frac{\partial \rho}{\partial t} + \Delta \cdot (\rho \vec{v}) = 0 \quad (18)$$

A transient cuttings-transport model makes it possible to better predict downhole conditions that evolve over time. Effects related to change in operational parameters are taken into account to represent the simulation as realistic as possible. By real estimation of downhole conditions, it is possible to provide better operational recommendations to avoid stuck pipe and pack-off incidents. Thus, by adjusting the hydraulic drilling parameters, such as drillstring rotational speed, flow rate and ROP one can avoid the formation of cuttings bed or deliver a proper method of removing them. For more theory on transient flow models, see Appendix A [18, 19].

Nevertheless, a transient flow model would have been too advanced to implement using only Excel formulas. Hence, the steady state model shown in Eq. 21 was considered instead. The equation is based on a no-slip model [20].

$$\%C = \frac{(ROP) \cdot \left(\frac{\pi}{4} D_{hole}^2\right) \cdot (1 - \phi)}{Q + (ROP) \cdot \left(\frac{\pi}{4} D_{hole}^2\right) \cdot (1 - \phi)} \quad (19)$$

where ϕ is reservoir porosity and D_{hole} is the hole size. Since the annulus volume and the flow rate is known; the time it takes between cuttings is generated at bottom and when they are observed at shaker can be determined. In order to get the transient behavior that reflects that the response evolves over time, the following time interpolation has been implemented:

$$xint = \frac{time - timenewrop}{timebottomsup} \quad (20)$$

where $xint$ is the interpolation coefficient, $time$ is the cumulative time that runs through the operation, $timenewrop$ is the time when the new ROP is initiated, and $timebottomsup$ is the calculated time it takes to transport the cuttings from bottom to surface.

The following limits needs to be established for transient flow determination:

$$\begin{aligned} xint &= 0 \text{ if } time = timenewrop \\ xint &= 1 \text{ if } time = timenewrop + timebottomsup \end{aligned}$$

Eq. 21 determines the transient cuttings concentration at the shaker during the bottoms-up circulation.

$$\%C_{transient} = (1 - xint) \cdot \%C_{old} + xint \cdot \%C_{new} \quad (21)$$

The transient model takes into consideration the increasing mud weight in the annulus as we circulate. After the bottoms-up circulation the new mud weight is established in the annulus.

2.3 Modeling in Discovery Web

The following rheology models have been implemented into Discovery Web for creation of hydraulic visualization scenarios.

2.3.1 Bingham frictional model

The majority of these formulas are taken from Data Drilling Handbook [16]. For more formula details see Appendix B.

2.3.1.1 Frictional pressure loss calculation inside the drillstring

Determination of average velocity and critical velocity value for drillpipe:

Average velocity:

$$V_{avg} = \frac{Q}{\frac{\pi}{4}(D_P^2)} \quad (22)$$

where V_{avg} is average velocity, D_P is string inside diameter and Q is fluid flow rate.

Critical velocity:

$$V_{Cr} = \frac{2.48}{D_P d} \left(\mu_P + \sqrt{\mu_P^2 + 73.57 \cdot \tau_y \cdot D_P^2 \cdot d} \right) \quad (23)$$

Flow regime determination:

(With critical $Re = 2100$ for a Bingham fluid.)

If $V_{avg} < V_{Cr}$ the flow is laminar.

If $V_{avg} > V_{Cr}$ the flow is turbulent.

Frictional pressure loss calculation inside the drillstring:

- Laminar flow:

$$\left(\frac{dp}{dL} \right) = \frac{Q \cdot \mu_P}{612.95 D_P^4} + \frac{\tau_y}{13.26 D_P} \quad (24)$$

- Turbulent flow:

$$\left(\frac{dp}{dL} \right) = \frac{d^{0.8} Q^{1.8} \mu_P^{0.2}}{901.63 D_P^{4.8}} \quad (25)$$

2.3.1.3 Frictional pressure loss calculation inside the annulus

Determination of average velocity and critical velocity value for annular flow:

Average velocity:

$$V_{avg} = \frac{Q}{\frac{\pi}{4}(D_2^2 - D_1^2)} \quad (26)$$

Critical velocity:

$$V_{Cr} = \frac{3.04}{(D_2 - D_1)d} \left(\mu_p + \sqrt{\mu_p^2 + 40.05 \cdot \tau_y \cdot (D_2 - D_1)^2 \cdot d} \right) \quad (27)$$

where V_c is critical fluid velocity, D_2 is annulus outside diameter, D_1 is annulus inside diameter (outside string), μ_p is plastic viscosity, τ_y is yield value, and d is fluid specific gravity.

Flow regime determination:

(With critical Re = 2100 for a Bingham fluid.)

If $V_{avg} < V_{Cr}$ the flow is laminar.

If $V_{avg} > V_{Cr}$ the flow is turbulent.

Frictional pressure loss calculation inside the annulus:

- Laminar flow:

$$\left(\frac{dp}{dL} \right) = \frac{Q \cdot \mu_p}{408.63(D_2 + D_1)(D_2 - D_1)^3} + \frac{\tau_y}{13.26(D_2 - D_1)} \quad (28)$$

- Turbulent flow:

$$\left(\frac{dp}{dL} \right) = \frac{d^{0.8} Q^{1.8} \mu_p^{0.2}}{706.96(D_2 + D_1)^{1.8} (D_2 - D_1)^3} \quad (29)$$

2.3.2 Herschel-Bulkley frictional model

The majority of these formulas are taken from the doctoral thesis “Analysis of drilling fluid rheology and tool joint effect to reduce errors in hydraulics calculations” [13]. For more formula details see Appendix B.

2.3.2.1 Frictional pressure loss calculation inside the drillstring

Determination of Reynolds number and critical Reynolds number value for drillpipe:

Reynolds number:

$$N_{Re} = \left[\frac{2(3n+1)}{n} \right] \left[\frac{\rho v_p^{(2-n)} \left(\frac{D_p}{2}\right)^n}{\tau_0 \left(\frac{D_p}{2v_p}\right)^n + K \left[\frac{(3n+1)}{nC_c}\right]^n} \right] \quad (30)$$

Critical Reynolds numbers value:

$$N_{Re\ cr} = \left[\frac{4(3n+1)}{n} \right]^{\frac{1}{1-z}} \quad (31)$$

Flow regime determination:

If $N_{Re} < N_{Re\ cr}$ the flow is laminar.
If $N_{Re} > N_{Re\ cr}$ the flow is turbulent.

Frictional pressure loss calculation inside the drillstring:

- Laminar flow:

$$\left(\frac{dp}{dL}\right) = \frac{4K}{14400D_p} \left\{ \left(\frac{\tau_0}{K}\right) + \left[\left(\frac{3n+1}{nC_c}\right) \left(\frac{8Q}{\pi D_p^2}\right)\right]^n \right\} \quad (32)$$

- Turbulent flow:

$$\left(\frac{dp}{dL}\right) = \frac{f_p Q^2 \rho}{144\pi^2 D_p^2} \quad (33)$$

2.3.2.2 Frictional pressure loss calculation inside the annulus

Determination of Reynolds number and critical Reynolds number value for annular flow:

Reynolds number:

$$N_{Re} = \left[\frac{4(2n+1)}{n} \right] \left[\frac{\rho v_p^{(2-n)} \left(\frac{D_2 - D_1}{2} \right)^n}{\tau_0 \left(\frac{D_p}{2v_a} \right)^n + K \left[\frac{2(2n+1)}{nC_a} \right]^n} \right] \quad (34)$$

Critical Reynolds number value:

$$N_{Re\ cr} = \left[\frac{8(2n+1)}{ny} \right]^{\frac{1}{1-z}} \quad (35)$$

Flow regime determination:

If $N_{Re} < N_{Re\ cr}$ the flow is laminar.
If $N_{Re} > N_{Re\ cr}$ the flow is turbulent.

Frictional pressure loss calculation inside the annulus:

- Laminar flow:

$$\left(\frac{dp}{dL} \right) = \frac{4K}{14400(D_2 - D_1)} \left\{ \left(\frac{\tau_0}{K} \right) + \left[\left(\frac{16(2n+1)}{nC_a(D_2 - D_1)} \right) \left(\frac{Q}{\pi \left((D_2/2)^2 - (D_1/2)^2 \right)} \right) \right]^n \right\} \quad (36)$$

- Annular flow:

$$\left(\frac{dp}{dL} \right) = \frac{f_a Q^2 \rho}{144\pi^2 (D_2 - D_1) (D_2^2 - D_1^2)^2} \quad (37)$$

2.3.3 Robertson-Stiff frictional model

The majority of these formulas are taken from doctoral thesis “Analysis of drilling fluid rheology and tool joint effect to reduce errors in hydraulics calculations” [13]. For more formula details see Appendix B.

2.3.3.1 Frictional pressure loss calculation inside the drillstring

Determination of Reynolds number and critical Reynolds number value for drillpipe:

Reynolds number:

$$N_{Re} = \frac{89100\rho v_p^{2-B}}{A} \left(\frac{0.416D_p}{3 + \frac{1}{B}} \right)^B \quad (38)$$

Critical Reynolds numbers value for laminar flow:

$$N_{Re\ Cr\ Lam} = 3470 - 1370B \quad (39)$$

Critical Reynolds numbers value for turbulent flow:

$$N_{Re\ Cr\ Turb} = 4270 - 1370B \quad (40)$$

Flow regime determination:

If $N_{Re} < N_{Re\ Cr\ Lam}$ the flow is laminar.

If $N_{Re} > N_{Re\ Cr\ Turb}$ the flow is turbulent.

If $N_{Re\ Cr\ Lam} < N_{Re} < N_{Re\ Cr\ Turb}$ the flow is transient and a interpolation has been introduced to ensure that all models are smooth and continuous. If not, this can cause problems for well flow models.

Frictional pressure loss calculation inside the drillpipe:

- Laminar flow:

$$\left(\frac{dp}{dl} \right) = 8.33 \cdot 10^{-4} \times 2^{2+B} \times A \left\{ \left(\frac{1+3B}{B} \right) \left[\frac{0.2v_p + \frac{C}{6}D_p}{D_p^{\left(\frac{1+B}{B}\right)}} \right] \right\}^B \quad (41)$$

- Turbulent flow:

$$\left(\frac{dp}{dl} \right) = \frac{f_p v_p^2 \rho}{25.81D_p} \quad (42)$$

2.3.3.2 Frictional pressure loss calculation inside the annulus

Determination of Reynolds number and critical Reynolds number value for annular flow:

Reynolds number:

$$N_{Re} = \frac{109000\rho v_a^{2-B}}{A} \left(\frac{0.0208(D_2 - D_1)}{2 + \frac{1}{B}} \right)^B \quad (43)$$

Critical Reynolds numbers value for laminar flow:

$$N_{Re\ Cr\ Lam} = 3470 - 1370B \quad (44)$$

Critical Reynolds numbers value for turbulent flow:

$$N_{Re\ Cr\ Turb} = 4270 - 1370B \quad (45)$$

Flow regime determination:

If $N_{Re} < N_{Re\ Cr\ Lam}$ the flow is laminar.

If $N_{Re} > N_{Re\ Cr\ Turb}$ the flow is turbulent.

If $N_{Re\ Cr\ Lam} < N_{Re} < N_{Re\ Cr\ Turb}$ the flow is transient and a interpolation has been introduced to ensure that all models are smooth and continuous. If not, this can cause problems for well flow models.

Frictional pressure loss calculation inside the annulus:

- Laminar flow:

$$\left(\frac{dp}{dL} \right) = 8.33 \cdot 10^{-4} \times 4^{1+B} \times A \left\{ \left(\frac{1 + 2B}{B} \right) \left[\frac{0.2v_a + \frac{C}{8}(D_2 - D_1)}{(D_2 - D_1)^{\left(\frac{1+B}{B}\right)}} \right] \right\}^B \quad (46)$$

- Annular flow:

$$\left(\frac{dp}{dL} \right) = \frac{f_p v_a^2 \rho}{25.81(D_2 - D_1)} \quad (47)$$

All flow models require continuous models. It is therefore very important to include a transient interpolation in all friction models to ensure that the flow models do not go unstable.

- Transient flow interpolation:

$$x_{int} = \frac{N_{Re} - N_{Re\ Cr\ Lam}}{N_{Re\ Cr\ Turb} - N_{Re\ Cr\ Lam}} \quad (48)$$

$$\left(\frac{dp}{dL} \right) = (1.0 - x_{int}) * \left(\frac{dp}{dL} \right)_{lam} + x_{int} \cdot \left(\frac{dp}{dL} \right)_{turb} \quad (49)$$

3. Drilling Parameters, Problem Detection and Remedial Action

Measurement and recording of hydraulic parameters and the quality of these are essential for our interpretation and understanding of wellbore conditions. Measurement gauges are constantly evolving, but the hydraulic parameters remain the same. This section discusses the various parameters we measure during a drilling operation and what they represent.

Recording of wellbore parameters includes measuring, reading and storing of data. On the Norwegian shelf it is a requirement that there should be two independent systems for measuring parameters. In practice, this can be used somewhat differently on the different installations. However, it should be interpreted and applied so that the entire supply chain should have two independent systems. A similarity can be drawn towards primary and secondary barrier when considering well barriers [21]. This means that there should be two sets of sensors, transmitters and measurement gauges to prevent unexpected errors, thus giving us an equivalent maximum coverage on a back-up system [22].

3.1 Drilling parameters

The parameters are recorded and used directly for carrying out the drilling operation. In order to process and analyze the necessary borehole parameters, we start by measuring the following quantities:

- Applied torque for make-/break-up of pipe connections [kNm]
- Tensile force - weight of drillstring/weight on drill bit [tons]
- Fluid balance for drilling fluid in/out of borehole [m³]
- Pump pressure from the mud pumps [bar]
- Applied torque on drillstring [kNm]
- Pipe tally [m] [pieces (joints) run]
- Mud weight and ECD [sg]
- Rate of penetration [m/h]
- Height of DDM [m]
- Flow rate [lpm]

In addition to these we also measure the temperature and gas content in the return drilling mud.

3.1.1 Applied torque for make-/break-up of pipe and pipe connection

The applied torque mentioned above, whether it is for rotation of the drill string or make-/break-up of pipe connections it is obtained by measuring the force applied directly to the drillstring. The way it is performed is that the torque on the tong is measured with a hydraulic transducer in the tong line. We are gauging the tension in the tong line and not the torque. It is therefore necessary to calibrate the measurement by multiplying the length of the tong arm times the tension in the tong line. It is important to note that the tong line must be perpendicular to the tong arm when the measurement is performed, a slight angle will reduce the actual value. However, a few degrees will not make an appreciable difference [22]. A correct measurement will lead to proper make-up torque; avoiding running loose (little torque applied) and pin breakage (to much torque applied). When drilling, torque is measured continuously, if applied torque is increasing this may be the result of pack-off/bridging.

3.1.2 Tensile force - weight on drill string/ weight on drill bit

To get a direct reading from the weight indicator on the weight of the drillstring, the tensile force in the drilling line must be calibrated for the number of times it has been cut and then again adjusted for any known weight of surface equipment such as e.g. travelling block and DDM. Any deviation from this measurement is correlated for by use of the neutral weight and provides again the weight on the drill bit as a secondary direct reading [22]. Note that when we not are drilling, the tensile force at the top of the drillstring will be equal to the buoyed weight of the entire drillstring. In deep wells, the tensile force may approach pipe tensile strain. For normal drilling operations, the optimum conditions are met when the bottom part of the heavy weight drillpipe (HWDP) is in compression and the drill bit carries the weight, the top part of the HWDP and the entire drillstring above are in tension and carried by the drawworks. A good weight indication sensor should give information on high over-pull when POOH, which may be the result of pack-off [14].

Today, most of the measurements are performed downhole using measurement while drilling (MWD). A sensor is mounted above the downhole motor (because the mud pulses used for data transmission in the drillstring cannot go through the motor). Vibration and noise from the drill bit makes it difficult to make precise measurements, this is due to the sensor and other electronics are subjected to large vibrational loads. Having equipment that is reasonably robust and reliable eliminates this. Another issue that has not been completed satisfactorily is the transmission of signals to surface. The transfer rate is too slow to get up all the information. Storing some information downhole and just sending up the information needed reduces this problem. To handle this, the sensor needs to be equipped with a mini computer, which is driven by mud flow through a small turbine [14]. However, new technology makes it possible to bring more and more information back to surface [23]

3.1.3 Volume control for drilling mud in/out of borehole

By using volume control for all active mud pits in the surface system and by measuring the return volume from the borehole, it is possible to record the fluid balance within the circulation system. The way this is being practiced is that there are placed level sensors in all active pits and in the mud return line. For good well control practices it is crucial to always be aware of changes in total fluid volume. Direct measurement of return flow is the first measurement that can provide indication of well control or circulation problems [22].

In addition to the pump rate, the volume control gives indications of a variety of conditions. A sudden and large reduction in the return flow of drilling mud indicates that the formation may be fractured, and that mud flows into the formation downhole (lost circulation).

Certainly, there will always be some net loss of drilling fluid because we are supposed to fill a borehole that is getting longer while drilling, but this is compensated for by the cuttings mass that is suspended in the return flow. If the amount of returned mud begins to increase exponentially, this may suggest inflow of liquid or gas downhole, and a kick may be under development [14].

3.1.4 Pump pressure

The drilling mud is pumped by one or several mud pumps, each of which can deliver about 2000 lpm at a pumping pressure of up to 386 bar (figures will obviously depend on the design of the system). It is worth noticing that a higher pressure increases the load on the equipment greatly, resulting in excessive wear and frequent interruptions. Pump pressure is measured from a sensor that is placed on the high-pressure manifold which the mud line runs through on the drill floor, and another one placed on the pressure side of the mud pumps. When performing these measurements, the theoretical pressure calculations should be adjusted for the placement of each sensor point. It is because we actually measure the pressure loss (friction) within the circulation system. The mud goes from the mud pumps through a fixed pipe (standpipe) on the drill floor, through a flexible high-pressure hose on top of the DDM connected to a rotary coupling attached directly to the uppermost drillpipe [14, 22]. Between the two above-mentioned measurement points there will be a noticeable difference because of:

- The sensor located at the pressure manifold on the drilling deck does not measure the pressure loss between the mud pump and the manifold; instead the sensor located on the mud pumps measures this.
- Between the mud pump and manifold on the drill floor there is a significant height difference. In the largest installations in the North Sea this height may be in excess of 30 meters and more. This means that the sensor measures hydrostatic pressure in addition to the pressure loss in the system.

3.1.5 Flow rate

The flow rate has a close connection to the pump pressure. The flow rate is directly measured on a mechanical gauge mounted on the outlet of the mud pumps. Before the signal is sent to the computer screen, it is converted to the desired output (in our case lpm). To do this conversion, we need an input for cylinder volume (stroke length and diameter). In real terms the mud pumps will have a lower efficiency than the theoretical calculated value. Normally, this efficiency will vary as a percentage between at 95-98% [22]. Flow rate is one of the factors in addition to rheology that affects hole cleaning. If proper hole cleaning of the wellbore is not achieved, several drilling problems may occur. Drilling problems such as lost circulation, stuck pipe, pack-off and more will be discussed later.

3.1.6 DDM height and ROP

Sometimes it is necessary to know the length of the drillpipe above the drill floor that you have to work with in case of an accident, or when it is time to do a new connection of drillpipe. This height can be measured mechanically, optically or with a pressure sensor, which may be directly readable. Together with the measured length of the drillstring there is also made calculations to reveal the depth of the wellbore, and provide the distance from the drill bit to bottom, during tripping in/out of hole [22]. When change in elevation per unit of time is recorded, it is common to convert the value to drilling speed (ROP) in meters per hour. Drilling speed is the rate that the drill bit moves through the formation, it is dependent on the formation type, but tend to vary between 2 to 30 meters/hour.

Other factors affecting drilling speed are drill bit type, rotary speed, weight on bit (WOB), well pressure (depth) and hydraulics (flow and pressure of drilling fluid). ROP management ensures good hole cleaning. If there is an indication of lower cuttings concentration compared to what we should anticipate, considered the chosen ROP, there might be development of cutting beds, and jamming of the string might occur [14, 22].

3.1.7 Mud weight and equivalent circulating density (ECD)

Drilling fluid density is often referred to as mud weight. By regulating the mud weight, we have the ability to manipulate and balance the borehole pressure, keeping us inside the drilling window. While drilling a well, the well pressure should be kept within two limiting values. The pressure must be greater than the formation pore pressure to prevent influx of formation fluids (kick), and at the same time, be lower than the formation fracture pressure to prevent fracturing formation (lost circulation). It is the interval between these two yielding values that creates the basis for the drilling window (Figure 1). This drilling window differs surely from well to well, dependent on depth and rock characteristics. Hematite and barite are used to increase the hydrostatic gradient in the wellbore, thus by regulating the mud weight. Eq. 52 gives the hydrostatic gradient.

$$P_{hydrostatic} [bar] = 0.0981 \cdot Depth_{TVD} [m] \cdot Mudweight [sg] \quad (50)$$

When working within the drilling window, it is not enough to simply keep track of the hydrostatic pressure. When drilling, drilling mud is circulated through the drillpipe, and cuttings are transported back to surface. This tells us that the mud weight can be divided into three different categories. The static mud weight as given in the Eq. 52, a differential pressure that is applied to the wellbore to get the fluid to flow, and cuttings that are suspended within drilling mud on its way to surface. The sum of all these three has been given the definition equivalent circulating density (ECD) and the expression is given in Eq. 1. To sum it up, the mud weight is divided into static mud weight and the frictional pressure loss in the annulus. The generated cuttings have an increasing effect on the ECD by increasing the static and the frictional contribution. If the ECD is higher than expected, one might expect that cuttings are packed around the bit. The annular space is blocked and the cuttings are creating additional friction. This condition could occur due to poor hole cleaning.

3.2 Typical equipment and wellbore problems

The data collected and the equipment that has been used to complete the job can be seen as a status report of the wellbore. Just as a motor or another form of electrical equipment is being monitored, whether it is increased temperature in a bearing, decreased oil pressure in a lubrication system, experience helps us predict how long the machinery can run without any critical problems. Experience can help us interpret the measured parameters and give us warnings on undesired events. For example, if the measurement of torque is flicking. These operational parameters can be compared with the hydraulic parameters used for drilling operations, and can show trends that can tell us what might go wrong.

When looking at different issues that arise in the wellbore and operational equipment, the different parameters we measure and record changes through time. They can change gradually over time or abruptly, if we for instance obtain a change in the drilled formation. This means that the hydraulic parameters change if there e.g. is an alteration in force, fluid flow or rotation. Trends in the measured parameters can be directly related to downhole problems. It is true that MWD equipment in the drillstring may fail by accident or that an internal leak may occur, but the majority of all downhole problems do not come without a warning.

Just look at the Macondo accident, here it was shown in hindsight that it was the combination of lack of understanding the trends and the failed equipment that caused the accident [1]. Indication of upcoming problems can therefore be detected by studying error in trends or change in the trends for one or more of the measured parameters. This section focuses upon wellbore failures and the related equipment respectively.

Nevertheless, we must note the importance of conditioning and maintenance of surface equipment, since successful drilling is dependent on continual preservation of the equipment on the drilling unit. For example, the failure of surface equipment may lead to incidents such as loss of pull force, drillstring rotation and pump capacity, which over a short period of time can lead to severe wellbore problems. Incidents such as stuck pipe, lost circulation and well control issues. These problems are usually the result of adverse trends over time [22].

3.2.1 Failure of surface equipment

In case of unexpected changes in the parameters that have no obvious explanation, it is recommended to first check the surface equipment. This is in fact a golden rule before pulling the drillstring out of the wellbore due to downhole problems. You should always eliminate the possible sources of error in the surface equipment. Obviously, each situation must be considered individually. One does not make an effort to check the surface equipment if there is an influx of hydrocarbons (kick) or if there is only a few seconds differing from free to stuck pipe [22]. Just to mention a few examples of common situations, and what to look for:

- Measurement of reduced surface volume: The reason for this can be as simple as transferring drilling mud between pits, without informing the right personnel. It could also be a sensor malfunction, or that there is a leakage out of the active system. In the worst case it could be a kick or lost circulation.
- It is common to check general sensor and/or instrument measurement if there is an unexpected change in parameter.
- If the pump pressure should decrease unexpectedly during drilling. This cause might be as simple as a valve leak in the pump system. The liquid portion of the pump must be checked (valves and pistons) or in worst case, it may be due to washouts and the string needs to be POOH.
- Loss of pressure during a pressure test or a leak test against formation (FIT or LOT): It is recommended to check all valves that are in contact with the cement pump system first. In worst case, the formation is not strong enough to handle the maximum acceptable differential pressure, and a leakage to the formation has occurred.
- A consequence of strong vibration/fluctuation of pump pressure is control of the pulsation bafflers on the mud pumps.

It is worth noticing the importance of having two independent systems for controlling hydraulic parameters (the rig's own system and mud loggers). If something happens unexpectedly there should be an inspection of pumps, lines, valves, sensors and all data should be checked against a secondary system [22].

3.2.2 Wellbore problems, detection and remedial action

Technical drilling issues can be related to everything from weakness in formation properties to drillstring failure, or a combination of both. This category includes wrong choice of equipment and equipment not suited for the specific job. For example, during operations in HPHT wells, the downhole equipment must be qualified and tested against the needed properties of such wells. High temperatures affect both mechanical and electronic equipment, and may in worst-case cause equipment failure. However, by establishing good routines, proper equipment may be selected. It is through experience we can study and better interpret the hydraulic parameters to keep us away from unnecessary problems. Experienced data is reflected in the following tables to come. These are examples of drilling problems that not only explain what to look for, but also various causes and suggestions for how these can be resolved. The following tables are based on [22] and are slightly modified.

The tool we have for determining wellbore problems is precisely the interpretation and comprehension of drilling parameters referred to in 3.1.1. The events given below addresses problems that can occur, some are simple, some are more complex and can have complex causes. There are dozens of variables and conditions in a drilling process shown in trends, so a 100% correct recipe on problem solving is almost impossible, but technological innovations can help us to move a step closer.

Event	Tearing-off drillstring.
Characteristics	Immediate loss of pull weight, torque and pump pressure.
Cause	Incorrect dimensioning of pipes and pipe connections. Cracking due to wear and overload. Incorrect make-up torque of pipe connections. Washouts not detected in time.
Action	POOH for possible fishing job.

Event	Washouts in drillstring.
Characteristics	Continuous loss of pump pressure. May have a sudden loss of pressure when a leakage occurs.
Cause	Cracking due to wear and overload. Incorrect dimensioning of pipes and pipe connections.
Action	Stop the mud pumps immediately. Eliminate the possibility of leaks in surface equipment. If doubt, pull out of hole. Pull out "wet" of the hole, observe continuously for leaks. Check the entire drill string. If there is a high resistance pulling the pipe, use no or minimal flow rate. Replace the component above / below the leak point.

Event	Wear of downhole motor and "stalling".
Characteristics	"Stalling" i.e. the rotor stops. Harder to get started with a control sequence. Several pieces of elastomer from the stator in the return flow.
Cause	The limit of the engine operating time is reached. In advanced long-range wells, downhole motors are often pushed to the limit of performance, so that the life expectancy might be somewhat reduced.
Action	Assess the need for steering, or whether one can continue in rotation mode. Assess risk of further rotary drilling with regard to being able to loose rotator in the well. POOH to replace downhole motor.

Event	Stalling.
Characteristics	Pump pressure increases rapidly. Tool face turns over. No ROP.
Cause	Wear of motor. Jammed stabilizer or drill bit. Formation change, drill bit hits new formation too aggressively.
Action	Quick response is required: - Shut down the mud pumps. - Pull off bottom. - Start up pumps. - Adjust tool face and resume steering.

Event	Drill bit related problems.
Characteristics	The new drill bit delivers poor or no ROP or too high torque has to be applied. Abrupt increase in pump pressure. Abrupt reduction/stop in ROP. Gradual reduction of ROP, trouble steering.
Cause	Wrong selection of drill bit. Plugged nozzle(s). Formation conditions (e.g. hard rock) Drill bit: The roller cone bit may have lost a cone, or junk in the hole may have torn off some of the cutters on the PDC drill bit. Wear of drill bit.
Action	Continue drilling ahead with same rate as long as the pressure is acceptable. Consider reducing pump rate. When drilling ahead, a sudden pressure drop may indicate that the plugs have been washed away. Consider the event, control eventual negative development in torque and pump pressure. If it is not formation related, POOH with drillstring for replacement of bit. Optimization of drilling parameters and steering intervals. May be combined wear of stabilizers and drill bit. Consider the total life of the drill bit, requirements of wellbore path, and the remaining length to TD.

Event	Failure of MWD-signals.
Characteristics	Poor/incomplete signals. “Noise” in signals. Total loss of signals.
Cause	The pressure drop in the drillstring is insufficient (too low). Failure of surface equipment. Failure of MWD tools, surface or downhole.
Action	Can control the pressure loss by calculating the total loss through MWD and the drillstring under the current pumping rate and mud conditions. If the calculation shows less than the requirement. Increase the pumping rate so that the required pressure drop is achieved (if possible). POOH with drill string to replace the drill bit nozzles or reset the sensors choke setting. Check pressure bafflers on the mud pumps. Check for leaks or loose parts in the mud line valves. MWD operator will check the receiver / computer. If failure downhole, POOH to replace MWD.

3.3 Stuck pipe

Stuck pipe events are costing the industry hundreds of millions of dollars each year. Stuck pipe incidents are unplanned events, which require the drilling contractors and operators to make quick decisions in order to minimize or ease the sticking condition. There are multiple conditions that can cause stuck pipe, one is not just stuck; there are a number of problems and combinations of problems that lead up to this problem. These problems include mechanical sticking, junk sticking, under gauge sticking, sloughing-hole sticking, lost-circulation sticking, differential sticking and blow out sticking. Thus there are some similarities between the events, each stuck pipe event has a distinctive set of conditions involving a combination of the well geometry, geology, conditions, depth and sticking mechanisms [22, 24].


It is important to perform correct planning and selection of the appropriate equipment to minimize stuck pipe incidents. When a stuck pipe situation occurs, one must act quickly and correctly in order to get free. It is important to identify the situation and the mechanism causing it. In almost all cases, there have been trends showing warning signs. The industry should focus on stuck pipe events in planning, covering both proper reaction and cleanup (fishing) [22].

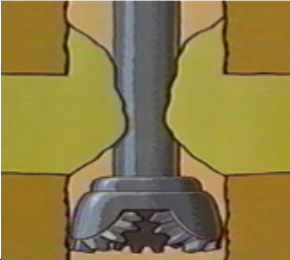
The mechanisms behind stuck pipe incidents is divided into three main groups:

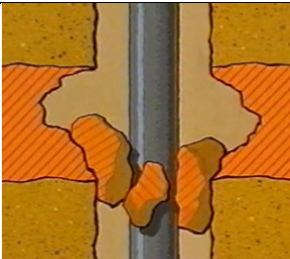
- 1) Pack-off/ Bridging.
 - Pack-off: Cuttings or caved in solids that wraps around the drillstring.
 - Bridging: Medium to large pieces of hard formation that jams the pipe.
- 2) Differential sticking.
- 3) Wellbore geometry.

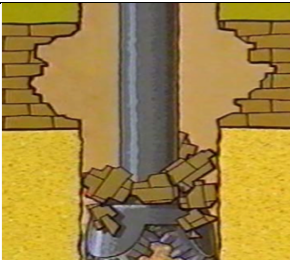
Behind each of these main mechanisms there are several causes that lead to stuck pipe. The tables below shows a systematic set of these causes. The tables takes basis in [22] and are slightly modified. The illustrations are taken from [25]. Take notice of how the hydraulic parameters can give indications of problems, and how they can be used to help, prevent and cure a stuck pipe situation.


3.3.1 Pack-off / Bridging

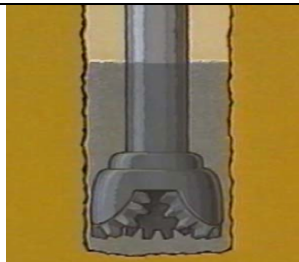
<p>Poor hole cleaning</p> <ul style="list-style-type: none"> – Cuttings do not stay in suspension, instead they drop to the bottom or at the low side of the pipe and causes pack-off. 	
<p>Avoid getting stuck:</p> <ul style="list-style-type: none"> • ROP management to ensure optimal hole cleaning. • Maintain correct mud specifications and annular velocities. • Monitor cuttings volume changes in shakers. • Recognize increased over-pull. • If allowed, always reciprocate and rotate pipe while circulating. • Use recommended viscous sweeps. • Consider back reaming and use regular wiper trips. 	<p>Free stuck pipe:</p> <ul style="list-style-type: none"> • Establish circulation and try to reciprocate. • Use viscous pills dependent on hole characteristics (depth, angle, size). • Try to rotate string in order to get the cuttings in suspension.

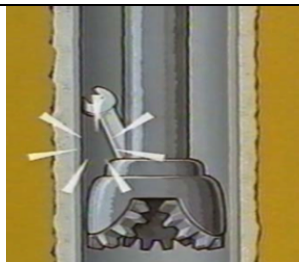
<p>Reactive formations</p> <ul style="list-style-type: none"> – Reactive shale is swelling up and creating clay balls and mud rings around the drillstring. 	
<p>Avoid getting stuck:</p> <ul style="list-style-type: none"> • Plan regular wiper trips, be prepared to stop and clean wellbore. • Avoid long periods without circulation in problem areas. • Watch out for potential surge and swab pressures. • Prepare for back reaming while tripping. • Recognize changes in mud properties. 	<p>Free stuck pipe:</p> <ul style="list-style-type: none"> • Establish circulation. • Concentrate on working drillstring downwards. • Gradually apply freeing force. • Once circulation is established, increasing MW might be beneficial.

<p>Unconsolidated formation</p> <ul style="list-style-type: none"> – Poorly consolidated formations fall out of the borehole and results in pack-off or bridging. 	
<p>Avoid getting stuck:</p> <ul style="list-style-type: none"> • Prepare to ream during a stand. • Control ROP. • Use solids removal equipment. • Prepare to use shaker screen blinding. • Clean out of hole before drilling ahead. • Avoid excessive periods of circulation in these formations. • Wipe each connection and avoid excessive swab and surge pressures. • Prepare for loose fill when RIH. 	<p>Free stuck pipe:</p> <ul style="list-style-type: none"> • Establish circulation. • Disturb bridge by working string downwards. • Increase force gradually, and ensure that the cavings are removed before further drilling.

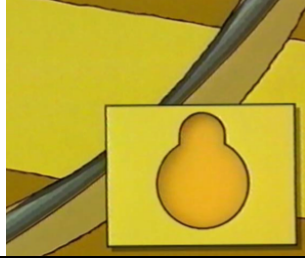
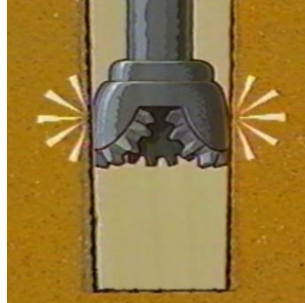
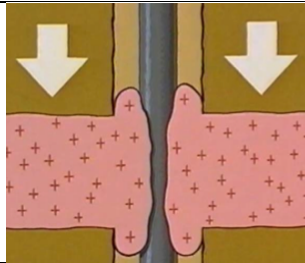
<p>Fractured formations</p> <ul style="list-style-type: none"> – Fractured formations fall into the wellbore and causes pack-off or bridging. 	
<p>Avoid getting stuck:</p> <ul style="list-style-type: none"> • Clean-out excess fill before drilling ahead. • Hole conditioning and preparation for LCM. • Minimize surge pressure and restrict tripping speed. • RIH with JAR on BHA. • Prepare to wash and ream when tripping in. 	<p>Free stuck pipe:</p> <ul style="list-style-type: none"> • Reciprocate to disturb bridge. • If annulus is not packed off, apply large forces in the beginning of procedures for getting free.

<p>Cementing</p> <ul style="list-style-type: none"> - Cement blocks fall out the borehole and results in bridging. 	
<p>Avoid getting stuck:</p> <ul style="list-style-type: none"> • Minimize rat hole below casing shoe. • When drilling out the rat hole and cement, always ream section carefully before drilling further. • Always be aware when tripping through casing shoe and past cement plugs. 	<p>Free stuck pipe:</p> <ul style="list-style-type: none"> • Work drillstring up and down to break down the cement blocks. • Acid may be used to break down the cement. • Gradually start to increase freeing forces.

<p>Cementing</p> <ul style="list-style-type: none"> - Wet cement results in pack-off 	
<p>Avoid getting stuck:</p> <ul style="list-style-type: none"> • Treat the mud if green cement is suspected. • Know theoretical TOC and start circulation above. • Control the returns of cement at shakers. • Do not rely on weight indicator • Restrict ROP when cleaning out cement. 	<p>Free stuck pipe:</p> <ul style="list-style-type: none"> • Immediately apply maximum force while working string upwards and start to jar. • Attempt to start circulation

<p>Junk</p> <ul style="list-style-type: none"> - Junk from BHA or surface results in bridging. 	
<p>Avoid getting stuck:</p> <ul style="list-style-type: none"> • Use maintained equipment in good condition. • Inspect equipment (MWD and BHA) regularly. • Be careful when working around rotary table. • Cover the hole, use fishnets. • Install wiper on drillpipe when possible. 	<p>Free stuck pipe:</p> <ul style="list-style-type: none"> • Work and jar drill string up and down. • Gradually increase freeing forces.

3.3.2 Wellbore geometry

<p>Key seating</p> <p>– Key seating: Short section with high dogleg (high angle change) where the drillstring is worn around the track in the borehole wall. The hole diameter gets the profile as a keyhole, the diameter of the track is too small for the BHA.</p>	
<p>Avoid getting stuck:</p> <ul style="list-style-type: none"> • Minimize rotation of pipe. • Minimize dogleg severity. • Consider design and configuration of BHA. • Minimize the rat hole length below casing. • Consider string reamer or installing a wiper. • Attempt to cure before further drilling. 	<p>Free stuck pipe:</p> <ul style="list-style-type: none"> • Reciprocate drill string while jarring or by rotating. • When free, gradually work pipe upwards. • Avoid jamming pipe in key seat. • Rotate pipe with minimum tension through key seat. • May use back reaming. • Minimize the risk of wall sticking.
<p>Under gauge</p> <p>– Reduction in hole diameter and ovality in the borehole cross-sectional area. Abrasive formation wears down the diameter of the drill bit. Core drilling can stipulate a hole diameter slightly less than the nominal diameter. A BHA equipped with motor creates an oval hole diameter, while a BHA used for rotation does not do this. In all cases the BHA and drill bit may be stuck.</p>	
<p>Avoid getting stuck:</p> <ul style="list-style-type: none"> • Always use gauge bit and stabilizers. • Ream to bottom if a problem is suspected. • Never force bit to bottom. • Proper bit selection. • Be careful running PDC after tricone bits. 	<p>Free stuck pipe:</p> <ul style="list-style-type: none"> • Jar bit upwards using maximum force. • Work drillstring upwards.
<p>Mobile formation</p> <p>– Overburden or tectonic stresses creates movement in plastic clay or salt formations so that some parts of the hole are smaller in diameter than the nominal diameter.</p>	
<p>Avoid getting stuck:</p> <ul style="list-style-type: none"> • Regular wiper trips. • Condition mud prior to penetrating salt. • Consider eccentric PDC bits. • Increase mud weight. • Minimize open hole time. • Importance of minimizing reaction time. 	<p>Free stuck pipe:</p> <ul style="list-style-type: none"> • Establish circulation; concentrate working string downwards, with gradually increasing force. • If squeezing salt, pump freshwater pill while working pipe, do not delay pumping water pill. • OBM systems: Use water input spacer ahead of pill. • Use maximum pull on pipe while circulating pill. Increase mud weight afterwards.

3.3.3 Differential sticking

The combination of a static drillstring in contact with a permeable formation and the development of filter cake provide a pressure differential that holds the string firmly against the borehole wall. High overbalance enhances this effect. In practice differential sticking usually occurs when the pipe is stationary during a connection or when taking survey. First indication of sticking is when there is full circulation through the pipe and no up/down mobility or rotary abilities, other than pipe torque and stretch. When solids in the mud no longer are suspended, they settle out, increasing the sticking force. The sticking force may be calculated by using the definition of differential pressure and the drill collar contact area [22].

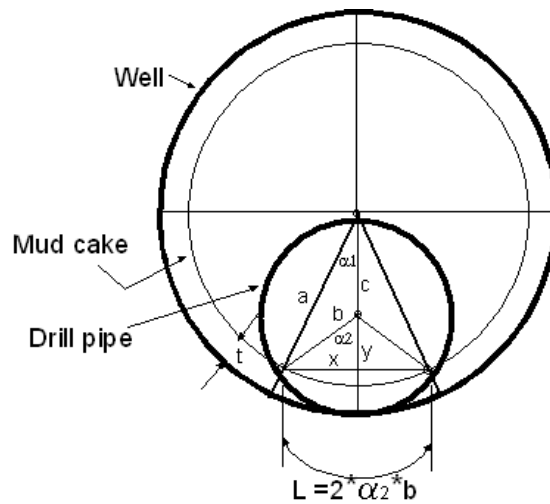


Figure 7 - Illustration of drill collar without centralizer sticking in a well [26].

Eq. 51 calculates the sticking force:

$$F = \mu \cdot \Delta P \cdot A \quad (51)$$

where ΔP is the difference between the outside mud pressure and the pore pressure inside the rock. By the absence of centralizers in the calculation, assuming it is only drill collars that is in contact with the mud cake, the contact length can be determined and the sticking force calculated by Eq. 52 [26]:

$$F = \mu \cdot \Delta P \cdot 2R_p \cos^{-1} \left(\frac{(R_w - t)^2 - R_p^2 - (R_w - R_p)^2}{2R_p(R_w - R_p)} \right) \cdot L_{DC} \quad (52)$$

where R_w is well radius, R_p is b shown in Figure 7, t is the mud cake thickness and L_{DC} is length of drill collar. The formula for a deviated well is shown in Eq. 53 [27]. The force needed to pull the drillstring is expressed as the sum of the pipe weight, the drag force and the differential sticking force.

$$F = \beta wh(\cos\alpha + \mu\sin\alpha) + \mu \cdot \Delta P \cdot A \quad (53)$$

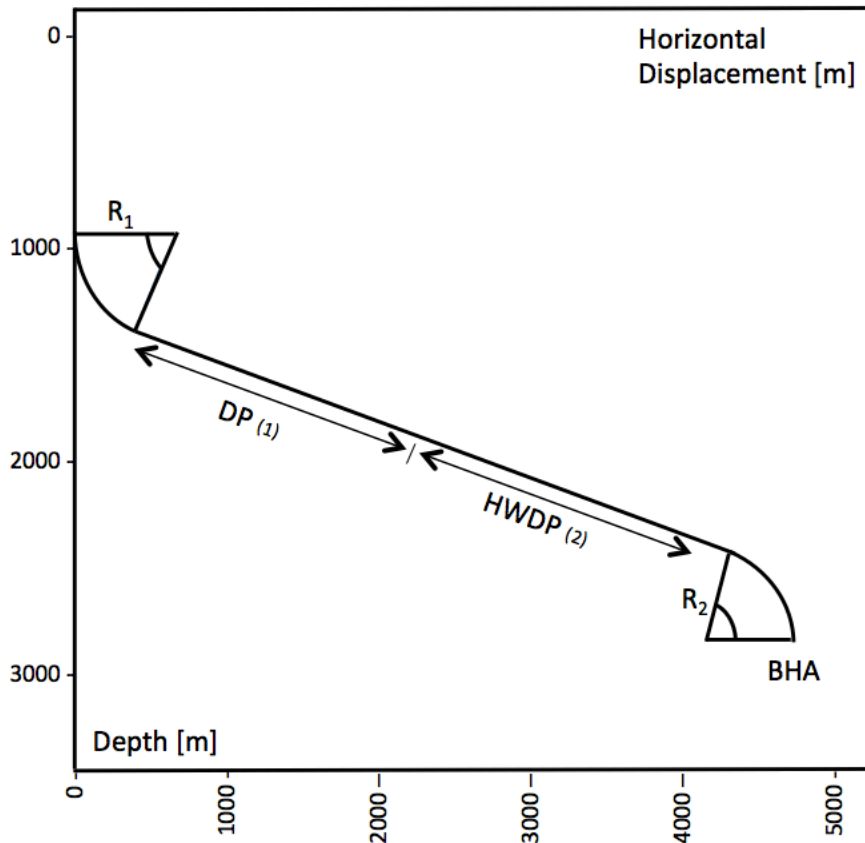


Figure 8 - Well path for stuck point derivations.

Sometimes it is not possible to work the pipe free. In the worst-case scenario it is therefore necessary to determine the stuck point for eventual cutting of pipe or drill collar. Models can determine the point of stuck. For stuck point determination, a tensile test needs to be performed to measure an additional force F and the corresponding elongation, ΔL . Aadnøy et al [27] derived a model for a well geometry shown in Figure 8. For a complex geometry one can develop a model based on torque and drag and for any loadings.

Aadnøy et al [27] derived a model based on the following assumptions:

- Negligible BHA (much stiffer than drillpipe).
- Only one size of drillpipe.
- No friction applied (force is acting directly on the stuck point).

If drag is included, some of the pulling force will transform to friction. However when pulling, the pull-rate is usually slow and nearly static, so we can easily assume that the drag forces in a vertical well are neglected. A golden rule is that pull force is assumed unaffected of friction for vertical wells. It is therefore reasonable to say that for straight section in deviated wells, friction is assumed neglected or dealt with by measuring the drag forces before the drillstring got stuck. Conversely, for curved section the friction is taken into account. Similarly to Figure 8 assume now that our well consists only of a vertical section, build section and sail section down to TD. The build section with a radius, R builds up to an angle, α . Then the sail section is drilled holding this angle down to the stuck point. Assume now that drag is neglected, and the pipe is pulled slowly with a force dF and a length dl .

The depth estimation down to the stuck point is given by Eq. 54 [27]:

$$l = AEe^{\mu\alpha} \frac{dl}{dF} - (e^{\mu\alpha} - 1) \left(l_1 + \frac{1}{2} R\alpha \right) \quad (54)$$

Eq. 54 is only valid for a constant drillpipe size, and for a well consisting of the three following sections; vertical, build-up and sail. Surely it is possible to assume two drillpipe sizes, referring to indexes, top pipe size is index 1 and bottom pipe size is index 2. Eq. 55 applies for the depth to stuck point if two different drillpipe sizes are used [27]. For example using drillpipe in combination with HWDP.

$$l = A_2 E e^{\mu\alpha} \frac{dl}{dF} - \frac{A_2}{A_1} (e^{\mu\alpha} - 1) \left(l_1 + \frac{1}{2} R\alpha \right) - l_2 \left(\frac{A_2}{A_1} - 1 \right) \quad (55)$$

When the situation is at point, quick and proper evaluation of hydraulic drilling parameters and reaction may be essential to prevent an eventual catastrophe. Nevertheless, either if you are lucky enough to get the pipe free or a preferable sidetrack is initiated, there are a few good practices to follow in order to bring the situation back to normal drilling. They are as follow; proper hole cleaning and removal of cuttings, activation of the jar, POOH and replace components of the BHA that may have been damaged due to large impact forces.

3.4 Lost circulation

Lost circulation is another problem that also lead to increased NPT. An illustration of a lost circulation scenario is shown in Figure 9. During a drilling operation there will be a continuous change in the mud system. This is because the system is continuously given additives such as basic fluids, solids, and chemicals to compensate for the gradually increasing hole volume. A certain amount of liquid may be bound to the cuttings or lost to permeable zones within the wellbore. This is a mass balance equation that we easily can keep track of. Lost circulation is therefore a measurable loss of the total drilling fluid to the formations.

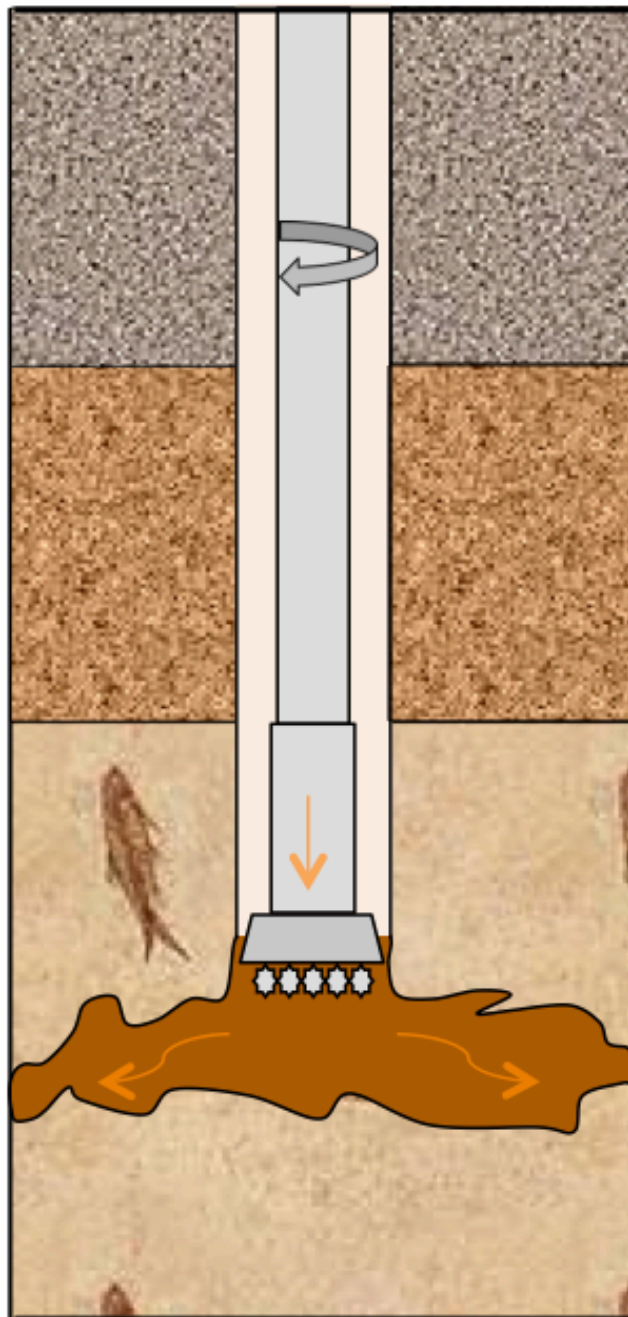


Figure 9 - Illustration showing total loss of circulation.

Table 5 shows that the severity of the downhole problem can be divided and graded according to the amount of lost mud [22]:

Grade:	Type:	Description:
1	Seepage loss	Continuous loss of up to $3m^3$ per hour under normal drilling conditions. This is an indication that we are on the threshold of what the exposed formations can withstand.
2	Partial loss	Continuous loss of more than $3m^3$ per hour under normal drilling conditions, but we do still have returns from the wellbore annulus. This indicates that there are conditions in the wellbore which means that we are in excess of the tolerance limit of the formations.
3	Total loss	The tolerance limit of the formation is clearly exceeded. We have no return flow from the annulus. Lost circulation may also cause the mud level in the annulus to decrease (tens of meters is not uncommon).

Table 5 - Severity of lost circulation [22].

As seen in Table 5 there is a development scale, and it is then often the case that the first two conditions (1st and 2nd) may be a warning of the 3rd (total loss circulation). The problems that can result in lost circulation can be divided into two main categories; Natural and Induced. Induced lost circulation occurs when the pressure exerted to the wellbore exceeds the maximum pressure the wellbore can resist (fracture pressure). Natural lost circulation occurs when the drill bit is penetrating formations with large pores, high permeability, leaky faults and natural fractures. Also here the formation is exposed to a fluid pressure in the wellbore, which exceeds the tolerance limit of loss [22, 28].

Pressure induced fractures may be the result of different causes. For example, the mud weight may simply be too high for the exposed formations, or alternatively the ECD too high. As mentioned earlier, ECD is a sum of the mud weight plus the friction in the annulus and the cuttings suspended in the mud. It is important that we understand that the greatest ECD is at the drill bit. It is the friction in the annulus that makes the contribution to the ECD measurement. Most of the total friction force in the drilling mud within the annulus is between the BHA and the wellbore. Here, the distance between the annulus and the pipe is at its smallest, ergo higher fluid velocity and higher friction. For a particular point in the well, the fluid pressure in the borehole reaches its maximum as the drill bit passes, it will diminish as the components with large diameter is passing [22].

Pressure waves transferred within the drilling fluid may also lead to total or partial lost circulation. For example, the pressure in the wellbore that builds up during pack-off of cuttings or cavings from the borehole wall may exceed the fracture pressure in the underlying formation causing lost circulation. Similarly, a shut in pressure could fracture weaker zones. Drilling through formations with low formation pressure may cause circulation losses. As we drill, the formation pressure and the fracture pressure will follow each other, so that when the drill bit intrudes a low-pressure zone, it will have a lower fracture gradient than the overlying zone. If we have been drilling with a drilling fluid that provides a borehole pressure greater than the fracture pressure of the low-pressure zone, the formation would fracture [22].

Similarly, naturally fractured and high permeability formations also have the same basic mechanism, that the wellbore pressure is higher than the strength of the weaker zone. Natural fracturing in a formation will have an additional weakness because the initial fracture is already there; the question is whether or not the pressure will exceed the fracture opening pressure. Likewise a fault that has not been sealed will also act as a trap for circulation losses. High permeable zones are often poorly consolidated, for instance sand zones where the cementations between the sand grains are weak. Drilling with high mud weight to control unstable clay further up will often lead to drilling into the sand zone with too high mud weight. Some formations may have cavities. Drilling through these cavities with an excess pressure of the mud relative to the formation fluid pressure can result in total or partial lost circulation. Prevention of circulation loss should be included in the planning processes and in the operational procedures that focuses on minimizing the risk for failures. By giving the proper concern, one also focuses on minimizing the risk of stuck pipe, because lost circulation often have a high risk of escalating into a stuck pipe situation [22].

For an optimized and efficient drilling operation, it is important to consider the following issues during the design phases: [22]:

- Design the casing so that it isolates the low-pressure zones and estimated loss zones as soon as possible after penetration.
- Good hole cleaning is essential. The more cuttings, the higher ECD.
- Plan for a minimum mud weight to control the known formation pressure. The weight must be balanced against the desire for high mud weight to keep the other formations from caving in.
- Drilling mud must have a certain rheology to purge the borehole properly.
- Excessively viscous mud increases friction and also provides higher ECD.
- Pre-treat the drilling mud with loss circulation material (LCM) before penetrating the known loss zone. Additives may be helpful to keep a zone with little or partial loss under control.
- Avoid pressure waves, plan for quiet tripping into / out of the borehole, "soft" start and stop all movements before making connections. Break up the mud gel strength when circulation starts by initiating rotation first. Start the mud pumps gently and increase incrementally with full return before the next increase.
- If possible, eliminate annulus restrictions; unstable formations should be back-reamed at fixed intervals.
- Control the ROP to keep down the amount of cuttings in the annulus.
- Assemble a BHA that is able to manage LCM in the drilling mud, especially in terms of MWD/LWD equipment.
- Have clear procedures for how the rig crew deals with LCM on the surface. It can be associated a high risk, having to stop circulation completely for a period time, due to plugging of surface equipment.

4. Examples of other Software Tools

Calibrated models for optimizing oil and gas production has been around for some time now, and usage of process models to control drilling processes is getting more and more common. A few examples of integrated drilling control systems are presented in this chapter [29].

4.1 Sekal DrillScene

The advanced monitoring system DrillScene is based on 20 years of modeling research and development in Stavanger at the International Research Institute of Stavanger (IRIS). The software system is based upon a continuous comparison of transient flow model predictions against real-time measurements at the rig site. The model can be used for giving warnings about possible unwanted events that is developing in the well and may in that context be a proactive tool [29].

4.1.1.1 Drilling Simulation Environment for Testing Drilling Automation Techniques

The purpose of the DrillScene wellbore simulator is to generate response from a “real” well, submitted to the drilling actions simulated in a virtual rig. Simulation of realistic well incident responses is therefore integrated into the wellbore simulator. Such incidents include for example influx, losses, pack-off, formation collapse and various stuck pipe situations. The advantage of such a simulator is the possibility to play through the simulation in fast-forward mode, pause or use multiverse-like capabilities. Figure 10 illustrates drilling through an unexpected depleted region causing fracture and loss [30, 31].

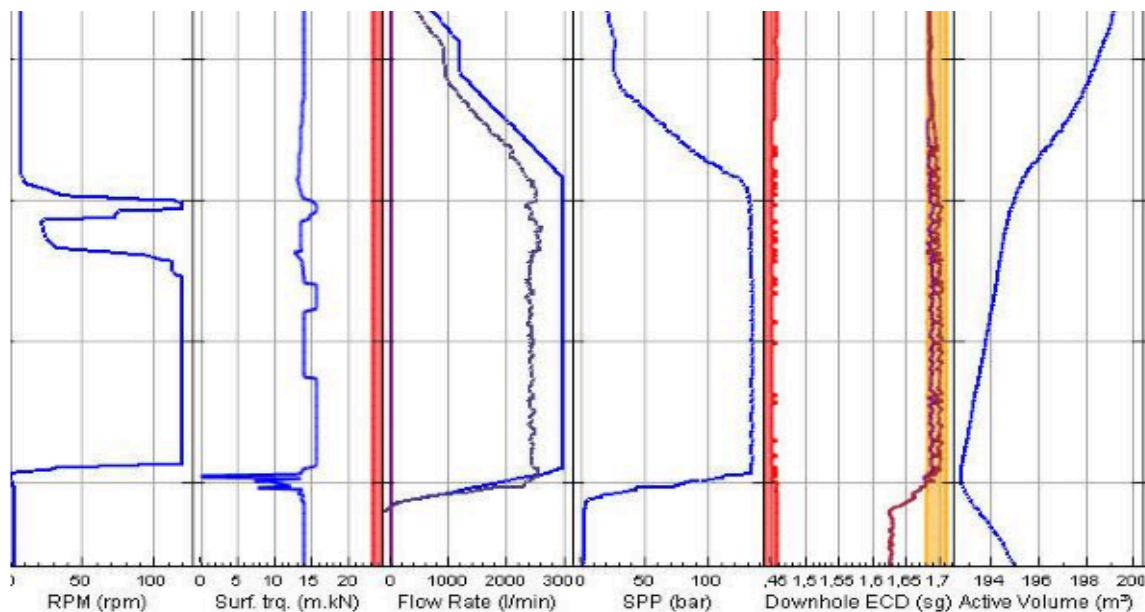


Figure 10 - DrillScene: Drilling through a depleted region. Time frame is 2 minutes [31].

One of the drilling methods used for simulations are MPD. The MPD solution is based on back-pressure, which means that a back-pressure pump is used at surface to control the well pressure. Figure 11 shows how the annulus needs to be sealed to be able to apply pressure at the surface. This makes it possible to continuously control the downhole pressure by changing the surface back-pressure. The back-pressure in the system is generated by a choke that

creates a pressure drop when drilling fluids are circulated through it. However, if there is zero or too low circulation through the well, an additional pump is used to create the required pressure drop by circulating the drilling fluid directly through the choke [30].

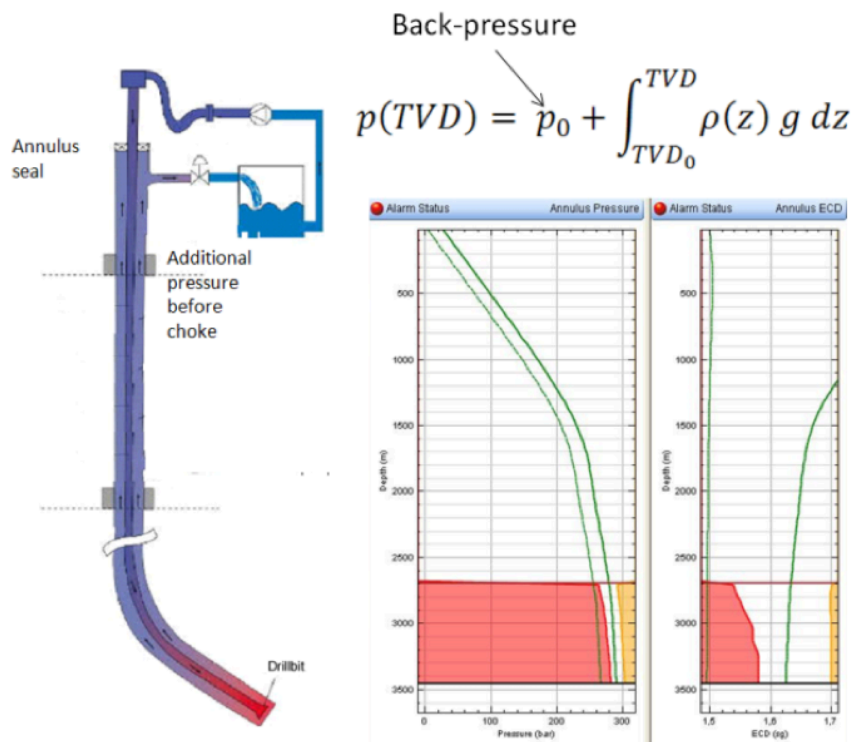


Figure 11 - DrillScene: MPD solution based on back-pressure [30].

4.2 eDrilling Solutions

eDrilling has a company mission that contributes to increased value creation, safety and profitability for its customers through solutions for planning, training, optimization and control of drilling operations. eDrilling has been around for a few years now and is an innovative system for real-time drilling simulation, 3D visualization and control from a remote drilling expert center. The concept processes all available real-time drilling data (both surface and downhole) in combination with real-time modeling to monitor and optimize the drilling processes most effectively. By implementing this information into the model it is possible to visualize the wellbore in 3D real-time. eDrilling has been implemented in an Onshore Drilling Center on the Ekofisk field in Norway. The system has for instance given very early warnings on ECD and friction related problems [32].

4.2.1.1 Supervision of ECD with automatic diagnosis embedded

During drilling, the eDrilling system will continuously be monitoring the ECD and compare it with calculations executed by an advanced dynamic pressure and temperature model. The model will continuously be calibrated where it is considered sufficiently reliable for that purpose. Figure 12 and Figure 13 shows an illustration of the flow model calculations using input from real drilling data. The simulations are based on washing/reaming (12-14 hours), drilling 18 meters (14-16.8 hours), back reaming, and tripping out (last half hour). At this stage, data was recorded while replaying data after operations had finished. If accurate pore and fracture pressures were available, the calculated ECD, both at the bottom and at other positions along the OH section, would have been compared continuously to the given pressure profiles. If getting close to or exceeding boundaries a visual notification would have been triggered in the 3D view [32].

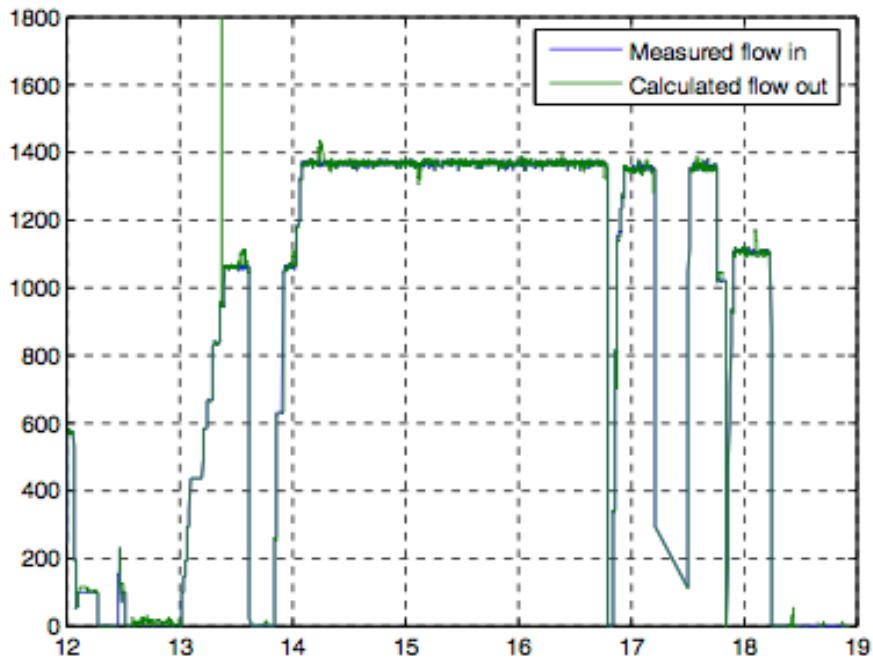


Figure 12 - eDrilling: Pump rate [32].

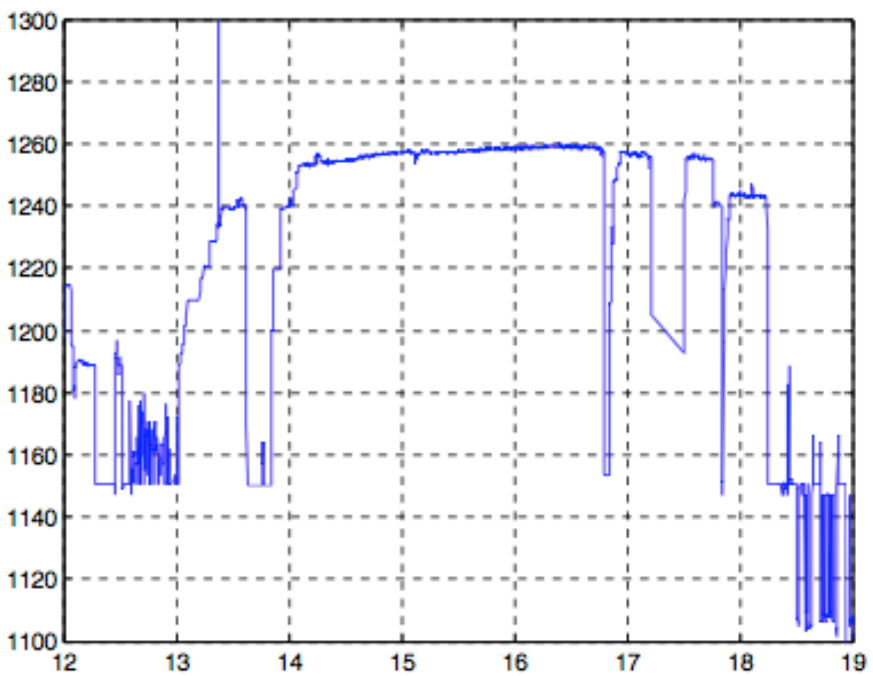


Figure 13 - eDrilling: Calculated bottomhole ECD [32].

4.3 DrillBench

DrillBench is a software tool for design and evaluation of all drilling operations. It is designed significantly for wells with narrow margins (i.e. narrow drilling window). DrillBench considers both transient and steady state conditions, and enables engineers to model wells with diverse and extreme complexities that has been verified extensively against actual data. The model can be used to model all types of wells and scenarios (HPHT, deep-water, ERD and MPD). The interface is user friendly and designed for both drilling engineers and drillers. Schlumberger is now the current owner of DrillBench [33].

4.3.1.1 Dynamic Modeling in drilling of the Gullfaks C-5A Well

During drilling of new wells in the Gullfaks field, Statoil in the early 2000 observed an increased trend in amount of drilling problems in the Shetland formation. Underbalanced drilling was initially considered as a remedial action to this problem (drilling with a hydrostatic pressure that is lower than the formation pressure). In general, this helps to increase productivity by reducing formation damage in the reservoir section and solves problems such as low ROP, kick/losses due to pressure depletion. At Gullfaks there was a problem related to small margins and it was difficult to drill conventionally. In the planning phase, the operational window was defined by means of steady state modeling. To ensure that the bottomhole pressure could be controlled, various combinations of influx rates and choke pressures were simulated. It was also important to ensure proper hole cleaning during the operations. By modeling the 7" liner, they were able to quantify the surge/swab pressures that again created the basis for the 7" liner running procedure. In order to evaluate the dynamics of the system, a number of scenarios were developed by introducing transient simulations (for instance if drilling through a high productivity fracture). This would assist the rig team in detecting drilling problems and making correct choke adjustment to maintain bottomhole pressure [34].

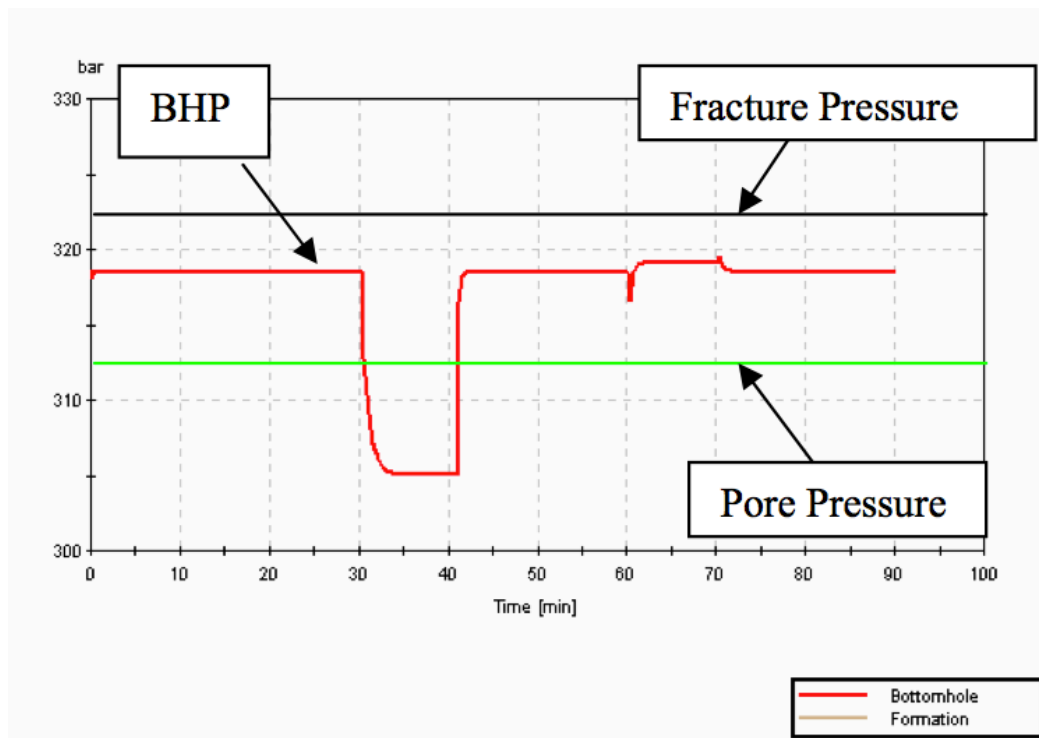


Figure 14 - DrillBench: Kick during connection [34].

Gullfaks is a mature field entering the final production stage. The Shetland formation, which makes up the cap rock of the Gullfaks field, has by high-pressure water injection been pressured up to reservoir pressure. This has re-activated old faults along the annulus of poorly cemented water injector wells. By increasing the pressure, which is below the cap rock, the Shetland formation has become extremely difficult to drill using normal overbalanced drilling techniques. It was when performing a re-entry job in well C-5A in 2002 that the well took a high-pressure kick, resulting in production shutdown.

It was assumed that the high-pressure water injection was the cause. From the kick data the pore pressure and fracture gradient was calculated to be 1.84 sg and 1.90 sg, respectively. This makes it an almost impossible drilling window to drill in a conventional manner since the difference between the ECD and the static mud weight can be larger than the margin, and it will be impossible to avoid kick or losses. An underbalanced method was therefore considered. Figure 14 shows that a kick will be taken if the well is drilled in overbalanced condition when performing a connection, which again can lead to fracturing of the formation. Figure 14 is not considering the pressure build-up during conventional well control. Dynamic modeling was successfully used for the planning and preparation phase for Gullfaks C-5A, which was the first underbalanced well drilled offshore in Norway by Statoil. It was by the use of dynamic modeling that it was possible to identify potential transient events and create remedial actions. The transient modeling results were also used as support material in training of rig crews, increasing the general understanding of flow dynamics during both overbalanced and underbalanced drilling [34].

5. Architecture of Discovery Web

SiteCom is Kongsberg Oil & Gas Technologies solution to enable real-time monitoring and analysis of all data from well operations. A typical system setup topology is presented in Figure 15 below. The SiteCom Suite delivers in addition to real-time monitoring, historical data storage for post-well analyses and training. At the well site it also provides an aggregator for data gathering from all the different service companies [35].

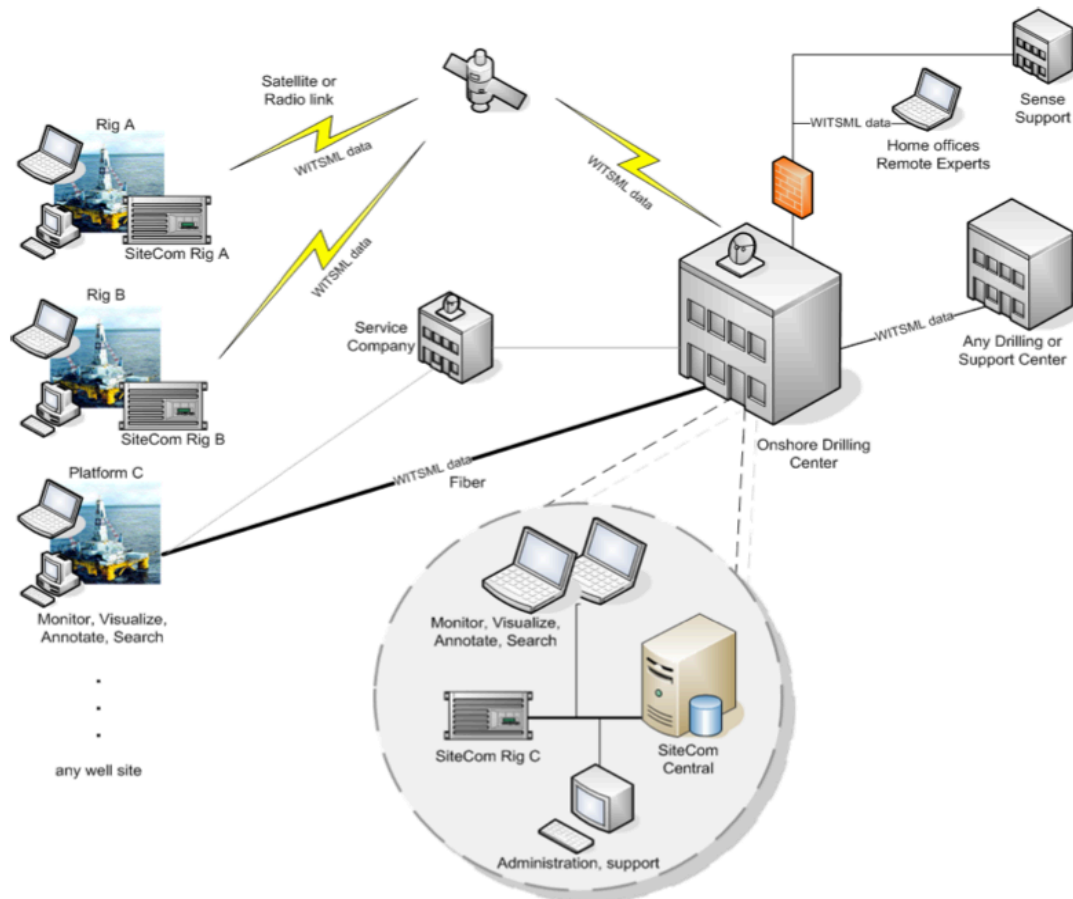


Figure 15 - SiteCom setup [35].

By using an aggregated system for collecting data from all service companies, operators are able to gather real-time data from multiple data sources. Data is taken from the rig systems in many different formats (OPC, WITS0, NMEA, WITSML) and then aggregated into the onshore drilling databases. By using a single link to shore (that replaces systems from mud logger, LWD & drilling systems) it is possible to use a standard application for analyzing and processing of data. This enables secure and flexible data, and standardized processes and workflows. Nevertheless, this helps us to create corporate standards independent of contractor that gives the client end-user quality data using only one interface (Discovery Web). This is because all data is transmitted, hosted and managed completely within the client domain, and the data management is independent of rig site service provider. Figure 16 illustrates how SiteCom aggregates all data sources at all rigs and transfers the data back to the central database (<WITSML/>), which the client end-user can connect to from his interface at home or at the office via a web browser and the Discovery Web application [35].

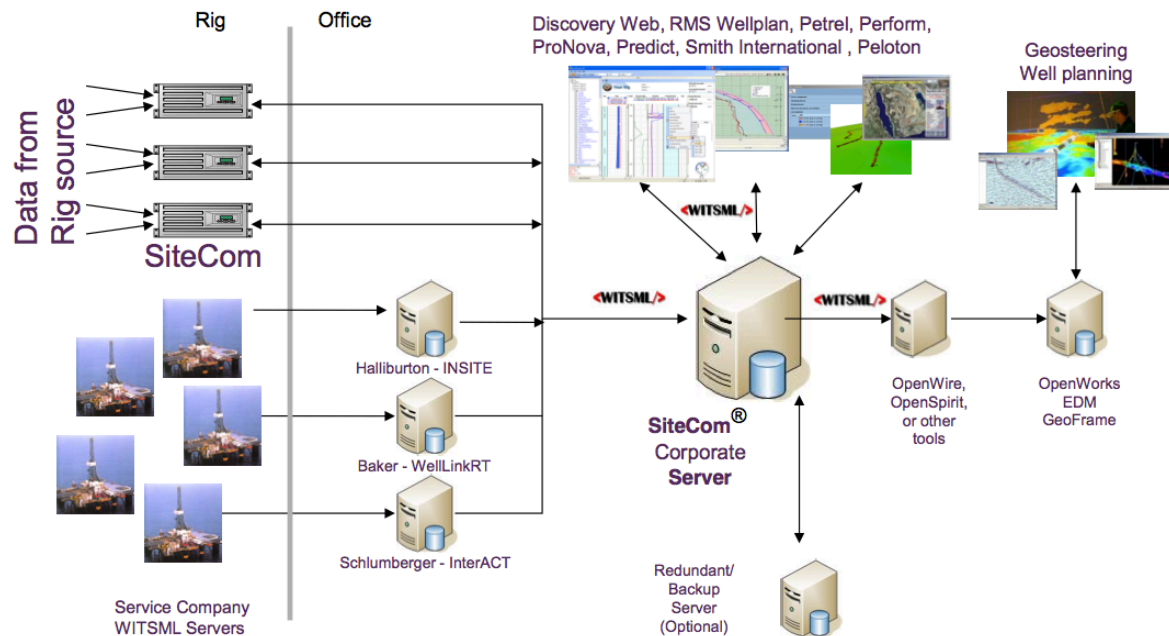


Figure 16 - Workflows of SiteCom [35].

The client-end user uses Discovery Web that has a standard flexible interface hosted in Internet Explorer that allows consoles to be easily configured to monitor all key drilling and evaluation (D&E) processes to maximize efficiency and minimize NPT. To help improve the D&E processes, Discovery Web is implemented with the following instruments [35]:

- Real-time drilling dashboard.
- Access to all rigs and wells with just a single click.
- Pumps 'n' Pits (Information about pits and pumps, flow in/out, PVT gain/loss and basic kick detection).
- Drilling calculations (Drilling parameter cross-plots and drilling diagnostics).
- Very rich feature set (i.e. Chat, Print, Export, Widgets, Formulas, Maps).

A basic drilling console illustration from Discovery Web is shown in Figure 17. As mentioned the application can be accessed and viewed from anywhere. Custom templates can be easily designed and distributed with the following benefits [36]:

- Enable a full overview over well site status.
- Improve client access to real-time data.
- Improve collaboration between teams and across disciplines.
- Easily distribute information.
- Reduce overall costs.
- Reduce the need for training.
- Helps to overcome contractual and geographical hurdles.

The combination of time-indexed, depth-indexed, real-time and historical data makes it a powerful tool in data gathering and processing. Data is displayed in widgets and can be viewed as bar graphs, log graphs, cross plots, image plots, lithology plots and circular gauges. Sources for data is everything from MWD, LWD, mud, cement, mud logging to weather and positioning [36].

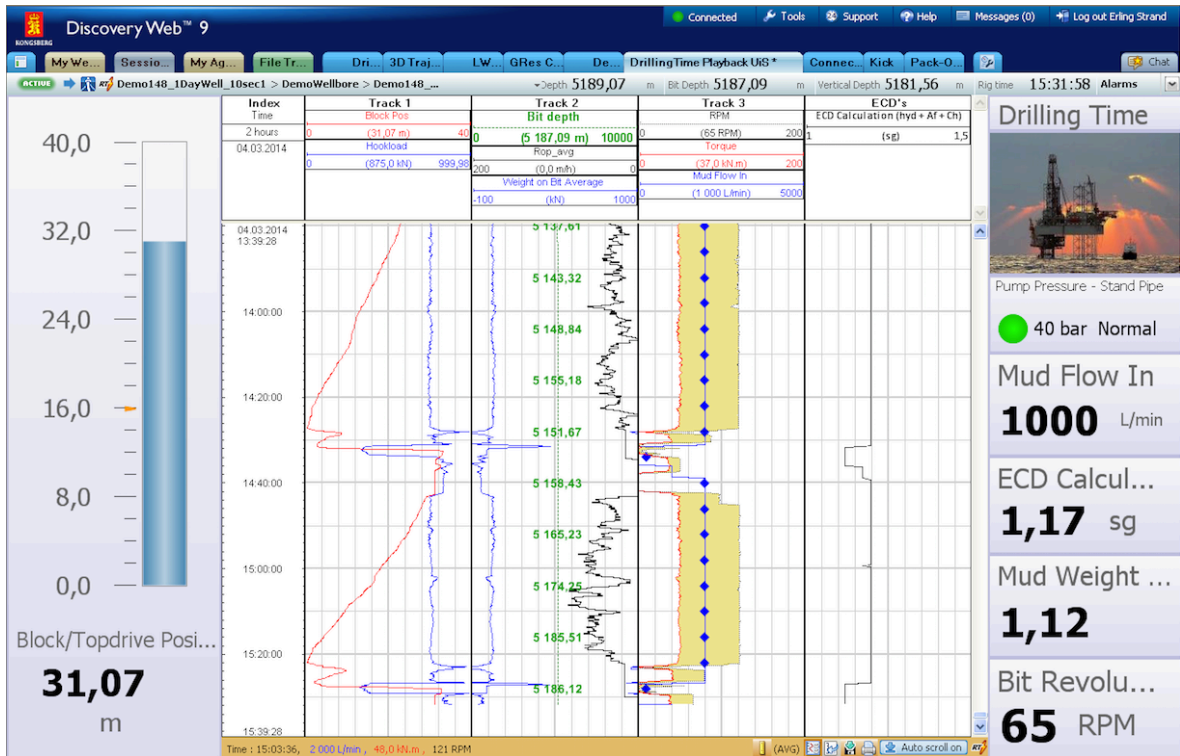


Figure 17 - Basic drilling console - DrillingTime Playback UiS [37].

In addition to real-time monitoring, the feature Discovery Web Formulas gives you the ability to create formulas (Figure 19). This makes it possible to include models that can be compared with real data. A formula consists of static parameters (static values), inputs (mnemonics) and outputs (formulas). Outputs from a formula can be visualized and used in the most common widgets (visualization elements) similar to log data, including log widgets, history table widgets and most single-value widgets. This is why outputs can utilize inputs and static parameters within the equation using predefined mathematical functions. Syntax for output formulas is taken from Microsoft Excel, where the supported Microsoft Excel functions are provided for. Figure 18 shows the calculation model used for Discovery Web Formulas and the Arithmetic Smart Agent. A graphical representation of an output equation is also provided for in Figure 19 and displays a rendered graphical display of the completed equation in a standard mathematical notation format [36].

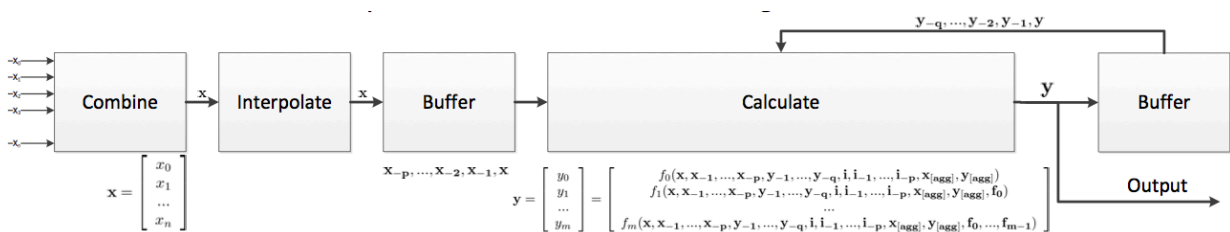


Figure 18 - Calculation model for Discovery Web Formula and Arithmetic Smart Agent [37].

ECD Calculation - Kick Scenario Description Formula for Kick Illustration

Input/output parameters

Time / Depth: Time Index unit: Interpolation: Configure

Formula symbol	Value/Mnemonic	Formula Unit	Description	Log Name	Buffer
AnnCsg...	8.5	inch	Annular OD 3		N/A
AnnCsg...	6.5	inch	Annular ID 3		N/A
ROP	20	m/h	Rate of Penetration		N/A
Q	FLOWIN	L/min	Flow Rate	Kick Scenario	0
d	MWIN	sg	Mud weight	Kick Scenario	0
TIME	CumTime	h	Cumulative time	Kick Scenario	0
DPL1	DPL1	m	Length of DP		0
AnnCsgL3	AnnCsgL3	m	Annulus Length 3		0
WellDe...	WellDepth	m	Current Well Depth		0

Formula(s)

Output	Formula	Use as output
SumAnnFric	IF(Q>0,(AnnFric1+AnnFric2+AnnFric3),0)	<input checked="" type="checkbox"/>
SumEqFric	IF(Q>0,(Motor+MWD+SurfEq),0)	<input checked="" type="checkbox"/>
SumDPFric	(DPFricTurb1+DPFricTurb2)	<input checked="" type="checkbox"/>
ChokePress	(d*FlowAChoke^2/(2959.41*0.95^2)/ChokeArea^2)/100	<input checked="" type="checkbox"/>
PumpPress	SumAnnFric+BitNozPloss+SumEqFric+SumDPFric+ChokePress	<input checked="" type="checkbox"/>
ECDCalc	((d*CumLAnn*0.0981)+SumAnnFric+ChokePress)/(CumLAnn*0.0981)	<input checked="" type="checkbox"/>

$$ECDCalc = \frac{((d \cdot CumLAnn \cdot 0.0981) + SumAnnFric + ChokePress)}{(CumLAnn \cdot 0.0981)}$$

Undo All Test Calculation Validate Save

Figure 19 - Discovery Web Formula [37].

6. Discovery Web Real-time ECD Control Design

6.1 Simulation based on our built data

Figure 20 shows the standard base-case that has been considered in the Discovery Web simulations. One is assuming drilling an 8 ½” hole from a platform rig through a reservoir section at 4000 meter with a 9 5/8” casing set at 3500 meters. The drillpipe is considered having an outer and inner diameter of 5” and 4.27” respectively. BHA outer and inner diameter is 6.5” and 2.5”. At 4000 meters, the length of drillpipe is 3800 meters and length of BHA is 200m. By assuming an average ROP of 40 m/h over a time interval of 4 hours, the following simulations are performed during drilling of 160 meters reservoir section.

Following assumptions are taken into considerations:

- Vertical well.
- Negligible pressure and temperature effects on the drilling fluid rheology and mud density.
- ROP value.
- Constant mud weight.
- Cutting particles are suspended in the drilling mud when there is no circulation.
- Cuttings are transported with the fluid velocity.
- Constant motor, MWD and surface equipment pressure effects.
- Implementation of Herschel-Bulkley rheology model.
- Appendix B: Rheology models.
- Appendix C: Rheology models and hydraulic calculations implemented in Discovery Web.
- Further assumptions will be explained through the different scenarios.

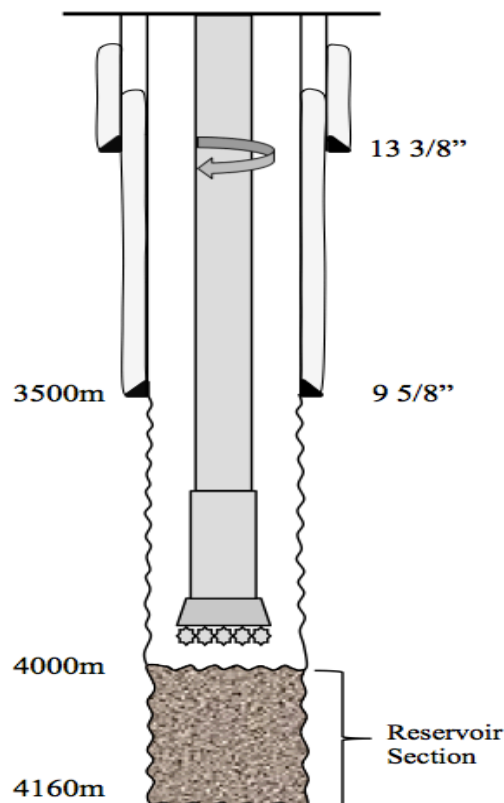


Figure 20 - Well schematics based on our built data.

6.1.1 Connection scenario

After drilling one stand (30 meter), the mud pumps have to be disconnected and a new stand has to be connected to the drillstring. Since there is no circulation, all friction in the system will disappear. This will be noticed as a drop in pump pressure from maybe 250-300 bars to 0. The drop in bottomhole pressure in the annulus will be approximately 6 bars for a 12 ¼” hole and 20-25 bars for an 8 ½” hole. The connection will last 5-10 minutes and we do not expect large temperature changes in the well. For the connection simulation scenario following parameters were considered. These are: mud weight in is 1.60 sg, flow rate in is 2000 lpm and average ROP is 40 m/h. Figure 21 shows that the pump pressure (SPP) varies from 293 to 0 bar during a connection. Bottomhole pressure (BHP) increases linearly due to the increased hydrostatic column and drops 40 bars during a connection. ECD varies from 1.60 to 1.695 sg.

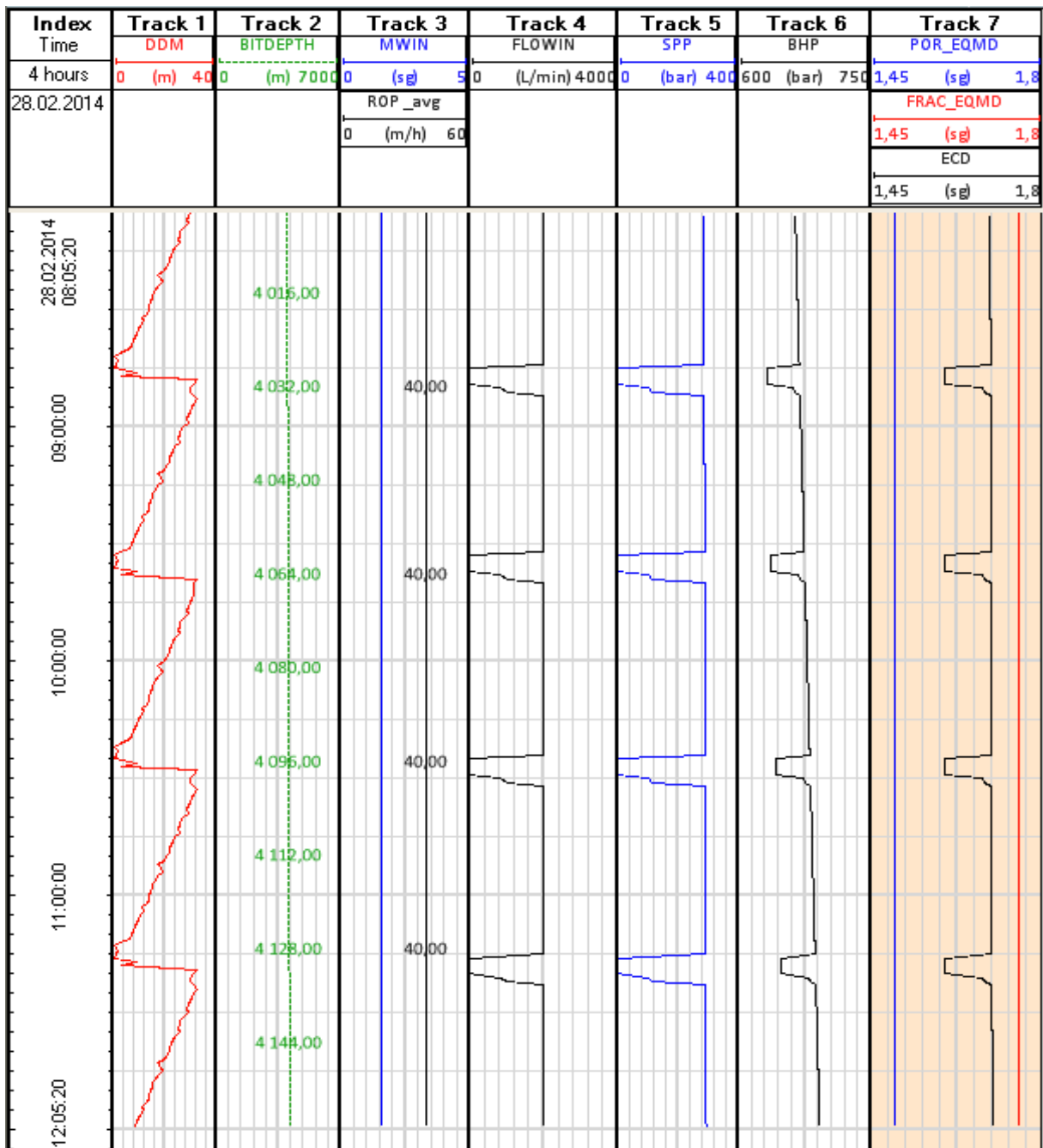


Figure 21 - Connection scenario.

6.1.2 Kick scenario during drilling

When drilling through a reservoir section, proper mud weight selection is essential to avoid a kick. Good simulation tools and real-time data can help in early detection of downhole problems. For the kick simulation scenario the following parameters were considered. The mud weight and flow rate is 1.6 sg and 2000 lpm, respectively. The simulation is shown in Figure 22. The kick occurred during drilling with insufficient mud weight to balance formation fluid. In time period 10.30-11.00, the ECD drops below the pore pressure curve, and a kick influx is taken into the well. We observe that the ECD becomes lower than the pore pressure.

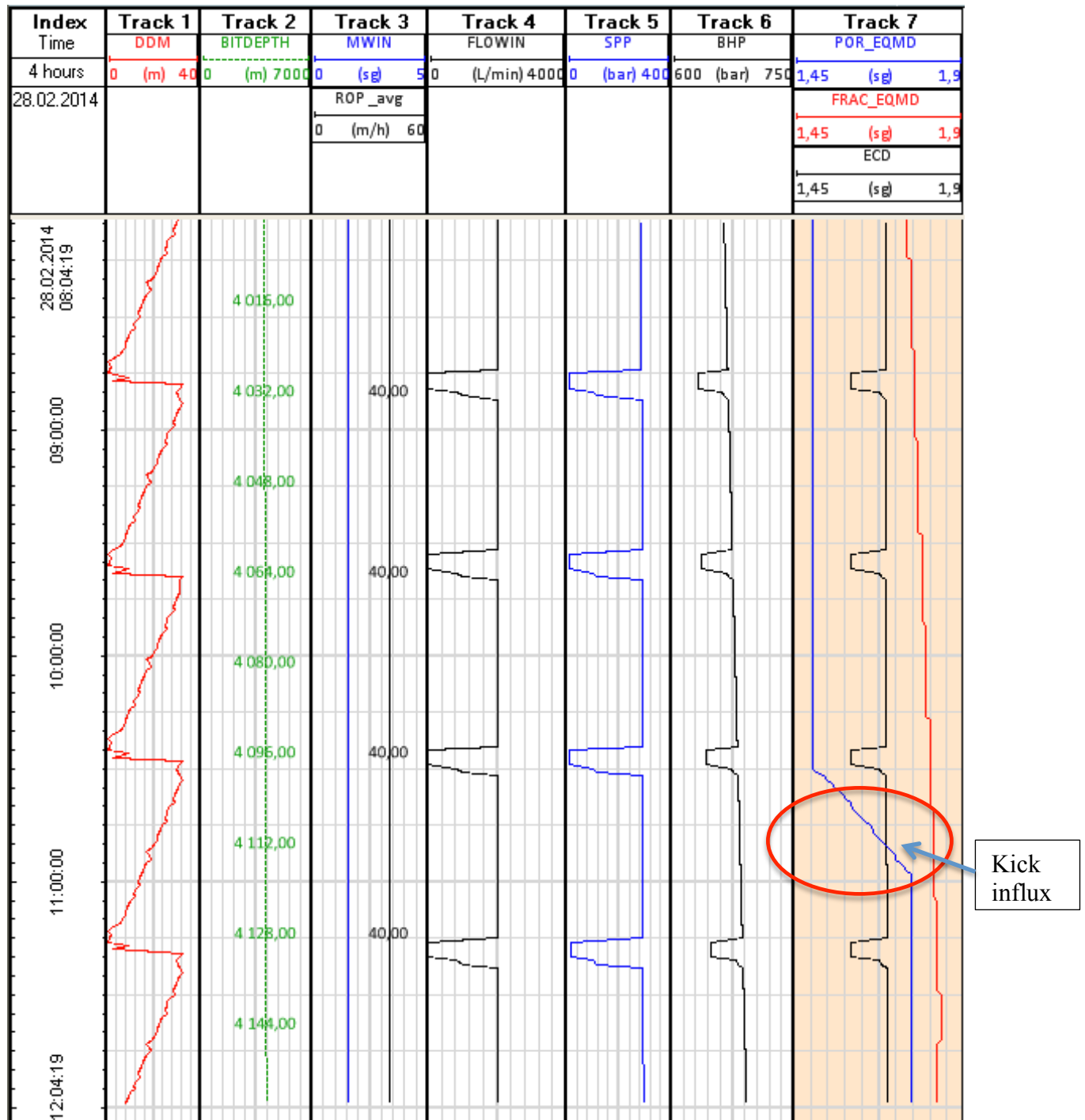


Figure 22 - Kick scenario during drilling.

6.1.3 Kick scenario during connection

In this scenario assume that an engineer has designed the ECD just a little bit higher than the formation pressure without the knowledge of safety margin considerations. The engineer did not consider that during a connection the dynamic part of the ECD would disappear (friction). This scenario is designed to illustrate the possible incident in a reservoir. For this kick during connection scenario, the following parameters were considered. ROP is 40 m/h and flow rate is 2000lpm. At around 4128 ft a connection was made and the mud weight was reduced below the reservoir pressure. Figure 23 shows that the kick influx will only be taken within the connection period. To prevent that the connection pressure drops below the pore pressure gradient, a safety margin between the static mud weight and pore pressure should have been considered. If an additional safety margin of 0.02 sg had been taken into account, the connection pressure drop would not have resulted in a kick.

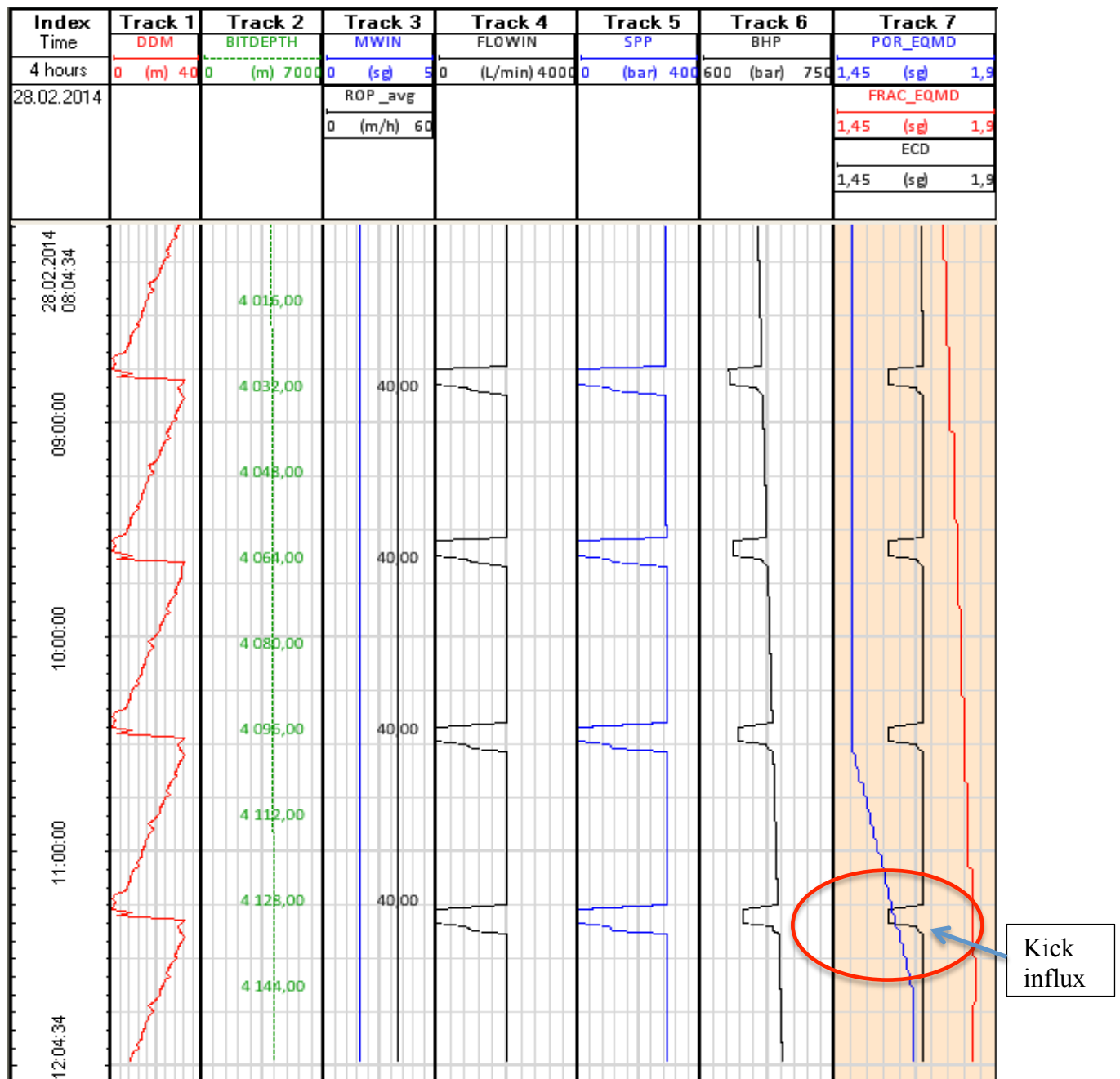


Figure 23 - Kick scenario during connection.

6.1.4 Pack-off scenario and sensitivity of pack-off

This scenario assumes that during drilling of unstable formations such as unconsolidated sandstone, brittle shale may fall into the wellbore and cause pack-off or bridging. It is assumed that the hole packs-off gradually behind the drill bit while drilling from 4000 m to 4160 m. Figure 24 shows an ideal pack-off illustrating the reduction of annular flow capacity by 10-20%. This section simulates the sensitivity of pack-off by gradually reducing the annular capacity. The annulus section above the pack-off point at 4000 m is considered unchanged (standard 8.5" hole). The following simulations have been executed for a 4 hours interval to illustrate the dramatic pressure build-up a pack-off can cause. During an actual drilling operation, the drilling operation would naturally stop earlier.

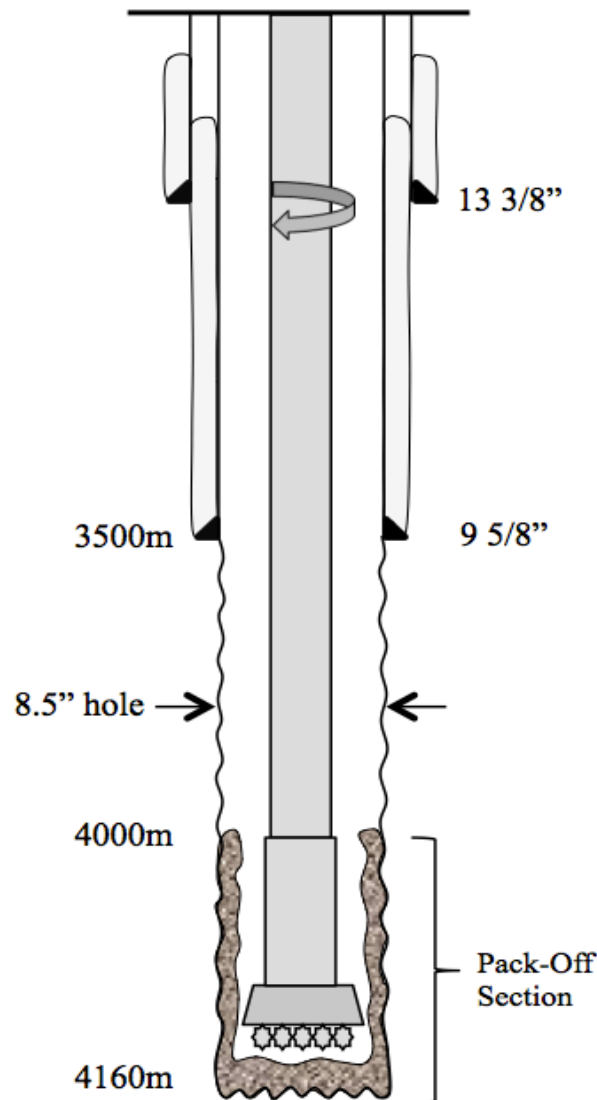


Figure 24 - Illustration of pack-off scenario.

Model input parameters used for the pack-off scenario:

- Mud weight in 1.60 sg
- Flow rate in 2000 lpm
- Average ROP 40 m/h
- Simulation time 4 hours
- BHA OD 6.5"

6.1.4.1 10% Pack-off effect

The simulation effect of 10% pack-off is presented in Figure 25. In Track 4 the outer diameter of the annulus is reduced from 8.5" to 7.65". This results in an increased ECD that approaches the fracture gradient. Accordingly, the pack-off effect also increases the pump pressure (SPP) and the bottomhole pressure (BHP), but the impacts does not show that clearly for a 10% pack-off.

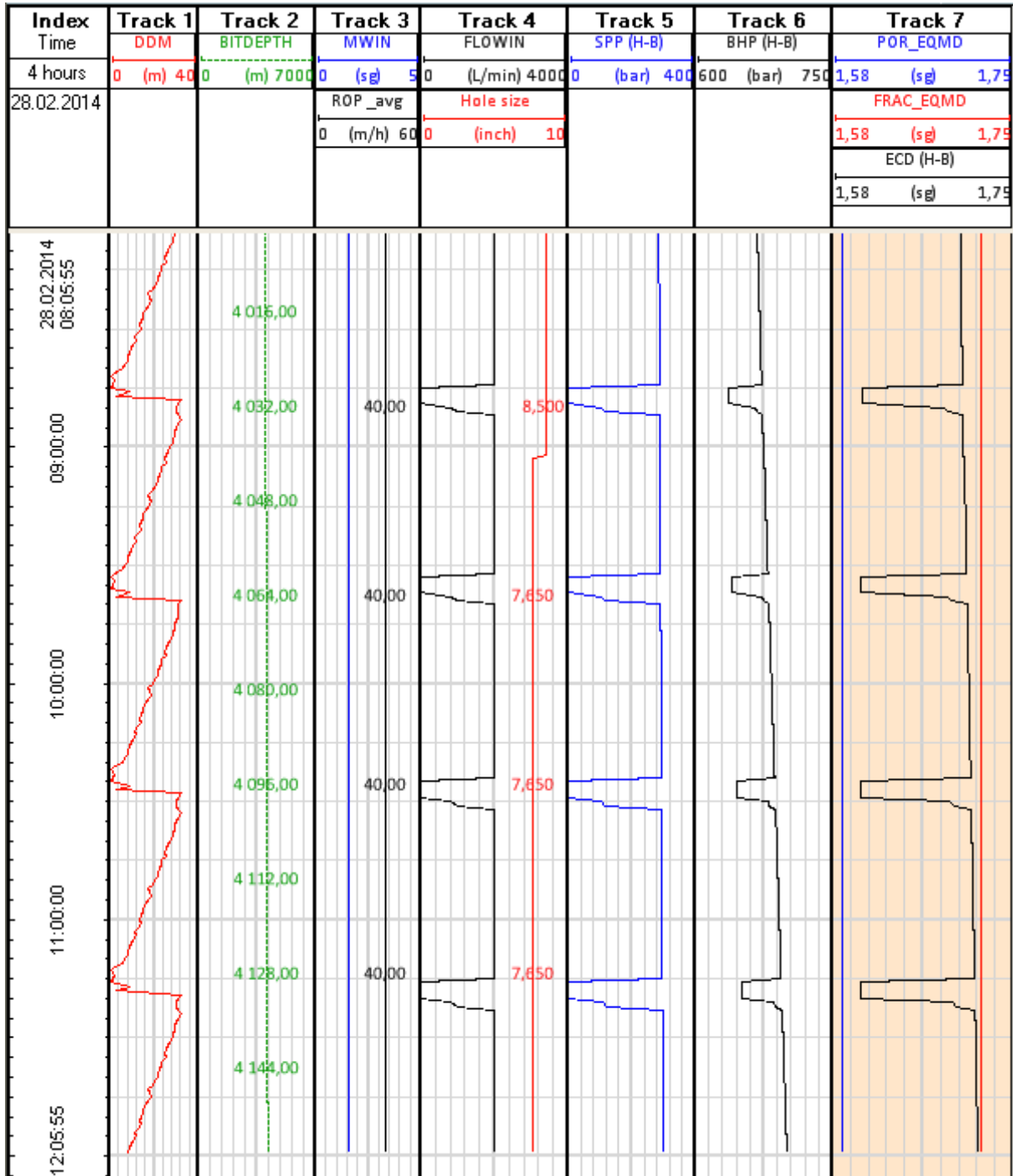


Figure 25 - Pack-off scenario 1 (10% reduction in annulus diameter).

6.1.4.2 16% Pack-off effect

The simulation effect of 16% pack-off is presented in Figure 26. In Track 4 the outer diameter of the annulus is reduced from 8.5" to 7.14". The 16% pack-off effect results in a sudden increase in SPP, BHP and ECD. Consequently, the formation fractures instantaneously when the hole packs off. The increase in SPP for the constant flow rate is symptom for the deterioration downhole due to pack off.

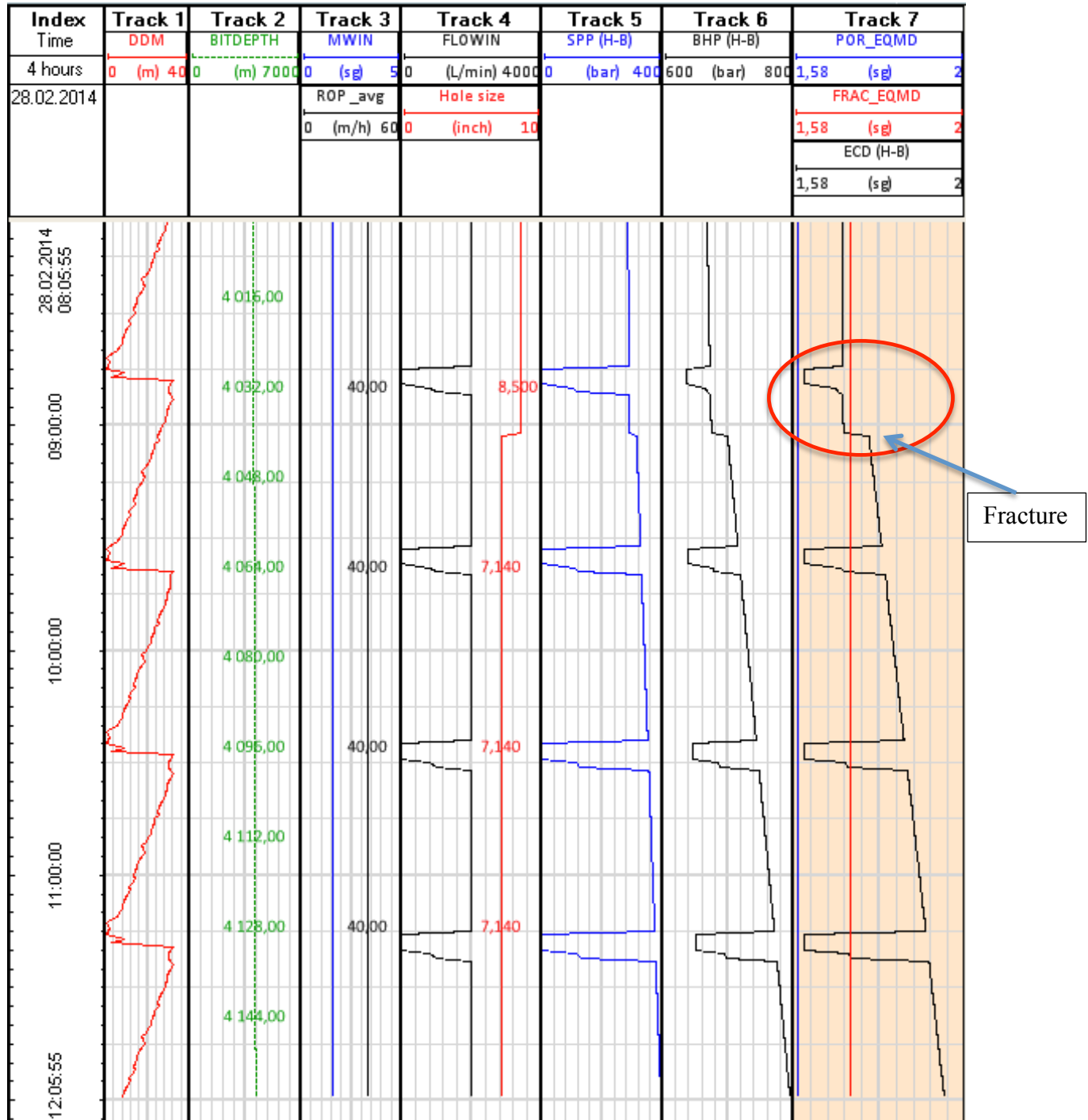


Figure 26 - Pack-off scenario 2 (16% reduction in annulus diameter)

6.1.4.3 20% Pack-off effect

This simulation assumes that the annular constriction is reduced by 20% due to pack-off. In Track 4 the outer diameter of the annulus is reduced from 8.5" to 6.8". The result of the simulation shows that pack-off increases the well pressure dramatically. As shown on Figure 27, until the clock is 9.00am, the ECD will not exceed the fracture gradient. It might not look like this, but this is due to scaling limits in Track 7. The linearly increasing ECD trend is due to the gradually increased pack-off length. For example at 9.00 am the pack-off length is 40 m, and at 12.00 am the pack-off length is 160 m. Again, it is important to emphasize that a drilling operation would never be continued as shown in this simulation, since the pack-off would have caused problems and led to a halt in the operation.

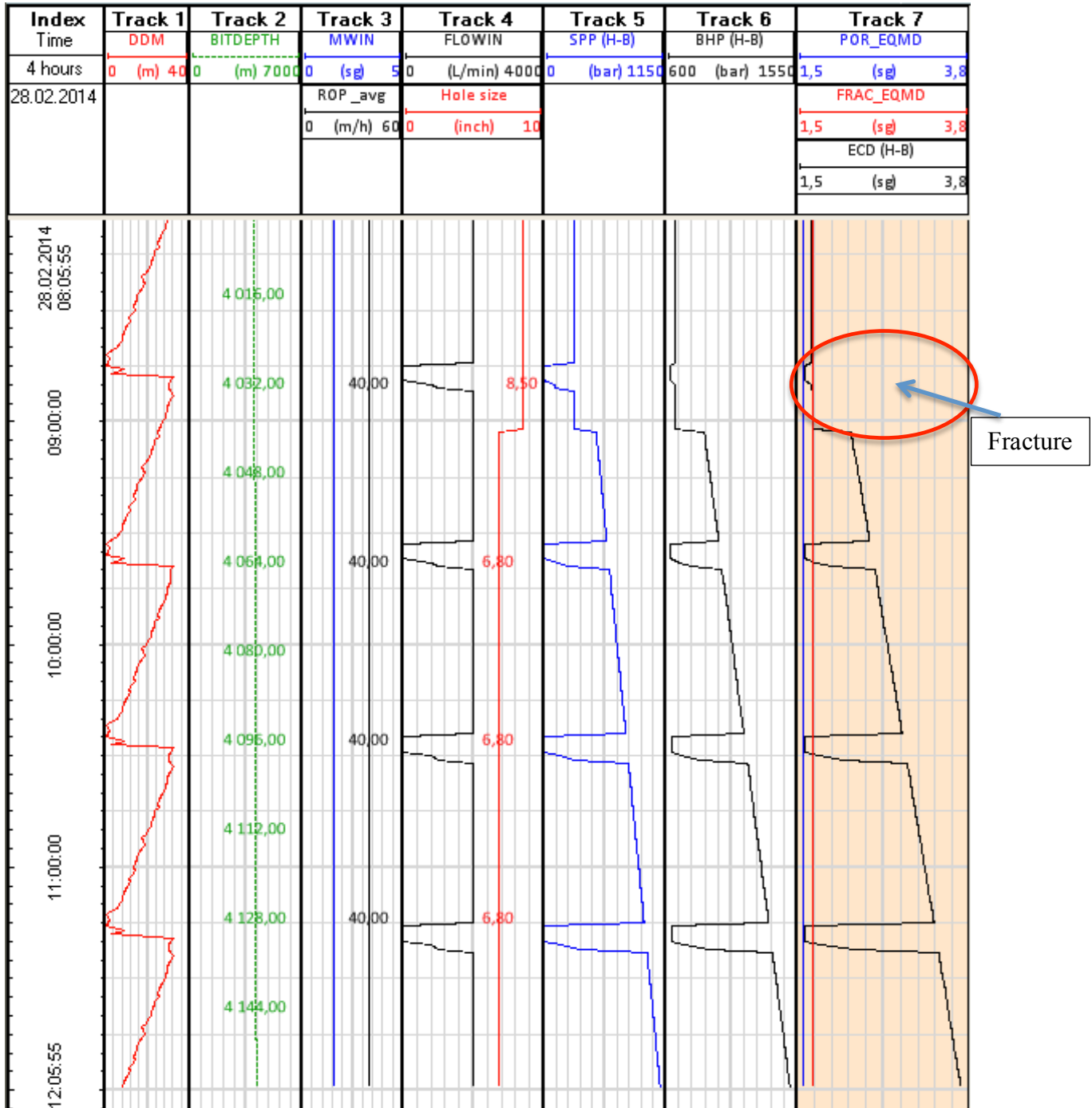


Figure 27 - Pack-off scenario 3 (20% reduction in annulus diameter).

6.1.5 Lost circulation scenario

During a drilling operation there will be a continuous change in the mud system. The system is continuously given additives such as basic fluids, solids, and chemicals to compensate for change in hole size, lost mud and volumes occupied by cuttings. A certain amount of liquid may be bound to the cuttings or lost to permeable zones within the wellbore. This is a mass balance equation that we easily can control. Lost circulation is a measurable loss of the total drilling fluid to the formations.

In this scenario, there are performed three different simulations, illustrating both partial and total loss to formation at the 9 5/8" casing shoe and total loss at 4120m. The operation is ongoing as normal until the point where mud is lost to the formation. An illustration for total loss at the 9 5/8" casing shoe is shown in Figure 28.

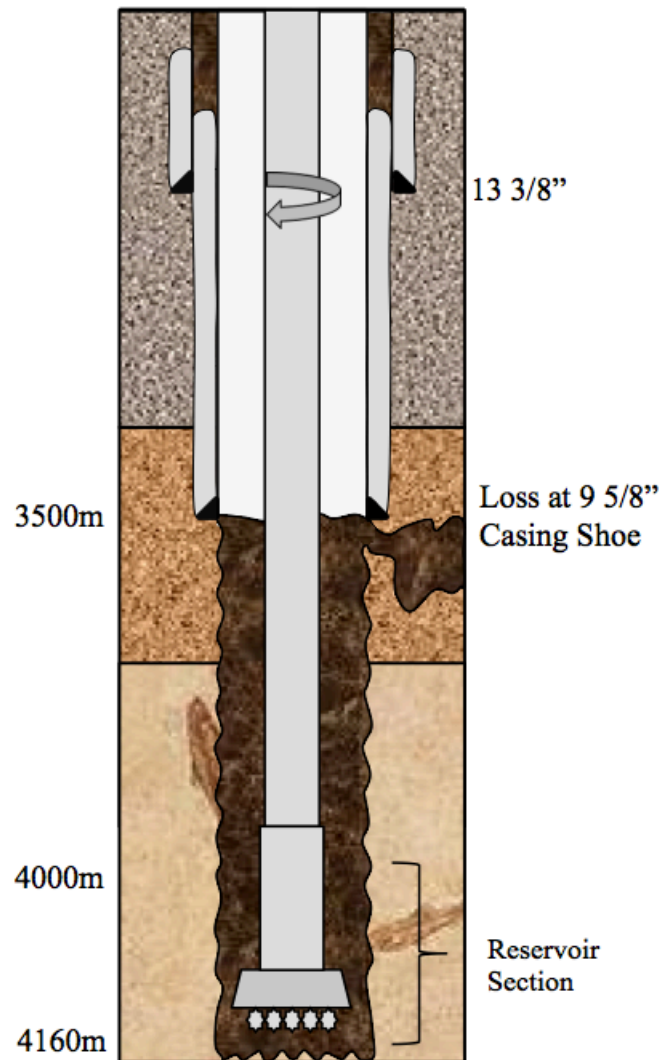


Figure 28 - Illustration of total loss of circulation at 9 5/8" casing shoe.

Parameters used for simulation of the lost circulation scenario:

- Mud weight in 1.60 sg
- Flow rate in 2000 lpm
- Average ROP 40 m/h
- Simulation time 4 hours

6.1.5.1 Partial loss at 9 5/8" casing shoe

Figure 29 shows the simulation result of partial loss to the formation below the 9 5/8" casing shoe. Drilling fluid is assumed to be partially lost into the formation at 9.00pm. In Track 4 flow rate out (FLOWOUT) decreases from 2000 lpm to 0 lpm in steps of 500 lpm. This results in an ECD that is trying to compensate for the decrease in flow rate (ECD decreases). However, since we are drilling deeper and deeper, the pressure in bar does not decrease since the hydrostatic column is increasing. However, the case is that we are losing mud and this is reflected in the ECD, which is given in sg, and more easily reflects the loss of frictional forces.

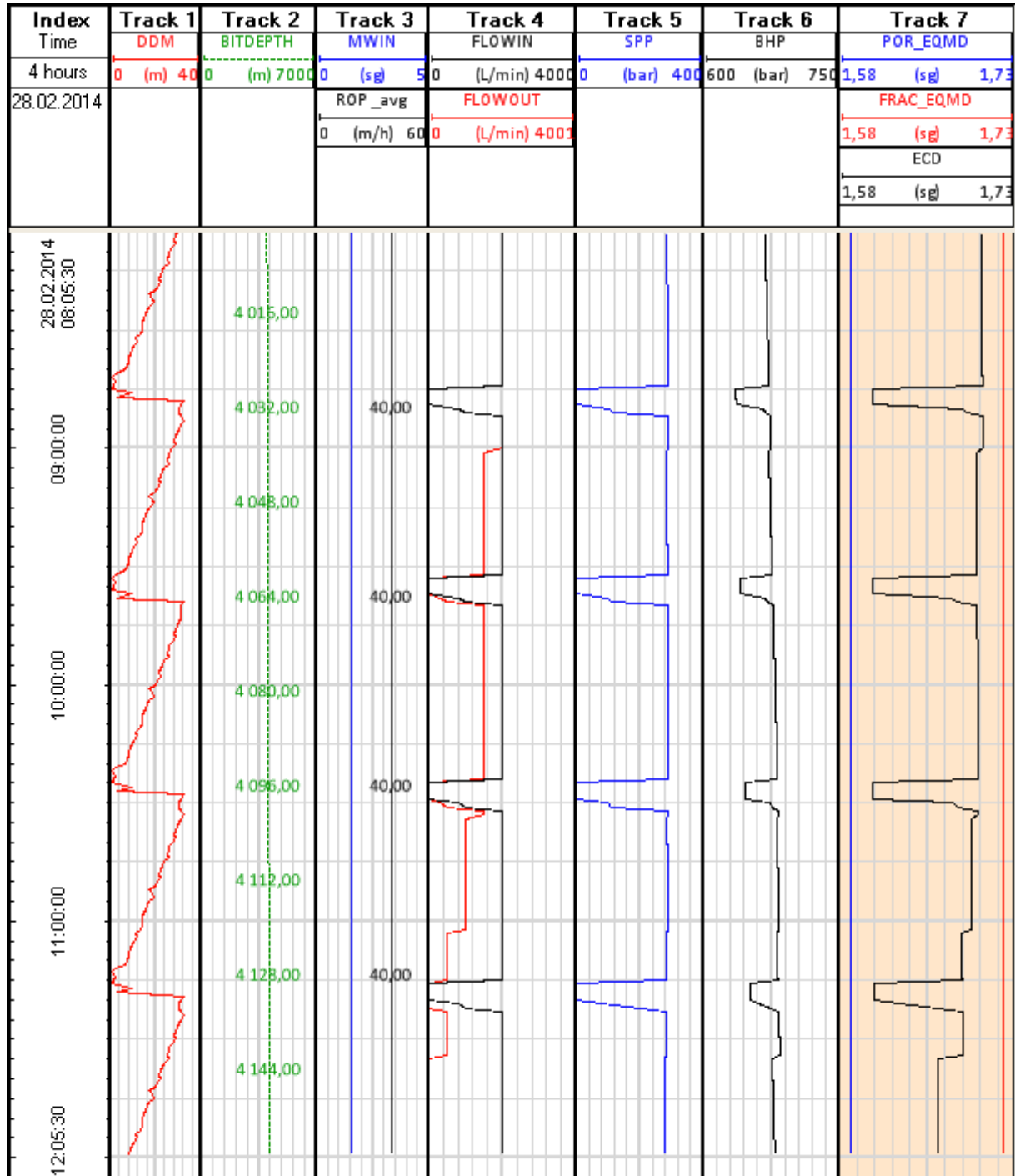


Figure 29 - Lost circulation scenario 1 (Partial loss at 9 5/8" casing shoe).

6.1.5.2 Total loss at 9 5/8" casing shoe

It is normal that we start losing mud gradually as shown in Figure 29. Figure 30 illustrates total loss below the 9 5/8" casing shoe. In this case we lose all the mud at once. When the flow rate out drops from 2000 lpm to 0 lpm in Track 4, this results in a strong reduction in the ECD at 9:00 am. Consequently, this also reduces the SPP and BHP, since the friction is lost in parts of the well.

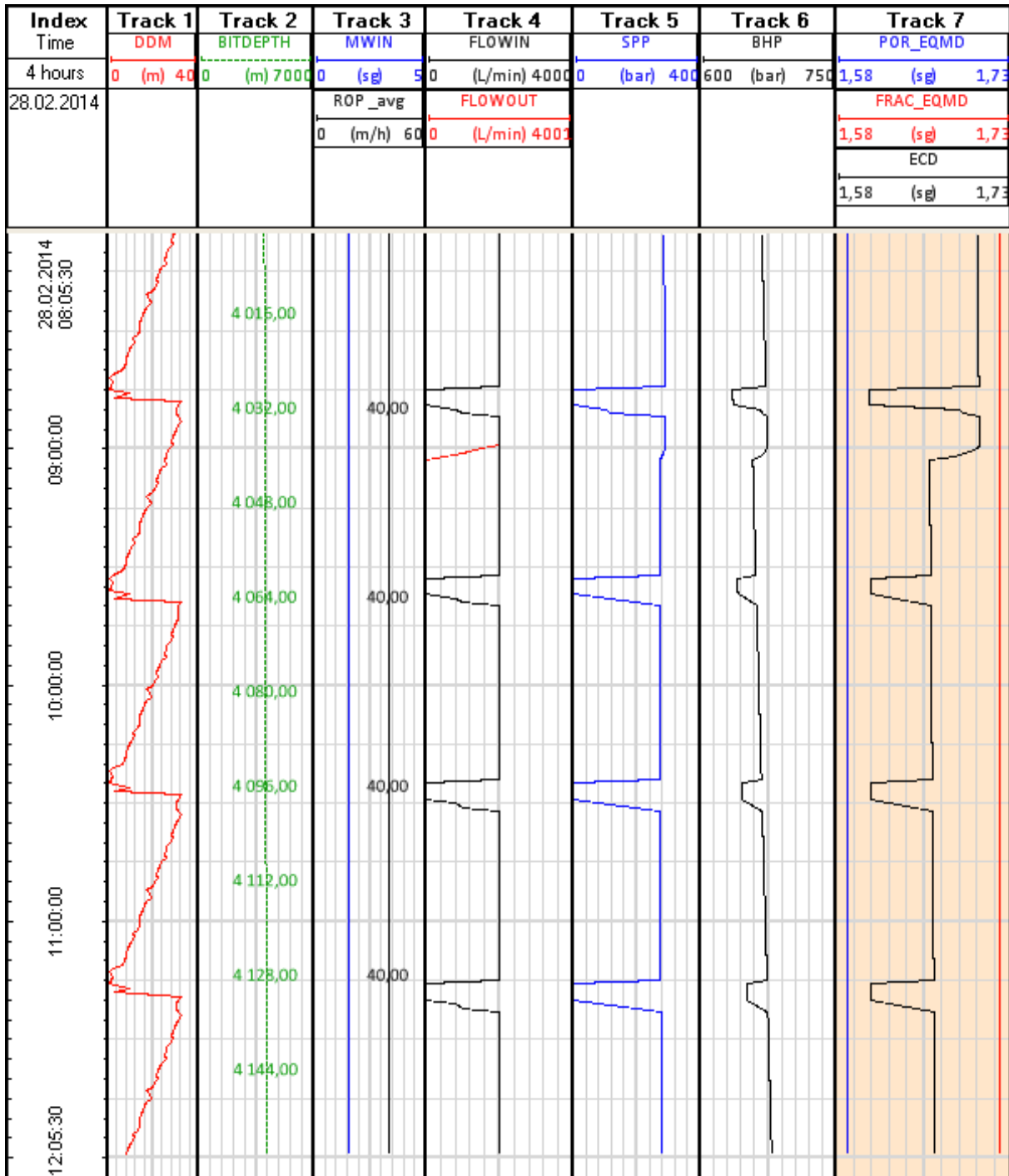


Figure 30 - Lost circulation scenario 2 (Total loss at 9 5/8" casing shoe).

6.1.5.3 Total loss at 4120 m

Figure 31 is similar to the simulation performed for total loss of circulation at the 9 5/8" casing shoe. The difference is that that the total loss of mud is at 4120 m.

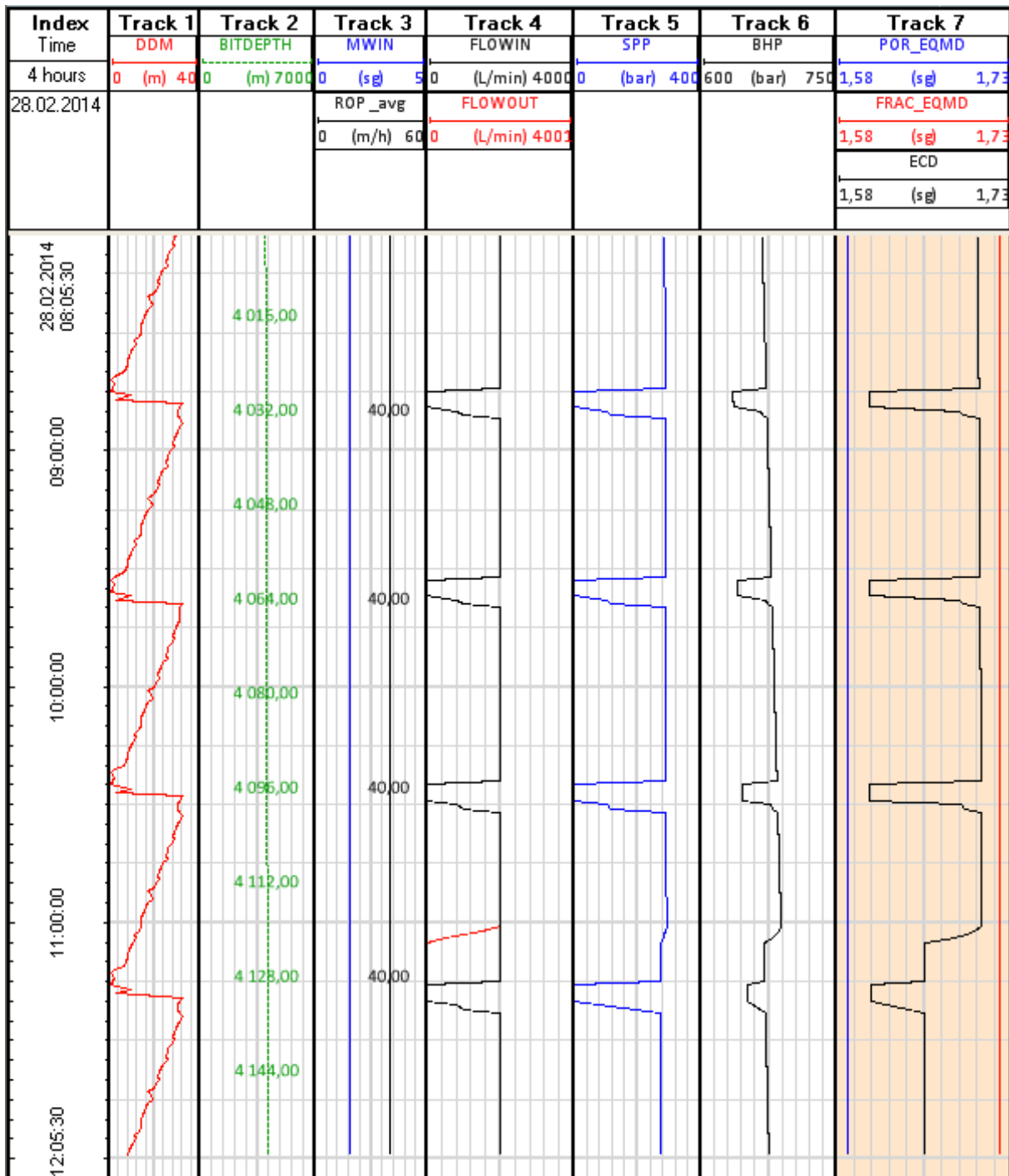


Figure 31 - Lost circulation scenario 3 (Total loss at 4120 m).

6.1.6 ROP vs. Cuttings concentration scenario

The simulation result of the ROP and cutting concentration effect scenario is illustrated in Figure 32, and shows how ramping up the average ROP from 20 to 80 m/h affects the mud weight and the cuttings concentration. In the model, we have assumed that the cuttings are transported with the liquid velocity. The sensor for measuring the cuttings concentration is located right above the bit and increases momentarily in Track 3 as the ROP increases. The sensor for measuring the mud weight out is located at the surface, shown in Track 4, and does not respond until there have been a bottoms-up circulation. In Track 7, the ECD formula is including the transient effect that takes into consideration the increasing mud weight in the annulus as we circulate. After the bottoms-up circulation the ECD stabilizes at a constant value, which reflects that the cuttings is present in the whole well.

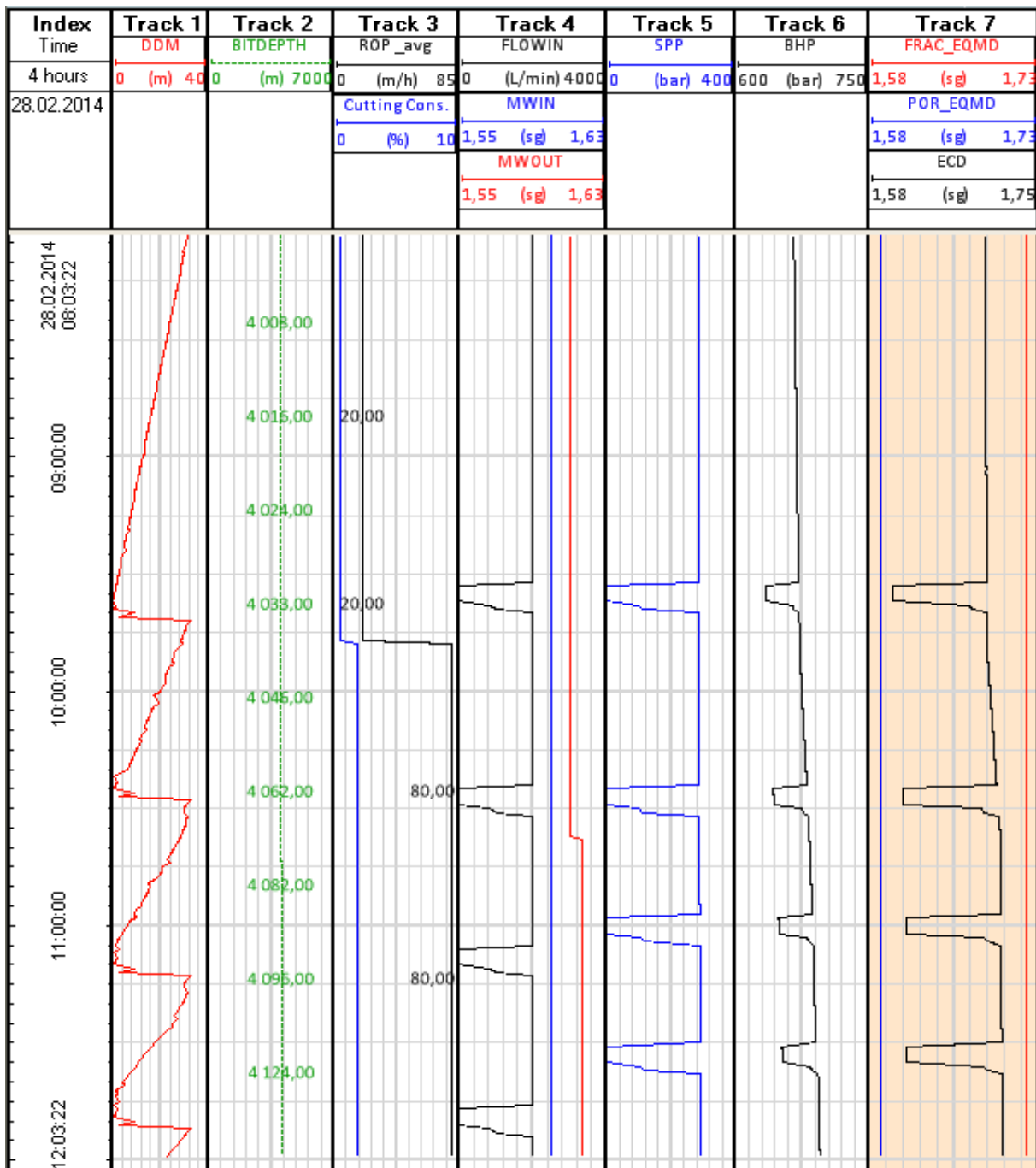


Figure 32 - ROP vs. Cuttings concentration scenario.

6.1.7 Comparison of different rheology models for hydraulic calculations

The different models were compared with respect to pressure predictions. These are Bingham (B), Robertson-Stiff (R-S), and Herschel-Bulkley (H-B). Figure 33 shows the simulation results. In Track 7, H-B and R-S give similar results, while B predicts lower pressure than the others in the annulus. For SPP in Track 5, H-B and B gave similar results, while R-S predicts lower pressure in drillpipe. This might fit with the theoretical part where it was said that B is not the best model to describe the annulus. Generally, it is said that three-parameter models are better than two-parameter models. This is also reflected in Track 7, where R-S and H-B model seems to fit quite well. H-B was chosen for the simulations, since the model did not show any large deviations compared to the other models.

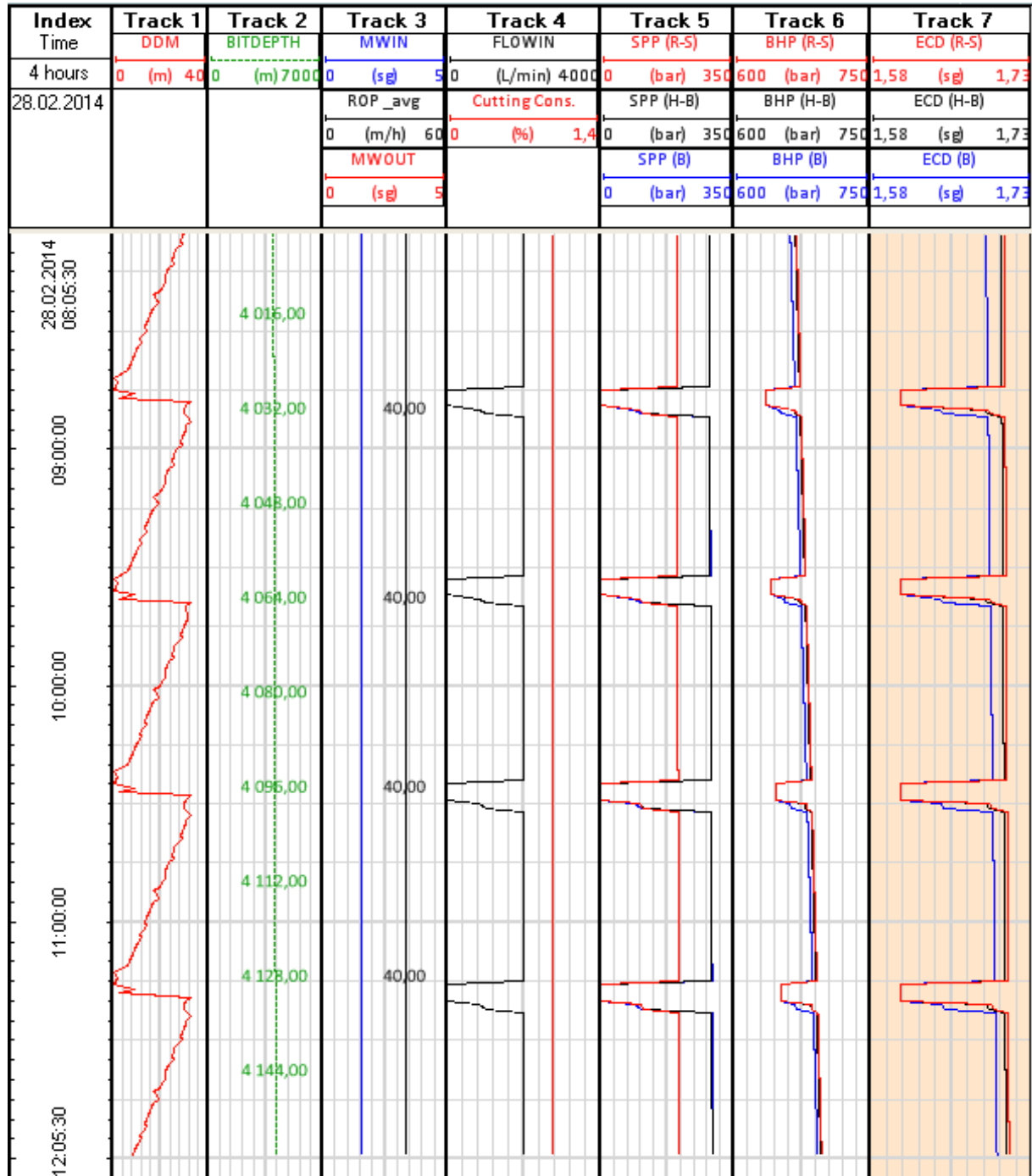


Figure 33 - Comparison of different rheology models for hydraulic calculations.

6.1.8 Washout scenario

Today, technology develops faster than before, which clearly is a mechanism that helps us to improve the way we operate. One of these new technologies is Intellipipe [23], a pipe that includes sensors along the drillstring to measure e.g. pressure and temperature at different locations in the wellbore in real-time. By using this equipment it will for instance be possible to detect a leak in the drillstring. In this scenario, we have placed three sensors, respectively at 1000 m, 2000 m and 3000 m. Unknowingly, a leak has occurred at 1500 m, and by using real-time monitoring it should be possible to locate the approximate position of the leak. Figure 34 shows an illustration of a washout scenario in drillpipe (Intellipipe).

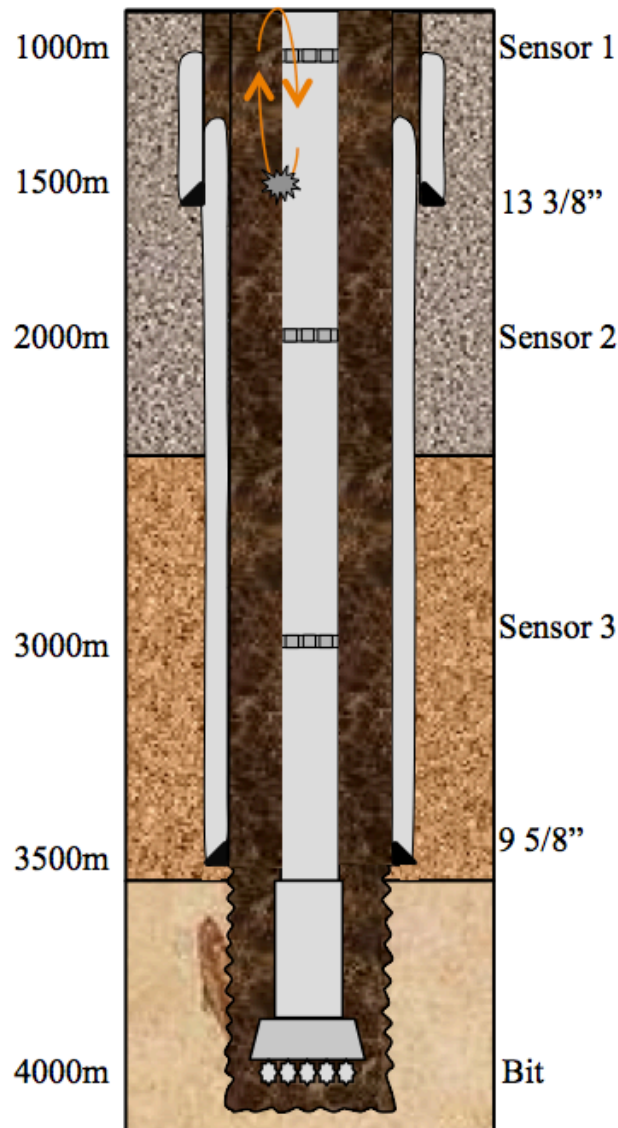


Figure 34 - Illustration of washout scenario in drillpipe (Intellipipe).

Model input parameters used for simulating the washout scenario:

- No reciprocation
- Flow rate in 2000 lpm
- Mud weight in 1.6 sg
- Simulation time 3 hours

6.1.8.1 Washout scenario

The washout scenario simulates loss of drilling fluid at 1500 m through a washout in drillpipe. The drilling fluid is lost from drillpipe to annulus from 0 lpm to 2000 lpm. At 2000 lpm loss rate, the well below 1500 m is dead, and is only affected by the weight of the hydrostatic column. Figure 35 illustrates that a washout simulation scenario is established at 10.00am. From Track 3-5 it is clear that the washout has occurred between Sensor 1 (1000 m) and Sensor 2 (2000 m). In Track 3, Sensor 1 takes no affect of the washout due to the fact that it is located above the loss point. Since Sensor 2 and 3 are located below the loss point, they will experience a loss in pressure. Sensor 3 more than Sensor 2 due to the distance from the leak point (would therefore sense that a large portion of the well is dead). Reduction of the annular friction will cause the ECD to drop, experiencing only the hydrostatic column from the loss point.

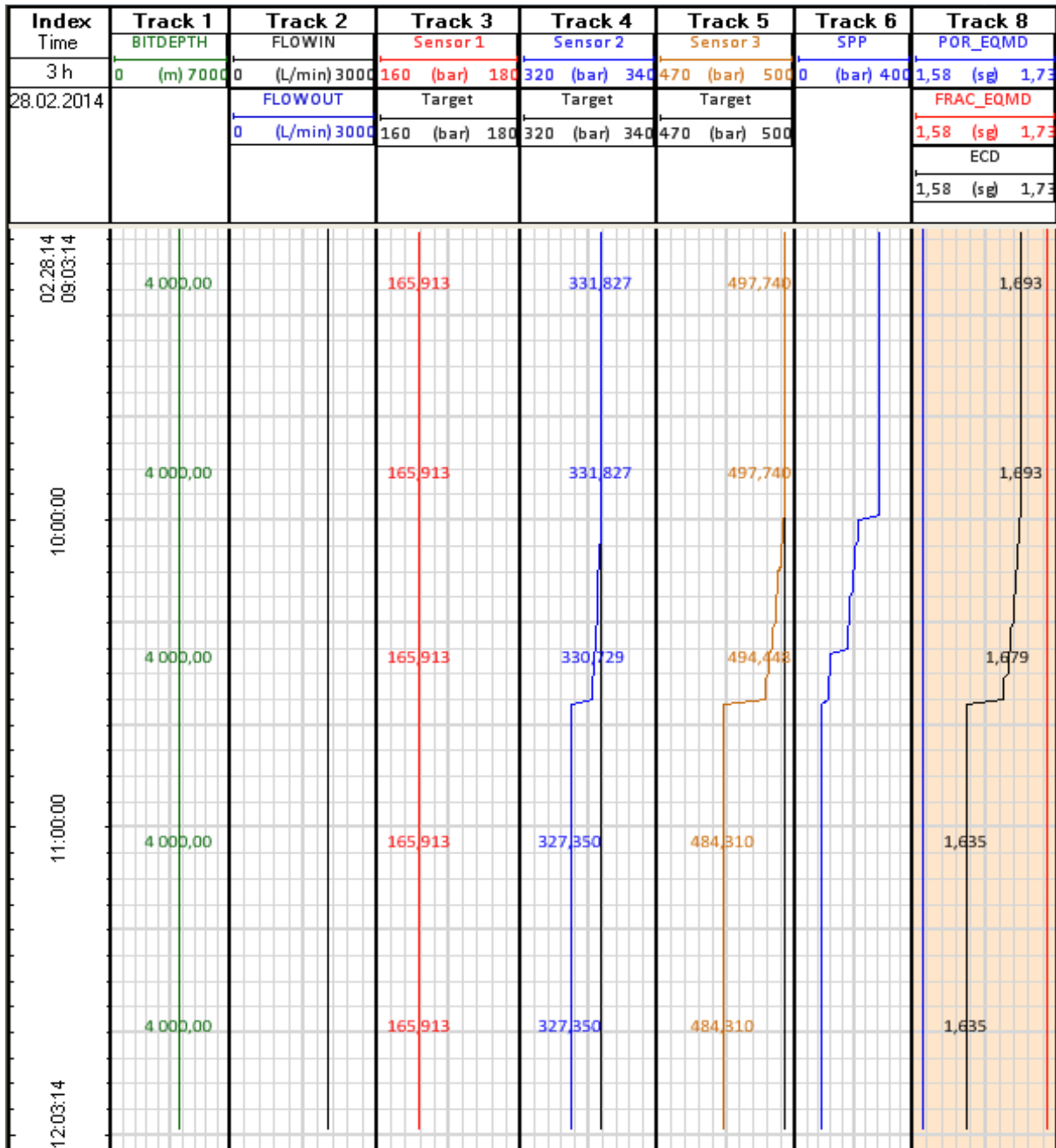


Figure 35 - Washout scenario in Intellipipe.

6.2 Simulation based on real well based data

In this work there have been several attempts to link the implemented model to a real well and create similar scenarios. However, in order to do this, additional parameters need to be more easily available in Discovery Web for real well consideration. This includes geometry data, as for instance hole diameter, casing depths, drillpipe and BHA components. It will also be very important to have the rheological data for the mud being used available from the vendors. In addition, if more advanced cuttings transport models were to be implemented [17], information about the cuttings size could also be a possible input parameter.

Due to the similarity of the self-made scenario, in terms of manually entering the parameters, it is decided not to retrieve data from old wells to rebuild similar scenarios. Nevertheless, it is determined that in the future it will be possible to run the model through a real-time system, and automatically retrieve the necessary parameters. Further follow-up work to this task will be given in the future work chapter.

7. Summary and Discussion

Since the introduction of petroleum exploration and exploitation the drilling technology is showing advancement. However, as the energy demand increases, the industry is expanding exploration activities in very challenging environments. These are to mention, deep-water, depleted formations, gas hydrated formations, HPHT, arctic and extended reach formations.

Drilling with conventional methods in challenging environments limits the operations and may cause undesired problems. It is not possible to say it too often, the E&P challenges are only increasing. By increased costs, falling production and stricter environmental regulations, it is essential to be aware of the challenges and reach strategic goals. During drilling operations today, many operators are facing increased NPT, due to drilling incidents (pack-off, kick, poor hole cleaning, fracture, collapse and lost circulation). Early symptom detection, armed with real-time calibrated process models, will help us to manipulate hydraulic drilling parameters and avoid unexpected events. Wellbore condition evaluation is based on detailed process models that are capable of predicting downhole hydraulic, thermal and mechanical affects during a drilling operation. By introducing the model to multiple drilling problem symptoms, the possibility for decreasing the NPT only increases [2, 3, 35].

In order to solve the conventional drilling problems, the industry is introducing new advanced drilling methods such as MPD, UBO, casing and liner drilling. For instance, the company Reel Well [38] has introduced a new drilling solution that aims of drilling wells that reaches beyond 20 km. All these technologies use control and monitoring systems that are based on real-time measured data.

It is no doubt that the introduction of good IO tools will help the ongoing drilling operations. Information is internally transferred through network systems to remote users, operators or managing systems in order to tie together different specialists, improve capacity and reduce costs. By using an aggregated system for collecting data from all service companies, operators are able to gather real-time data from multiple data sources. Data is taken from the rig systems in many different formats and then aggregated into the onshore drilling databases [35].

Discovery Web is a web-based browser that will help us to reach out to all the people involved by implementing a visualization and collaboration tool for multi-disciplinary target groups. Having developed a model that simulates different drilling scenarios, using only static values, mnemonics and outputs, I am confident that Kongsberg Oil & Gas Technologies brings an equally good tool to the market. In addition to real-time monitoring, the feature Discovery Web Formulas gives you the ability to create your own formulas. By this it is possible to create models that can be compared with real data in order to evaluate the predictive capability of the model. Outputs from a formula can be visualized and used in the most common widgets similar to log data. In addition, when having models running along with real-time data, deviating trends may be an indicator of unwanted events taking place in the well. There must be a reason why the model does not fit the data anymore. Hence, they can in theory function as warning indicators. By building a monitoring panel in Discovery Web, based on the proper rheological models and hydraulic calculations, this thesis have been used to show how models and simulations can be combined in Discovery Web. The next step would be to compare the developed model against a real well. In addition, the model implemented can also be made more advanced [3, 35].

The experience has been that it was easy to implement the model using Discovery Web Formulas. Another strength of the software is that it is very easy to visualize and import data from real wells in this application. Hence, it is a very good tool for comparing models with real data. This real-time data handling capability and visualization flexibility is considered as one of the major strengths.

Proper training combined with new advanced tools is a key element in preventing undesirable incidents. No matter how good and advanced the models are, it is important to not only be critical with respect to data, but also know how to be able to interpret the data in the best possible way. Nevertheless how advanced new tools are, it does not help if the people do not know how the tools work and how to use them. By allowing new students to play around with powerful tools such as Discovery Web (by building models and interpreting data), it will raise the awareness around drilling incidents and enable students to easily pick up and understand new information when they start working after graduation.

In this thesis, three hydraulic simulation models were implemented in Discovery Web. These are: Bingham, Robertson-Stiff and Herschel-Bulkley. In order to illustrate the applicability of the implemented models, a case study was presented which was based on drilling a well from 4000 m. Based on the input of rheology, geometry, flow rate, mud densities and ROP, the following drilling scenarios have been simulated.

- Connection scenario
 - Stop in flow rate (in) reduces the SPP, BHP and ECD.
 - SPP is reduced from 293 to 0 bar during a connection.
 - BHP increases linearly due to the increased hydrostatic column when drilling deeper, and drops 40 bars during a connection.
 - ECD varies from 1.60 - 1.70 sg during a connection.
- Kick scenario during drilling
 - Unexpected high pore pressures cause this type of kick.
 - In this case, the ECD is lower than pore pressure.
 - The planned mud weight is insufficient.
- Kick scenario during connection
 - During a connection the well pressure caused by the static mud weight is lower than pore pressure and is inducing a kick.
 - One should always plan for having a static mud weight above pore pressure when including safety margins (swab or riser margin).
- Pack-off scenario and sensitivity of pack-off
 - Decrease in outer diameter of annulus increases the SPP, BHP and ECD.
 - In the simulation, pack-off length increases while drilling (after 1 hour the pack-off length is 40 m and after 4 hours the pack-off length is 160 m). In a real situation formation will break down when exceeding fracture pressure, but here we have demonstrated the pressure effects.
 - 10% pack-off: ECD varies from 1.61 - 1.72 sg, SPP 0 - 300 bar.
 - 16% pack-off: ECD varies from 1.61 - 1.95 sg, SPP 0 - 394 bar.
 - 20% pack-off: ECD varies from 1.61 - 3.68 sg, SPP 0 - 1100 bar.
 - ECD drops to 1.61 sg (MW 1.60 sg) due to the effect of cuttings concentration in the annulus.

- Lost circulation scenario and sensitivity of lost circulation
 - Decrease in flow rate (out) reduces the SPP, BHP and ECD.
 - While drilling deeper, the BHP in bar can increase even if we have losses, since the hydrostatic pressure is increased due to deeper wells. However, the ECD will be reduced.

- ROP vs. Cuttings concentration scenario
 - Increase in ROP will increase the cuttings concentration in the annulus, which again will increase the static mud weight and ECD.
 - The full response on the ECD will first be seen when the new cuttings concentration has been circulated bottoms-up. This was reflected in the simulation. This is also reflected in the sensor located at the bottom, while the mud weight out will first increase after one bottoms-up circulation.
 - In this case, no slip conditions were assumed. However, more advanced cuttings transport models should be considered, taking into account slippage (which will affect concentration profile) and bed build up [17].
 - The ECD increases 0.014 sg when changing the ROP from 20 to 80 m/h.

- Hydraulics and rheology model comparison
 - The three rheological models for hydraulic calculations were compared. These are: Bingham, Robertson-Stiff and Herschel-Bulkley.
 - For the given rheological and hydraulic data, the models gave similar result for SPP and ECD. However, some discrepancies could be observed.
 - SPP for Robertson-Stiff is 90 bars lower than for Bingham and Herschel-Bulkley, this is probably due to a lower frictional loss in drill pipe for this model. Bingham gave a slightly lower annular frictional pressure drop.
 - We chose to use Herschel-Bulkley since this model gave the least variations compared to the others. In addition, a three-parameter model is usually more accurate than a two-parameter model, like Bingham.

- Washout scenario
 - The purpose was to demonstrate the advantage of the new technology Intellipipe.
 - The simulation shows that it is possible to use drillpipe with implemented pressure sensors at different locations in the annulus to detect location of washout in drillpipe.
 - Three sensors are considered, and the washout takes place between the two uppermost sensors. Sensor 1 takes no affect of the washout due to the fact that it is located above the loss point. Sensor 2 and 3 are located below the loss point and will experience a loss in pressure. Sensor 3 will see the effect more than Sensor 2 due to the increased distance to the leak point.
 - Reduction of the annular friction will cause the ECD to drop, experiencing only the hydrostatic column of mud from the leak point.

8. Conclusion

Good real-time monitoring and control systems are one of the major factors for a successful drilling operation. By implementing good IO technology, several drilling related problems such as excessive torque and drag, kick, stuck pipe and lost circulation can be reduced and avoided. Real-time monitoring systems run both measurement and model based predictions in parallel. Whenever the measurement system fails, the model-based prediction can be used to monitor the downhole condition as illustrated in this thesis with Discovery Web. In addition, when we run models and measurements in parallel, the models can be calibrated to fit the real data. However, when discrepancies in trends of the measured data and the model-based predictions occur it can be a sign of detecting worsening downhole conditions and a first warning of an unexpected event. They can also be used for forward prediction based on a current real-time calibrated model state.

One example can be to have measured hydraulic data displayed along with models for predicting well pressures. Such models can be very complex when integrating fluid mechanics, solid mechanics and thermodynamics. Here relatively simple models for well pressure predictions were implemented and it was shown how one could visualize those data. In addition, it was shown how different parameters such as e.g. ROP and flow rate would affect the trends. It was also of importance to demonstrate different events/unwanted situations that can occur, and how that would affect the trend lines / pressure development. Since the introduction of real-time monitoring systems there have been several studies that have been carried out to investigate the behavior of hydraulic drilling parameters and how they can be used in early symptom detection.

This thesis comes to the conclusion that:

- Discovery Web is a very good tool for showing and taking into use real-time data from real wells.
- Knowledge about drilling problems and real-time monitoring systems are a combination that certainly should be more practiced by the universities to raise the awareness on decreasing NPT.
- It is shown that one can use Discovery Web Formulas to enter formulas and models, and how we can visualize them. Later these models can be compared against actual data when all input well data is available. In this case, it was focused on rheological models for hydraulic calculations.
- It is a tool that is very flexible in terms of visualization processing and it is made suggestions for how this can be visualized.
- It has also been shown how to embed events into the models, which later can be used as a basis for developing training scenarios and demonstrations in teaching.
- The results show how the models implemented can be the first step in introducing models in combination with real-time data for monitoring and handling drilling problems using this application. In terms of gathering information, the data needs to be of high quality and the equipment equally reliable when drilling in challenging environments.
- Advanced real-time monitoring systems can be used to drill difficult wells and aid in avoiding bad incidents that will have negative impacts on the operation. Future wells will be of the difficult type, hence there should be a need for such tools in order to be able to exploit complex hydrocarbon reserves.

9. Future Work

The following bullet points includes recommendations for future work:

- Implement pressure and temperature effects in density calculation and rheological models.

NORSOK D-010 [21] defines HPHT as a “well with expected shut-in pressure exceeding 690 bar, (10,000 psi), and a static bottomhole temperature higher than 150 °C”. HPHT has an impact on the mud properties and could cause well control issues. The surface mud weight should be adjusted correspondingly for thermal and pressure effects on the effective fluid density in the well. Temperature is the most critical parameter since it will lower the specific gravity of the mud. Similarly the pressure will increase the specific gravity. Figure 36 illustrates the temperature effect on density for a simulated scenario [39].

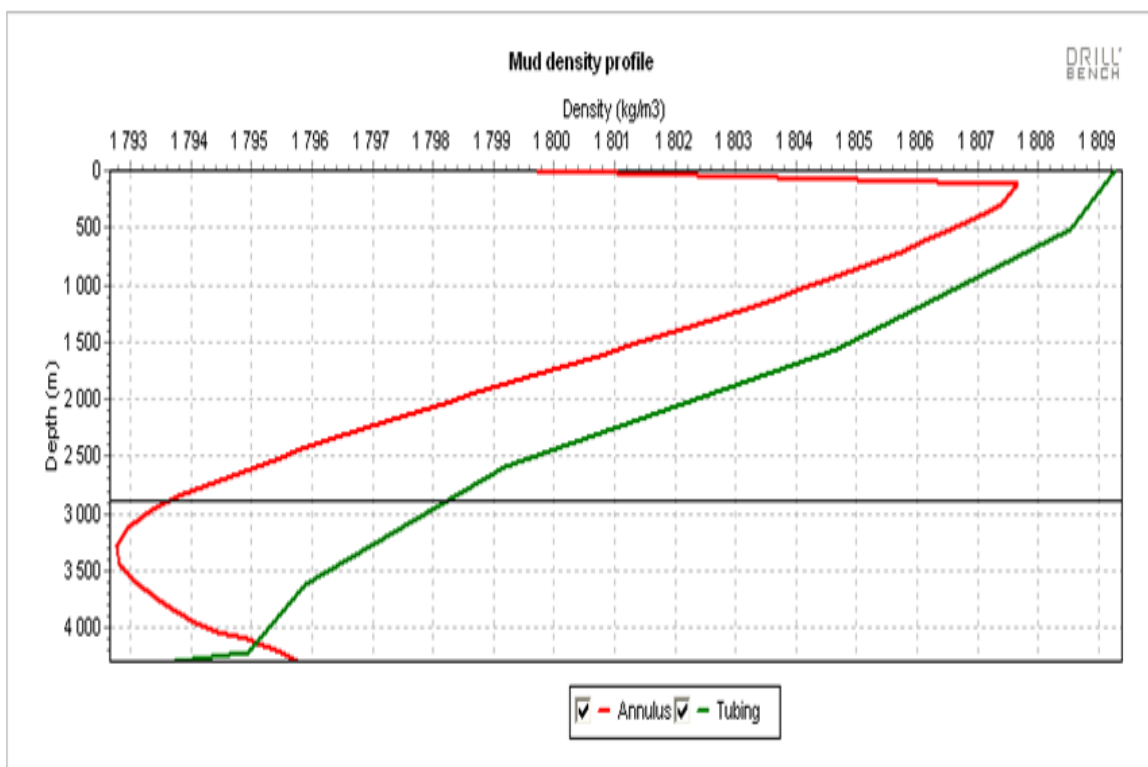


Figure 36 - Temperature effect on density [39].

- Implementing Matlab as a second programming language
The idea is that the Excel sheet will function as a very simplified steady state hydraulic model calculating pressures in a well. A steady state model gives only a snapshot of the well condition at a given time. However, by introducing Discovery Web we were able to do the simulations over time. Excel is a great tool if you need to have the values and formulas for inputs and outputs in tables in front of you. Matlab is best for “sophisticated” math, especially regarding large data sets; like matrix algebra and differential equations. If one were to implement a transient flow model, Matlab would have been the right tool due to the introduction of space discretization grids. Where local calculation of hydrostatic pressure and frictional losses will take into account increasing pressure and temperature versus depth, instead of assuming fixed values in the whole well.

- Improve graphical representation

By taking real-time monitoring a step further, one should make good graphical tools that clearly indicate when something is about to go wrong. For example, by creating a "speedometer look" for the mud weight trend, where the arrow was located in a green area if everything was ok and switched over to the red marked area if the mud weight was too high, or too low.

- Implement an MPD system

The code implemented in Discovery Web already contains the ability to manipulate the choke opening and activate a back-pressure pump. Furthermore, it could be possible to run simulations that show the optimal adjustments to maintain a constant well pressure during a connection. For a MPD system the ECD formula can be written as Eq. 56.

$$ECD = \rho + \frac{\Delta P_f + \textit{Choke pressure}}{gh} \quad (56)$$

By starting up the back-pressure pump, one could avoid the drop in ECD during a connection, thus keeping us inside drilling window in challenging environments.

References

1. BP, 2010, *Deepwater Horizon Accident Investigation Report*, [Report] [cited 03.03.2014], Available from: <https://http://www.itslearning.com/file/download.aspx?FileID=1055334&FileVersionID=-1>.
2. Cayeux, E., et al., 2012, *Early Symptom Detection Based on Real-Time Evaluation of Downhole Conditions: Principles and Results from several North Sea Drilling Operations*, [Conference Paper] SPE-150422-MS, presented at SPE Intelligent Energy International, Utrecht, The Netherlands, 27-29 March 2012.
3. Kongsberg Oil & Gas Technologies, 2012, *Discovery Web - an integrated IO / collaboration and visualization platform*, [PowerPoint presentation prepared for: SBBU].
4. Falconer, I.G., J.P. Belaskie, and F. Variava, 1987, *Applications of a Real Time Wellbore Friction Analysis*, [Conference Paper] SPE-18649-MS, presented at SPE/IADC Drilling Conference, New Orleans, Louisiana, February 28-March 3, 1989.
5. Niedermayr, M., et al., 2010, *Case Study--Field Implementation of Automated Torque-and-Drag Monitoring for Maari Field Development*, [Conference Paper] SPE-128243-MS, presented at IADC/SPE Drilling Conference and Exhibition, New Orleans, Louisiana, USA, 2-4 February 2010.
6. Cayeux, E. and B. Daireaux, 2009, *Early Detection of Drilling Conditions Deterioration Using Real-Time Calibration of Computer Models: Field Example from North Sea Drilling Operations*, [Conference Paper] SPE-119435-MS, presented at SPE/IADC Drilling Conference and Exhibition, Amsterdam, The Netherlands, 17-19 March 2009.
7. Aadnoy, B.S. and S. Ong, *Introduction to special issue on Borehole Stability*, Petroleum Science and Engineering, 2003, 38(3-4): p. 79-82.
8. Hovda, S., et al., 2008, *Potential of Ultra High-Speed Drill String Telemetry in Future Improvements of the Drilling Process Control*, [Conference Paper] SPE-115196-MS, presented at IADC/SPE Asia Pacific Drilling Technology Conference and Exhibition, Jakarta, Indonesia, 25-27 August 2008.
9. Strand, S., 1998, *Øvinger i bore- og brønnvæsker*, Høgskolen i Stavanger, Stavanger.
10. Kolle, G. and R. Mesel, 1998, *Brønnvæsker: for VK1 brønnteknikk*, Vett & Viten, Nesbru, ISBN: 82-412-0322-5.
11. Okafor, M.N. and J.F. Evers, 1992, *Experimental Comparison of Rheology Models for Drilling Fluids*, [Conference Paper] SPE-24086-MS, presented at Western Regional Meeting, Bakersfield, California, March 30-April 1, 1992.

12. Kok, M.V. and T. Alikaya, *Effect of Polymers on the Rheological Properties of KCl/Polymer Type Drilling Fluids*, Energy Sources, 2005, 27(5): p. 405-415.
13. Ochoa, M.V., 2006, *Analysis of Drilling Fluid Rheology and Tool Joint Effect to Reduce Errors in Hydraulics Calculations*, [PhD Thesis], Texas A&M University, p. 99.
14. Skaugen, E., 1997, *Kompendium i boring*, Høyskolen i Stavanger, Stavanger.
15. Azar, J.J. and G.R. Samuel, 2007, *Drilling engineering*, [Book], PennWell Corp., Tulsa, Oklahoma, USA.
16. Gabolde, G. and J.-P. Nguyen, 2006, *Drilling data handbook*, [Book], Editions Technip, Paris. ISBN: 2-7108-0871-4.
17. Larsen, T.I., A.A. Pilehvari, and J.J. Azar, *Development of a New Cuttings-Transport Model for High-Angle Wellbores Including Horizontal Wells*, SPE Drilling & Completion, 1997, 12(02): p. 129-136. SPE-25872-PA.
18. Cayeux, E., et al., 2013, *Real-Time Evaluation of Hole Cleaning Conditions Using a Transient Cuttings Transport Model*, [Conference Paper] SPE-163492-MS, presented at SPE/IADC Drilling Conference and Exhibition, Amsterdam, The Netherlands, 5-7 March 2013.
19. Evje, S. and K.K. Fjelde, *Hybrid Flux-Splitting Schemes for a Two-Phase Flow Model*, Journal of Computational Physics, 2002, 175(2): p. 674-701.
20. V. C. Kelessidis, G.M., A. Koutroulis, T. Michalakis, *Significant parameters affecting efficient cuttings transport in horizontal and deviated wellbores in coil tubing drilling: A critical review*, 1st International Symposium of the Faculty of Mines (ITU) on Earth Sciences and Engineering, 2002, 19(04): p. 213-227. SPE-81746-PA.
21. Standards Norway, *Well integrity in drilling and well operations*, in *NORSOK D-010 Rev. 4*. 2013.
22. Vett & Viten, E.A., 2008, *Borekunnskap: modul 0401*, Nesbru.
23. NOV, 2013, *Intelliserv Product Catalog*, [Web Page], [cited 04.06.2014], Available from:
http://www.nov.com/uploadedFiles/Business_Groups/Downhole/IntelliServ/LandingPage/IntelliServ-Product-Catalog-D392004875-MKT-001-Rev-01.pdf.
24. Segura, J. and Weatherford International, *Drillpipe Cutting at Ultrahigh Pressure Proven for Remediating Deepwater Stuck-Pipe Hazards*, SPE Drilling & Completion, 2011, 26(04): p. 569-577. SPE-139511-PA.
25. Nakhleh, J.T.Ø., 2009, *Drilling problem scenarios for Simulation and Training*, [BSc Thesis], Institute of Petroleum Technology, University of Stavanger, p. 55.
26. Belayneh, M., 2013, *MPB 110 Geology and Petro-physics lecture note*, [Lecture].

27. Aadnoy, B.S., K. Larsen, and P.C. Berg, 1999, *Analysis of Stuck Pipe in Deviated Boreholes*, [Conference Paper] SPE-56628-MS, presented at SPE Annual Technical Conference and Exhibition, Houston, Texas, USA, 3-6 October 1999.
28. Wang, H., et al., *Best Practice in Understanding and Managing Lost Circulation Challenges*, SPE Drilling & Completion, 2008, 23(02): p. 168-175. SPE-95895-PA.
29. Sekal, 2014, *DrillScene Advanced Monitoring*, [Web Page], [cited 11.03.2014], Available from: <http://sekal.com/?id=1017>.
30. Cayeux, E., et al., 2012, *Advanced Drilling Simulation Environment for Testing New Drilling Automation Techniques*, [Conference Paper] SPE-150941-MS, presented at IADC/SPE Drilling Conference and Exhibition, San Diego, California, USA, 6-8 March 2012.
31. Iversen, F., et al., *Drilling Automation: Potential for Human Error*, SPE Drilling & Completion, 2013, 28(01): p. 45-59. SPE-151474-PA.
32. Rommetveit, R., et al., 2008, *eDrilling used on Ekofisk for Real-Time Drilling Supervision, Simulation, 3D Visualization and Diagnosis*, [Conference Paper] SPE-112109-MS, presented at SPE Intelligent Energy Conference and Exhibition, Amsterdam, The Netherlands, 25-27 February 2008.
33. Schlumberger, 2014, *Drillbench Dynamic Drilling Simulation Software*, [Web Page], [cited 05.04.2014], Available from: <http://www.software.slb.com/products/foundation/Pages/drillbench.aspx>.
34. Rommetveit, R., et al., 2004, *Use of Dynamic Modeling in Preparations for the Gullfaks C-5A Well*, [Conference Paper] SPE-91243-MS, presented at SPE/IADC Underbalanced Technology Conference and Exhibition, Houston, Texas, USA, 11-12 October 2004.
35. Kongsberg Oil & Gas Technologies, 2014, *Drilling Software Business Unit*, [PDF handout].
36. Kongsberg Oil & Gas Technologies, 2012, *Welcome to Discovery Web*, [Help Manual], [cited 19.02.2014], Available from: http://kidemo.intellifield.no/DWeb/Help/Discovery_Web.htm - Topics/Welcome.htm.
37. Kongsberg Oil & Gas Technologies, 2014, *Discovery Web Interface*, [Pictures], Screenshots from program.
38. Reel Well AS, 2014, *JIP: ERD beyond 20 km*, [Web Page], [cited 27.05.2014], Available from: <http://www.reelwell.no/Extended-Reach-Drilling/JIP-ERD-beyond-20-km>.
39. Belayneh, M., 2014, *Chapter 6: Well Control*, PET-525, [Lecture].

Appendix A

Conservation laws

When dealing with mass balance there are three fundamental laws that also apply to well and pipe flow, they are as follow: conservation of mass, momentum and energy. If we consider conservation of mass in a pipe segment it can be expressed in the following manner [19]:

Mass flux in = Mass flux out

Mass at new time level (n+1) = mass at old time level (n) + [(mass flux in)-(mass flux out)]

By introducing the drift flux model, which is a simplified version of the more fundamental two fluid models, it is possible to describe one and two phase flow in pipe at a transient level. The model is derived from the Navier Stokes equations and combines the momentum equations for the mixture and an additional equation expresses the slippage between gas and liquid. This surely makes the model dependent on the type of two-phase flow pattern (bubble, dispersed bubble, slug and annular flow). The model describes 1D flow.

Transient flow model

Consider a well segment, where t is time and z is the flow direction through this segment.

The following nonlinear partial differential equations for conservation of mass and momentum across this segment can be expressed as follows [19]:

Conservation of liquid mass:

$$\frac{\partial}{\partial t}(A\rho_l\alpha_l) + \frac{\partial}{\partial z}(A\rho_l\alpha_lv_l) = s_1 \quad (57)$$

Conservation of gas mass:

$$\frac{\partial}{\partial t}(A\rho_g\alpha_g) + \frac{\partial}{\partial z}(A\rho_g\alpha_gv_g) = s_2 \quad (58)$$

Conservation of mixture momentum:

$$\frac{\partial}{\partial t}(A(\rho_l\alpha_lv_l + \rho_g\alpha_gv_g)) + \frac{\partial}{\partial z}(A(\rho_l\alpha_lv_l^2 + \rho_g\alpha_gv_g^2)) + A\frac{\partial}{\partial z}p = -A(\rho_{mix}g + \frac{\Delta p_{fric}}{\Delta z}) \quad (59)$$

where A is area, ρ_i is phase densities (liquid I = l, gas i = g), v_i is phase velocities, p is pressure, s_i is source (inflow, leakage, phase transfer between phases), g is gravity constant, α_i is phase volume fractions taking values between 0 and 1, $\rho_{mix} = \rho_l\alpha_l + \rho_g\alpha_g$, $v_{mix} = \alpha_lv_l + \alpha_gv_g$, μ_l is phase viscosities, $\mu_{mix} = \mu_l\alpha_l + \mu_g\alpha_g$, d_{out} is outer diameter in annulus and d_{in} is inner diameter in annulus and corresponds to outer diameter of drill string.

To be able to solve the equations, which contains a certain number of unknowns it might be necessary to add some closure laws, to ensure that the number of equations is the same as the number of unknowns [19].

Appendix B

1. Rheology and Hydraulics Equations for Bingham Plastics Model [13].

Pipe Flow	Annular Flow
$v_p = \frac{0.408Q}{D_p^2}$	$v_a = \frac{0.408Q}{D_2^2 - D_1^2}$
$\mu_p = \theta_{600} - \theta_{300}$ $\tau_y = \theta_{300} - \mu_p$	
$\mu_a = \mu_p + \frac{5\tau_y D_p}{v_p}$	$\mu_a = \mu_p + \frac{5\tau_y (D_2 - D_1)}{v_a}$
$N_{Re} = \frac{928D_p v_p \rho}{\mu_a}$ <p>If $N_{Re} < 2100$</p> $f_p = \frac{16}{N_{Re}}$	$N_{Re} = \frac{757(D_2 - D_1) v_p \rho}{\mu_a}$ <p>If $N_{Re} < 2100$</p> $f_p = \frac{16}{N_{Re}}$
$He = \frac{37,100\rho\tau_y D_p^2}{\mu_p^2}$ $N_{Re} = \frac{928D_p v_p \rho}{\mu_p}$	$He = \frac{37,100\rho\tau_y D_e^2}{\mu_p^2}$ $D_e = 0.816(D_2 - D_1)$ $N_{Re} = \frac{928D_e v_a \rho}{\mu_p}$
Hedström number.	$f_{a,p} = \frac{0.0791}{N_{Re}^{0.25}}$
$\left(\frac{dp}{dL}\right) = \frac{f_p v_p^2 \rho}{25.81D_p}$ $\Delta p = \left(\frac{dp}{dL}\right) \Delta L$	$\left(\frac{dp}{dL}\right) = \frac{f_p v_p^2 \rho}{25.81(D_2 - D_1)}$ $\Delta p = \left(\frac{dp}{dL}\right) \Delta L$
$\Delta p_{Nozzles,psi} = \frac{156\rho q^2}{(D_{n1}^2 + D_{n2}^2 + D_{n3}^2)^2}$	

2. Rheology and Hydraulics Equations for Herschel-Bulkley Model [13].

Pipe Flow	Annular Flow
$\tau_0 = \frac{\tau^{*2} - \tau_{min}\tau_{max}}{2\tau^* - \tau_{min} - \tau_{max}}$ $\gamma^* = \sqrt{\gamma_{min}\gamma_{max}}$ $\log(\tau - \tau_0) = \log(K) + n \log(\gamma)$	
$v_p = \frac{0.408Q}{D_p^2}$	$v_a = \frac{0.408Q}{D_2^2 - D_1^2}$
$N_{Re} = \left[\frac{2(3n+1)}{n} \right] \left[\frac{\rho v_p^{(2-n)} \left(\frac{D_p}{2}\right)^n}{\tau_0 \left(\frac{D_p}{2v_p}\right)^n + K \left[\frac{(3n+1)}{nC_c}\right]^n} \right]$	$N_{Re} = \left[\frac{4(2n+1)}{n} \right] \left[\frac{\rho v_p^{(2-n)} \left(\frac{D_2 - D_1}{2}\right)^n}{\tau_0 \left(\frac{D_p}{2v_a}\right)^n + K \left[\frac{2(2n+1)}{nC_a}\right]^n} \right]$
$N_{Re\ cr} = \left[\frac{4(3n+1)}{ny} \right]^{\frac{1}{1-z}}$	$N_{Re\ cr} = \left[\frac{8(2n+1)}{ny} \right]^{\frac{1}{1-z}}$
$y = \frac{\log n + 3.93}{50}$ $z = \frac{1.75 - \log n}{7}$	
Laminar if: $N_{Re} < N_{Re\ cr}$	
$\left(\frac{dp}{dL}\right) = \frac{4k}{14400D_p} \left\{ \left(\frac{\tau_0}{k}\right) + \left[\frac{(3n+1)}{nC_c}\right] \left(\frac{8Q}{\pi D_p^2}\right)^n \right\}$	$\left(\frac{dp}{dL}\right) = \frac{4k}{14400(D_2 - D_1)} \left\{ \left(\frac{\tau_0}{k}\right) + \left[\frac{16(2n+1)}{nC_a(D_2 - D_1)}\right] \left(\frac{Q}{\pi \left(\left(\frac{D_2}{2}\right)^2 - \left(\frac{D_1}{2}\right)^2\right)}\right)^n \right\}$
Turbulent if: $N_{Re} > N_{Re\ cr}$	
$f_p = y(C_c N_{Re})^{-z}$	$f_a = y(C_a^* N_{Re})^{-z}$
$C_c = 1 - \left(\frac{1}{2n+1}\right) \frac{\tau_0}{\tau_0 + k \left(\frac{(3n+1)Q}{n\pi \left(\frac{D_p}{2}\right)^3}\right)^n}$	$C_a^* = 1 - \left(\frac{1}{1+n}\right) \frac{\tau_0}{\tau_0 + k \left\{ \left[\frac{2(2n+1)}{n(D_2/2 - D_1/2)}\right] \left[\frac{Q}{\pi \left(\left(\frac{D_2}{2}\right)^2 - \left(\frac{D_1}{2}\right)^2\right)}\right] \right\}^n}$
$\left(\frac{dp}{dL}\right) = \frac{f_p Q^2 \rho}{144\pi^2 D_p^2}$	$\left(\frac{dp}{dL}\right) = \frac{f_a Q^2 \rho}{144\pi^2 (D_2 - D_1)(D_2^2 - D_1^2)^2}$
$\Delta p = \left(\frac{dp}{dL}\right) \Delta L$	
$\Delta p_{Nozzles,psi} = \frac{156\rho Q^2}{(D_{n1}^2 + D_{n2}^2 + D_{n3}^2)^2}$	

3. Rheology and Hydraulics Equations for Robertson-Stiff Mode [13].

Pipe Flow	Annular Flow
$C = \frac{\gamma_{min}\gamma_{max} - \gamma^{*2}}{2\gamma^* - \gamma_{min} - \gamma_{max}}$ $\log(\tau) = \log(A) + B \log(\gamma)$	
$v_p = \frac{0.408Q}{D_p^2}$	$v_a = \frac{0.408Q}{D_2^2 - D_1^2}$
$N_{Re} = \frac{89100\rho v_p^{2-B}}{A} \left(\frac{0.416D_p}{3 + \frac{1}{B}} \right)^B$	$N_{Re} = \frac{109000\rho v_a^{2-B}}{A} \left(\frac{0.0208(D_2 - D_1)}{2 + \frac{1}{B}} \right)^B$
Laminar if: $N_{Re} \leq 3470 - 1370B$	
$\left(\frac{dp}{dl} \right) = 8.33E - 4 \times 2^{2+B} \times A \left\{ \left(\frac{1+3B}{B} \right) \left[\frac{0.2v_p + \frac{C}{6}D_p}{D_p^{\left(\frac{1+B}{B}\right)}} \right] \right\}^B$	$\left(\frac{dp}{dl} \right) = 8.33E - 4 \times 4^{1+B} \times A \left\{ \left(\frac{1+2B}{B} \right) \left[\frac{0.2v_a + \frac{C}{8}(D_2 - D_1)}{(D_2 - D_1)^{\left(\frac{1+B}{B}\right)}} \right] \right\}^B$
Turbulent if: $N_{Re} \geq 4270 - 1370B$	
$a = \frac{\log B + 3.93}{50}$ $b = \frac{1.75 - \log B}{7}$	
$f_p = \frac{a}{N_{Re}^b}$ $\left(\frac{dp}{dL} \right) = \frac{f_p v_p^2 \rho}{25.81 D_p}$	$f_a = \frac{a}{N_{Re}^b}$ $\left(\frac{dp}{dL} \right) = \frac{f_a v_a^2 \rho}{25.81 (D_2 - D_1)}$
$\Delta p = \left(\frac{dp}{dL} \right) \Delta L$	
$\Delta p_{Nozzles,psi} = \frac{156\rho Q^2}{(D_{n1}^2 + D_{n2}^2 + D_{n3}^2)^2}$	

Appendix C

1. Excel Spreadsheet - FANN Rheology Data

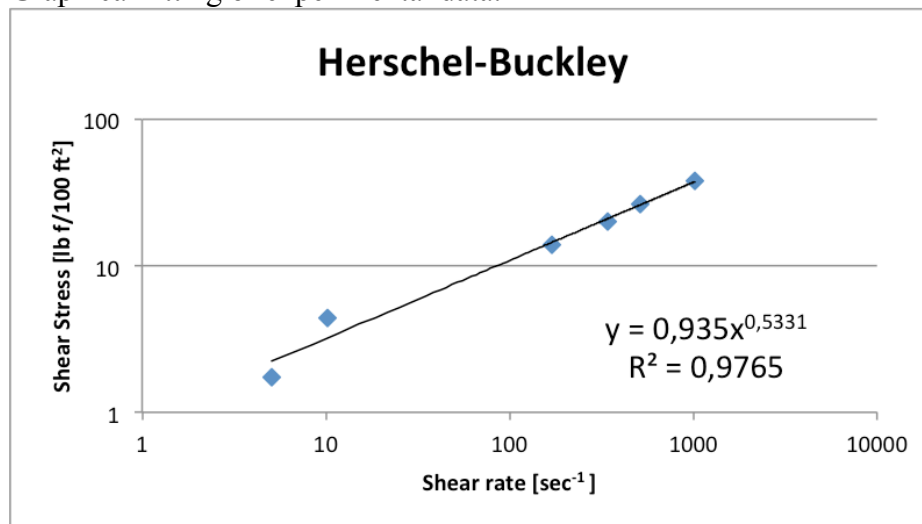
Excel Spreadsheet using Fann rheology data for determination of the different rheological model parameters.

Input:

Fann data				
Reading	Measured shear stress	Shear rate (RPM)	Shear rate (Oil Field)	Shear Stress (Oil Field)
θ_{600}	54,50	600	1021,8	58,15
θ_{300}	43,50	300	510,9	46,41
θ_{200}	37,50	200	340,6	40,01
θ_{100}	32,00	100	170,3	34,14
θ_6	23,00	6	10,218	24,54
θ_3	20,50	3	5,109	21,87

Output - Herschel-Bulkley:

Graphical fitting of experimental data:



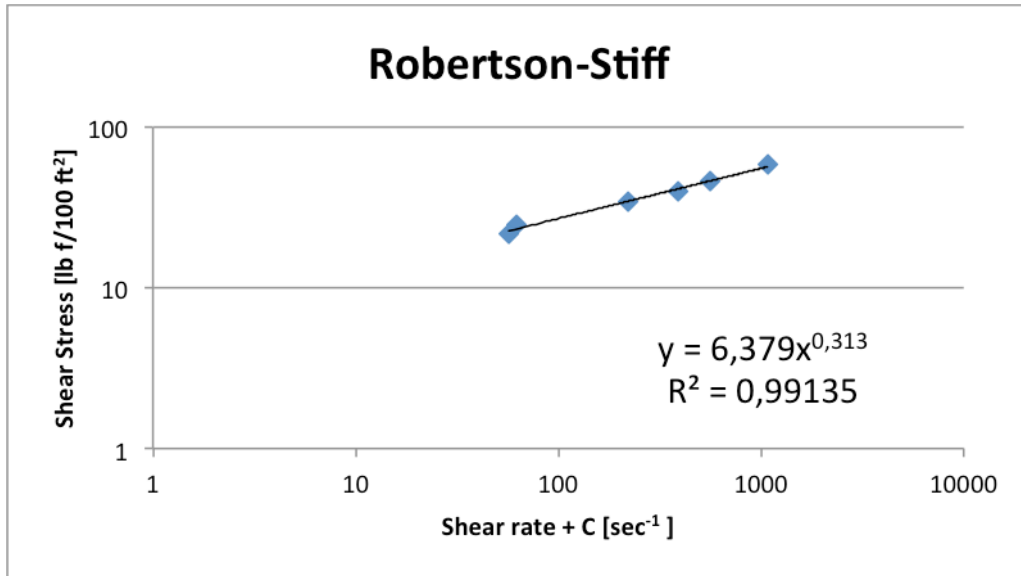
Regression used to fit of experimental data:

Herschel-Bulkley Model			
Shear Stress (corr) (Herschel-Bulkley)	Shear rate (Oil Field)	Shear Stress (Herschel-Bulkley)	error
38,01	1021,80	57,72	0,001
26,28	510,90	46,11	0,001
19,88	340,60	41,06	0,004
14,01	170,30	34,60	0,002
4,40	10,22	23,36	0,008
1,74	5,11	22,37	0,004
Total error:			0,344

Calculated values	
τ_0	28,26
τ^*	20,14
K	0,9350
n	0,5331

Output - Robertson-Stiff Model:

Graphical fitting of experimental data:



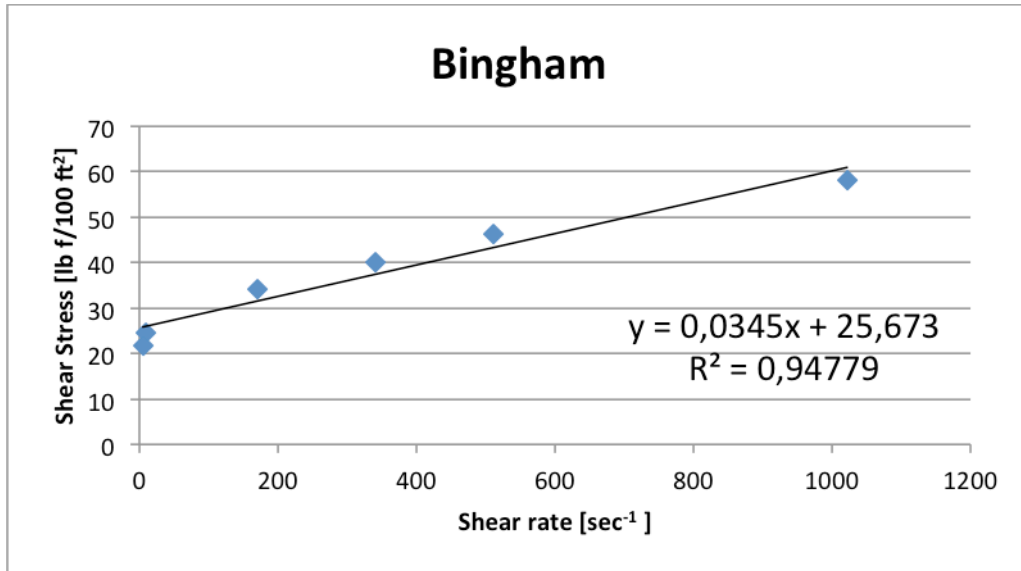
Regression used to fit of experimental data:

Robertson-Stiff Model			
Shear rate (corr) (Robertson-Stiff)	Shear Stress (Oil Field)	Shear Stress (Robertson-Stiff)	error
1073,81	58,15	56,70	0,004
562,91	46,41	46,32	0,000
392,61	40,01	41,38	0,006
222,31	34,14	34,63	0,002
62,23	24,54	23,25	0,009
57,12	21,87	22,63	0,006
Total error:			0,452

Calculated values	
AA	6.379
A	3054.25
B	0.313
C	52.01

Output - Bingham Model:

Graphical fitting of experimental data:



Regression and formula used to fit of experimental data:

Bingham Model			
Shear rate (corr) (Bingham)	Shear Stress (Oil Field)	Shear Stress (Bingham)	error
1021,8	58,15	60,96	0,008
510,9	46,41	42,32	0,011
340,6	40,01	37,43	0,011
170,3	34,14	31,55	0,013
10,2	24,54	26,03	0,010
5,1	21,87	25,85	0,030
Total error:			1,382

	Formula	Graphic
μ_p	11,00	16,53
τ_y	32,50	25,67

2. Implemented models in Discovery Web

Contains the Discovery Web code that is implemented into the simulations.

2.1. Bingham Frictional Model

Static Inputs:		
Parameter:	Value:	Unit:
YP	11,00	lb/100ft2
PV	32,50	cP
BackPPump	0,00	lpm
VcutTransp	1,02	m/s
ChokeOD	3,00	inch
ChokeOpen	1,00	0-1
AnnCsgL1	3500,00	m
AnnCsgL2	500,00	m
AnnCsgID1	5,00	inch
AnnCsgID2	5,00	inch
AnnCsgID3	6,50	inch
DPL2	200,00	m
DPID1	4,27	inch
DPID2	2,50	inch
BitNoz	6,00	
BitNozID	12,00	
Motor	13,80	bar
MWD	13,80	bar
SurfEq	2,00	bar
dcuttings	2,50	sg
PackOffAnnL1	0,00	(0-1) %
PackOffAnnL2	0,00	(0-1) %
PackOffAnnL3	0,00	(0-1) %
CutCons	0,01	(0-1) %
InitialWellDepth	4000,00	m

Variable Input:		
Parameter:	Value:	Unit:
Q	2000	lpm
d	1,60	sg
ROP	40	m/h
TIME	4	h

Output			
Parameter:	Value:	Unit:	Discovery Web Formula:
dout	1,61	sg	$((1 - \text{CutCons}) * \text{din} + \text{dcuttings} * \text{CutCons}) * 8.33$
AnnCsgOD1	8,53	inch	$\text{AnnCsgOD1} * (1 - \text{PackOffAnnL1})$
AnnCsgOD2	8,50	inch	$\text{AnnCsgOD2} * (1 - \text{PackOffAnnL2})$
AnnCsgOD3	8,50	inch	$\text{AnnCsgOD3} * (1 - \text{PackOffAnnL3})$
DPL1	3960,00	m	$(\text{AnnCsgL1} + \text{AnnCsgL2} - \text{DPL2}) + (\text{ROP} * \text{TIME})$
DPV1	3,61	m/s	$Q / 1000 / 60 / (3.14 / 4 * (\text{DPID1} * 0.0254)^2)$
DPV2	10,53	m/s	$Q / 1000 / 60 / (3.14 / 4 * (\text{DPID2} * 0.0254)^2)$
DPVCri1	1,15		$(2.48 / d / \text{DPID1} * (\text{PV} + \text{SQRT}(\text{PV}^2 + 73.57 * \text{YP} * \text{DPID1}^2 * d))) / 60$
DPVCri2	1,32		$(2.48 / d / \text{DPID2} * (\text{PV} + \text{SQRT}(\text{PV}^2 + 73.57 * \text{YP} * \text{DPID2}^2 * d))) / 60$
DPFricLam1	20,33	bar	$((\text{DPL1} * Q * \text{PV}) / (612.95 * \text{DPID1}^4)) + ((\text{YP} * \text{DPL1}) / (13.26 * \text{DPID1})) / 100$
DPFricLam2	6,09	bar	$((\text{DPL2} * Q * \text{PV}) / (612.95 * \text{DPID2}^4)) + ((\text{YP} * \text{DPL2}) / (13.26 * \text{DPID2})) / 100$
DPFricTurb1	105,72	bar	$(\text{DPL1} * d^{0.8} * Q^{1.8} * \text{PV}^{0.2} / (901.63 * \text{DPID1}^{4.8})) / 100$
DPFricTurb2	69,73	bar	$(\text{DPL2} * d^{0.8} * Q^{1.8} * \text{PV}^{0.2} / (901.63 * \text{DPID2}^{4.8})) / 100$

Parameter:	Value:	Unit:	Discovery Web Formula:
DPFricLamTurb1	105,72	bar	IF(DPV1<DPVCri1,DPFricLam1,DPFricTurb1)
DPFricLamTurb2	69,73	bar	IF(DPV2<DPVCri2,DPFricLam2,DPFricTurb2)
WellDepth	4160,00	m	InitialWellDepth+(ROP*TIME)
AnnCsgL3	160,00	m	(ROP*TIME)
LossShoe1	0,00	m	IF(LossShoe=1,IF(WellDepth>=4060,AnnCsgL1,0),0)
LossTD1	0,00	m	IF(LossTD=1,IF(WellDepth>=4120,AnnCsgL1,0),0)
LossTD2	0,00	m	IF(LossTD=1,IF(WellDepth>=4120,AnnCsgL2,0),0)
LossTD3	0,00	m	IF(LossTD=1,IF(WellDepth>=4120,AnnCsgL3,0),0)
VelAnn1	1,38	m/s	$(Q^4)/(60*1000*3.14*((AnnCsgOD1*0.0254)^2-(AnnCsgID1*0.0254)^2))$
VelAnn2	1,39	m/s	$(Q^4)/(60*1000*3.14*((AnnCsgOD2*0.0254)^2-(AnnCsgID2*0.0254)^2))$
VelAnn3	2,19	m/s	$(Q^4)/(60*1000*3.14*((AnnCsgOD3*0.0254)^2-(AnnCsgID3*0.0254)^2))$
LamTurb1	1,18		$(PV+SQRT(PV^2+40.05*YP*(AnnCsgOD1-AnnCsgID1)^2*dout))*3.04/(AnnCsgOD1-AnnCsgID1)/d/60$
LamTurb2	1,18		$(PV+SQRT(PV^2+40.05*YP*(AnnCsgOD2-AnnCsgID2)^2*dout))*3.04/(AnnCsgOD2-AnnCsgID2)/d/60$
LamTurb3	1,50		$(PV+SQRT(PV^2+40.05*YP*(AnnCsgOD3-AnnCsgID3)^2*dout))*3.04/(AnnCsgOD3-AnnCsgID3)/d/60$
AnnFricLam1	17,58		$(AnnCsgL1*Q*PV/(408.63*(AnnCsgOD1+AnnCsgID1)*(AnnCsgOD1-AnnCsgID1)^3))+YP*AnnCsgL1/13.26/(AnnCsgOD1-AnnCsgID1)/100$
AnnFricLam2	2,56		$(AnnCsgL2*Q*PV/(408.63*(AnnCsgOD2+AnnCsgID2)*(AnnCsgOD2-AnnCsgID2)^3))+YP*AnnCsgL2/13.26/(AnnCsgOD2-AnnCsgID2)/100$
AnnFricLam3	2,78		$(AnnCsgL3*Q*PV/(408.63*(AnnCsgOD3+AnnCsgID3)*(AnnCsgOD3-AnnCsgID3)^3))+YP*AnnCsgL3/13.26/(AnnCsgOD3-AnnCsgID3)/100$
AnnFricTurb1	26,57		$1.8*(AnnCsgOD1-AnnCsgID1)^3)/100$
AnnFricTurb2	3,91		$1.8*(AnnCsgOD2-AnnCsgID2)^3)/100$
AnnFricTurb3	5,55		$IF(LossTD3>=120,((120*dout^0.8*Q^1.8*PV^0.2/(706.96*(AnnCsgOD3+AnnCsgID3)^3))/100),((AnnCsgL3*d^0.8*Q^1.8*PV^0.2/(706.96*(AnnCsgOD3+AnnCsgID3)^3))/100),((AnnCsgL3*d^0.8*Q^1.8*PV^0.2/(706.96*(AnnCsgOD3-AnnCsgID3)^3))/100),((AnnCsgL3*d^0.8*Q^1.8*PV^0.2/(706.96*(AnnCsgOD3-AnnCsgID3)^3))/100))$
AnnFric1	26,57	bar	IF(LossShoe1=3500,0,IF(LossTD1=3500,0,IF((VelAnn1>LamTurb1),AnnFricTurb1,AnnFricLam1)))
AnnFric2	3,91	bar	IF(LossTD2=500,0,IF((VelAnn2>LamTurb2),AnnFricTurb2,AnnFricLam2))
AnnFric3	5,55	bar	IF((VelAnn3>LamTurb3),AnnFricTurb3,AnnFricLam3)
FlowAChoke	0	lpm	Q+BackPPump
CumLAnn	4160,00	m	AnnCsgL1+AnnCsgL2+AnnCsgL3
CumLDP	4160,00	m	DPL1+DPL2
ChokeID	1,200	(0-1)	ChokeOD-(ChokeOD*ChokeOpen)
ChokeArea	2,543	in2	$3.14/4*(ChokeOD-ChokeID)^2$
BitNozTFA	0,6623	inch2	$(BitNozID/32)^2*3.14/4*BitNoz$
BitNozPloss	54,62	bar	$(d*Q^2/2959.41/0.95^2/BitNozTFA^2)/100$
SumAnnFric	36,03	bar	IF(Q>0,(AnnFric1+AnnFric2+AnnFric3),0)
SumEqFric	29,60	bar	IF(Q>0,(Motor+MWD+SurfEq),0)
SumDPFric	175,45	bar	(DPFricTurb1+DPFricTurb2)
ChokePress	0	bar	$(dout*FlowAChoke^2/(2959.41*0.95^2)/ChokeArea^2)/100$
PumpPress	299,42	bar	SumAnnFric+BitNozPloss+SumEqFric+SumDPFric+ChokePress
ECDCalc	1,6983	sg	$((dout*CumLAnn*0.0981)+SumAnnFric+ChokePress)/(CumLAnn*0.0981)$
Hydrostatic	693.1	bar	ECDCalc*CumLAnn*0.0981

2.2. Herschel-Bulkley Frictional Model

Static Input:		
Parameter:	Value:	Unit:
BackPPump	0,00	lpm
ChokeOD	3,00	inch
ChokeOpen	1,00	0-1
AnnCsgL1	3500,00	m
AnnCsgL2	500,00	m
AnnCsgID1	5,00	inch
AnnCsgID2	5,00	inch
AnnCsgID3	6,50	inch
DPL2	200,00	m
DPID1	4,27	inch
DPID2	2,50	inch
BitNoz	6,00	
BitNozID	12,00	
Motor	13,80	bar
MWD	13,80	bar
SurfEq	2,00	bar
dcuttings	2,50	sg
PackOffAnnL1	0,00	(0-1) %
PackOffAnnL2	0,00	(0-1) %
PackOffAnnL3	0	(0-1) %
Porosity	0,2	
Washoutdepth	1500	m
Sensor1Depth	1000	m
Sensor2Depth	2000	m
Sensor3Depth	3000	m

Variable Input:		
Parameter:	Value:	Unit:
Qin	2000	lpm
Qloss	50	lpm
din	1,60	sg
ROP	40	m/h
TIME	4	h

Output - Above WashoutDepth			
Parameter:	Value:	Unit:	Discovery Web Formula:
d	13,33	ppg	$0.26417 * Q_{in}$
Q	528,34	gpm	$8.33 * d_{in}$
Ro	18,87	degree	$(2 * R_3 - R_6)$
To (FANN)	20,14		$0.511 * R_0$
n (FANN)	0,533	unitless	$3.32 * \log((R_{600} - R_0) / (R_{300} - R_0))$
K (FANN)	0,935	lbf. ⁿ /100f ^t	$0.511 * ((R_{300} - R_0) / (511^n))$ $(ROP * 0.000277778 * ((PI()/4) * (0.0254 * AnnCsgOD3)^2) * (1 - Porosity)) / ((Q_{in} * 1.66667 * 10^{-5}) + (((ROP * 0.000277778 * ((PI()/4) * (0.0254 * AnnCsgOD3)^2) * (1 - Porosity))))$
CutCons	0,010		
dout	13,40	ppg	$((1 - CutCons) * d_{in} + d_{cuttings} * CutCons) * 8.33$
AnnCsgOD1	8,53	inch	$8.53 * (1 - PackOffAnnL1)$
AnnCsgOD2	8,50	inch	$8.50 * (1 - PackOffAnnL2)$
AnnCsgOD3	8,50	inch	$8.50 * (1 - PackOffAnnL3)$

Parameter:	Value:	Unit:	Discovery Web Formula:
DPV1	11,82	ft/s	$0.408 * Q / DPID1^2$
DPV2	34,49	ft/s	$0.408 * Q / DPID2^2$
Cc1	0,7595	unitless	$1 - \frac{(1/(2^{*n+1})) * (T0/(T0+K * (((3^{*n+1}) * 0.002228 * Q) / (n * PI) * ((DPID1/12)/2)^3))^{*n})}{1 - \frac{(1/(2^{*n+1})) * (T0/(T0+K * (((3^{*n+1}) * 0.002228 * Q) / (n * PI) * ((DPID2/12)/2)^3))^{*n})}{(2^{*n+1})/n * (7.48 * d * DPV1^{(2-n)} * (0.5 * (DPID1/12))^{*n}) / ((T0 * ((DPID1/12) * 0.5 / DPV1)^n) + K * ((3^{*n+1}) / (n * Cc1))^{*n})}$
Cc2	0,8570	unitless	$1 - \frac{(1/(2^{*n+1})) * (T0/(T0+K * (((3^{*n+1}) * 0.002228 * Q) / (n * PI) * ((DPID2/12)/2)^3))^{*n})}{(2^{*n+1})/n * (7.48 * d * DPV2^{(2-n)} * (0.5 * (DPID2/12))^{*n}) / ((T0 * ((DPID2/12) * 0.5 / DPV2)^n) + K * ((3^{*n+1}) / (n * Cc2))^{*n})}$
ReDP1	3107	unitless	$\frac{(2^{*n+1})/n * (7.48 * d * DPV1^{(2-n)} * (0.5 * (DPID1/12))^{*n}) / ((T0 * ((DPID1/12) * 0.5 / DPV1)^n) + K * ((3^{*n+1}) / (n * Cc1))^{*n})}{(2^{*n+1})/n * (7.48 * d * DPV2^{(2-n)} * (0.5 * (DPID2/12))^{*n}) / ((T0 * ((DPID2/12) * 0.5 / DPV2)^n) + K * ((3^{*n+1}) / (n * Cc2))^{*n})}$
ReDP2	16014	unitless	$\frac{(2^{*n+1})/n * (7.48 * d * DPV1^{(2-n)} * (0.5 * (DPID1/12))^{*n}) / ((T0 * ((DPID1/12) * 0.5 / DPV1)^n) + K * ((3^{*n+1}) / (n * Cc1))^{*n})}{(2^{*n+1})/n * (7.48 * d * DPV2^{(2-n)} * (0.5 * (DPID2/12))^{*n}) / ((T0 * ((DPID2/12) * 0.5 / DPV2)^n) + K * ((3^{*n+1}) / (n * Cc2))^{*n})}$
y	0,073	unitless	$(\log(n) + 3.93) / 50$
z	0,289	unitless	$(1.75 - \log(n)) / 7$
NReDPCr	2584	unitless	$\frac{(4^{*n+1}) / (n * y)^{1/(1-z)}}{(4^{*n+1}) / (n * y)^{1/(1-z)}}$
DPFricLam1	0,026	psi/ft	$\frac{(4^{*n+1}) / (n * y)^{1/(1-z)}}{(4^{*n+1}) / (n * y)^{1/(1-z)}}$
DPFricLam2	0,057	psi/ft	$\frac{(4^{*n+1}) / (n * y)^{1/(1-z)}}{(4^{*n+1}) / (n * y)^{1/(1-z)}}$
fDPTurb1	0,00775	unitless	$y^{*n} * (ReDP1 * Cc1)^{-z}$
fDPTurb2	0,005	unitless	$y^{*n} * (ReDP2 * Cc2)^{-z}$
DPFricTurb1	0,132	psi/ft	$(fDPTurb1 * d * 7.48 * (0.002228 * Q)^2) / (144 * PI)^2 * (DPID1/12)^5$
DPFricTurb2	1,154	psi/ft	$(fDPTurb2 * d * 7.48 * (0.002228 * Q)^2) / (144 * PI)^2 * (DPID2/12)^5$
DPL1	3960	m	$(AnnCsgL1 + AnnCsgL2 - DPL2) + (ROP * TIME)$
DPFricLamTurb1	650	psi	$IF(ReDP1 < NReDPCr, (DPFricLam1 * WashoutDepth / 0.3048), (DPFricTurb1 * WashoutDepth / 0.3048))$
VelAnn1	4,51	ft/s	$(0.408 * Q) / (AnnCsgOD1^2 - AnnCsgID1^2)$
VelAnn2	4,56	ft/s	$(0.408 * Q) / (AnnCsgOD2^2 - AnnCsgID2^2)$
VelAnn3	7,19	ft/s	$(0.408 * Q) / (AnnCsgOD3^2 - AnnCsgID3^2)$
Ca1	0,649	unitless	$1 - \frac{(1/(1+n)) * T0 / (T0 + K * ((2^{*n+1}) / (n * ((AnnCsgOD1 * 0.5 / 12) - (AnnCsgID1 * 0.5 / 12)))) * ((0.002228 * Q) / (PI) * ((AnnCsgOD1 * 0.5 / 12)^2 - (AnnCsgID1 * 0.5 / 12)^2)))^{*n}}{(1/(1+n)) * T0 / (T0 + K * ((2^{*n+1}) / (n * ((AnnCsgOD2 * 0.5 / 12) - (AnnCsgID2 * 0.5 / 12)))) * ((0.002228 * Q) / (PI) * ((AnnCsgOD2 * 0.5 / 12)^2 - (AnnCsgID2 * 0.5 / 12)^2)))^{*n}}$
Ca2	0,651	unitless	$1 - \frac{(1/(1+n)) * T0 / (T0 + K * ((2^{*n+1}) / (n * ((AnnCsgOD2 * 0.5 / 12) - (AnnCsgID2 * 0.5 / 12)))) * ((0.002228 * Q) / (PI) * ((AnnCsgOD2 * 0.5 / 12)^2 - (AnnCsgID2 * 0.5 / 12)^2)))^{*n}}{(1/(1+n)) * T0 / (T0 + K * ((2^{*n+1}) / (n * ((AnnCsgOD3 * 0.5 / 12) - (AnnCsgID3 * 0.5 / 12)))) * ((0.002228 * Q) / (PI) * ((AnnCsgOD3 * 0.5 / 12)^2 - (AnnCsgID3 * 0.5 / 12)^2)))^{*n}}$
Ca3	0,738	unitless	$1 - \frac{(1/(1+n)) * T0 / (T0 + K * ((2^{*n+1}) / (n * ((AnnCsgOD3 * 0.5 / 12) - (AnnCsgID3 * 0.5 / 12)))) * ((0.002228 * Q) / (PI) * ((AnnCsgOD3 * 0.5 / 12)^2 - (AnnCsgID3 * 0.5 / 12)^2)))^{*n}}{(4^{*n+1}) / n * (7.48 * d * VelAnn1^{(2-n)} * (0.5 * ((AnnCsgOD1 - AnnCsgID1) / 12))^{*n}) / ((T0 * ((AnnCsgOD1 - AnnCsgID1) / 12) * 0.5 / VelAnn1)^n) + K * ((2^{*n+1}) / (n * Ca1))^{*n}}$
ReAnn1	756	unitless	$\frac{(4^{*n+1}) / n * (7.48 * d * VelAnn1^{(2-n)} * (0.5 * ((AnnCsgOD1 - AnnCsgID1) / 12))^{*n}) / ((T0 * ((AnnCsgOD1 - AnnCsgID1) / 12) * 0.5 / VelAnn1)^n) + K * ((2^{*n+1}) / (n * Ca1))^{*n}}{(4^{*n+1}) / n * (7.48 * d * VelAnn2^{(2-n)} * (0.5 * ((AnnCsgOD2 - AnnCsgID2) / 12))^{*n}) / ((T0 * ((AnnCsgOD2 - AnnCsgID2) / 12) * 0.5 / VelAnn2)^n) + K * ((2^{*n+1}) / (n * Ca2))^{*n}}$
ReAnn2	768	unitless	$\frac{(4^{*n+1}) / n * (7.48 * d * VelAnn2^{(2-n)} * (0.5 * ((AnnCsgOD2 - AnnCsgID2) / 12))^{*n}) / ((T0 * ((AnnCsgOD2 - AnnCsgID2) / 12) * 0.5 / VelAnn2)^n) + K * ((2^{*n+1}) / (n * Ca2))^{*n}}{(4^{*n+1}) / n * (7.48 * d * VelAnn3^{(2-n)} * (0.5 * ((AnnCsgOD3 - AnnCsgID3) / 12))^{*n}) / ((R0 * ((AnnCsgOD3 - AnnCsgID3) / 12) * 0.5 / VelAnn3)^n) + K * ((2^{*n+1}) / (n * Ca3))^{*n}}$
ReAnn3	1449	unitless	$\frac{(4^{*n+1}) / n * (7.48 * d * VelAnn3^{(2-n)} * (0.5 * ((AnnCsgOD3 - AnnCsgID3) / 12))^{*n}) / ((R0 * ((AnnCsgOD3 - AnnCsgID3) / 12) * 0.5 / VelAnn3)^n) + K * ((2^{*n+1}) / (n * Ca3))^{*n}}{(8^{*n+1}) / (n * y)^{1/(1-z)}}$
NReAnnCr	4959	unitless	$\frac{(8^{*n+1}) / (n * y)^{1/(1-z)}}{(8^{*n+1}) / (n * y)^{1/(1-z)}}$

Parameter:	Value:	Unit:	Discovery Web Formula:
AnnFricLam1	0,040	psi/ft	$(4 * K) / (14400 * ((AnnCsgOD1 - AnnCsgID1) / 12)) * ((T0 / K) + (((16 * (2 * n + 1)) / (n * Ca1 * ((AnnCsgOD1 - AnnCsgID1) / 12)))) * ((Q * 0.002228) / (Pi() * ((AnnCsgOD1 / 12)^2 - (AnnCsgID1 / 12)^2))))^n$
AnnFricLam2	0,040	psi/ft	$(4 * K) / (14400 * ((AnnCsgOD2 - AnnCsgID2) / 12)) * ((T0 / K) + (((16 * (2 * n + 1)) / (n * Ca2 * ((AnnCsgOD2 - AnnCsgID2) / 12)))) * ((Q * 0.002228) / (Pi() * ((AnnCsgOD2 / 12)^2 - (AnnCsgID2 / 12)^2))))^n$
AnnFricLam3	0,092	psi/ft	$(4 * K) / (14400 * ((AnnCsgOD3 - AnnCsgID3) / 12)) * ((T0 / K) + (((16 * (2 * n + 1)) / (n * Ca3 * ((AnnCsgOD3 - AnnCsgID3) / 12)))) * ((Q * 0.002228) / (Pi() * ((AnnCsgOD3 / 12)^2 - (AnnCsgID3 / 12)^2))))^n$
fAnnTurb1	0,012	unitless	$y * (Ca1 * ReAnn1)^{-z}$
fAnnTurb2	0,012	unitless	$y * (Ca2 * ReAnn2)^{-z}$
fAnnTurb3	0,0097	unitless	$y * (Ca3 * ReAnn3)^{-z}$
AnnFricTurb1	0,037	psi/ft	$(fAnnTurb1 * 7.48 * dout * (0.002228 * Q)^2) / (144 * Pi()^2 * ((AnnCsgOD1 - AnnCsgID1) / 12) * ((AnnCsgOD1 / 12)^2 - (AnnCsgID1 / 12)^2)^2$
AnnFricTurb2	0,038	psi/ft	$(fAnnTurb2 * 7.48 * dout * (0.002228 * Q)^2) / (144 * Pi()^2 * ((AnnCsgOD2 - AnnCsgID2) / 12) * ((AnnCsgOD2 / 12)^2 - (AnnCsgID2 / 12)^2)^2$
AnnFricTurb3	0,132	psi/ft	$(fAnnTurb3 * 7.48 * dout * (0.002228 * Q)^2) / (144 * Pi()^2 * ((AnnCsgOD3 - AnnCsgID3) / 12) * ((AnnCsgOD3 / 12)^2 - (AnnCsgID3 / 12)^2)^2$
AnnCsgL3	160,00	m	ROP * TIME
AnnFricLamTurb1	195	psi	IF(ReAnn1 < NReAnnCr, (AnnFricLam1 * WashoutDepth / 0.3048), (AnnFricTurb1 * WashoutDepth / 0.3048))
AnnFricLamTurb2	0	psi	
AnnFricLamTurb3	0	psi	IF(Washoutdepth > 0, IF(ReAnn3 < NReAnnCr, (AnnFricLam3 * AnnCsgL3 / 0.3048), (AnnFricTurb3 * AnnCsgL3 / 0.3048)))

Output - Below WashoutDepth			
Parameter:	Value:	Unit:	Discovery Web Formula:
QoutLoss	528,3	lpm	$0.26417 * (Qin - Qloss)$
DPV1Loss	11,8	ft/s	$0.408 * QoutLoss / DPID1^2$
DPV2Loss	34,5	ft/s	$0.408 * QoutLoss / DPID2^2$
Cc1Loss	0,7595	unitless	$1 - (1 / (2 * n + 1)) * (T0 / (T0 + K * (((3 * n + 1) * 0.002228 * QoutLoss) / (n * Pi() * ((DPID1 / 12) / 2)^3))))^n$
Cc2Loss	0,8570	unitless	$1 - (1 / (2 * n + 1)) * (T0 / (T0 + K * (((3 * n + 1) * 0.002228 * QoutLoss) / (n * Pi() * ((DPID2 / 12) / 2)^3))))^n$
ReDP1Loss	3107	unitless	$(2 * (3 * n + 1) / n) * (7.48 * dout * DPV1Loss^{(2 - n)} * (0.5 * (DPID1 / 12))^n) / ((T0 * ((DPID1 / 12) * 0.5 / DPV1Loss)^n) + K * ((3 * n + 1) / (n * Cc1Loss))^n$
ReDP2Loss	16014	unitless	$(2 * (3 * n + 1) / n) * (7.48 * dout * DPV2Loss^{(2 - n)} * (0.5 * (DPID2 / 12))^n) / ((T0 * ((DPID2 / 12) * 0.5 / DPV2Loss)^n) + K * ((3 * n + 1) / (n * Cc2Loss))^n$
DPFricLam1Loss	0,0263	psi/ft	$(4 * K) / (14400 * (DPID1 / 12)) * ((T0 / K) + (((3 * n + 1) / (n * Cc1Loss)) * ((8 * QoutLoss * 0.002228) / (Pi() * (DPID1 / 12)^2))))^n$
DPFricLam2Loss	0,0570	psi/ft	$(4 * K) / (14400 * (DPID2 / 12)) * ((T0 / K) + (((3 * n + 1) / (n * Cc2Loss)) * ((8 * QoutLoss * 0.002228) / (Pi() * (DPID2 / 12)^2))))^n$
fDPTurb1Loss	0,0077	unitless	$y * (ReDP1Loss * Cc1)^{-z}$
fDPTurb2Loss	0,0047	unitless	$y * (ReDP2Loss * Cc2)^{-z}$

Parameter:	Value:	Unit:	Discovery Web Formula:
DPFricTurb1Loss	0,1320	psi/ft	$(fDPTurb1Loss*dout*7.48*(0.002228*QoutLoss)^2)/(144*Pi()^2*(DPID1/12)^5)$
DPFricTurb2Loss	1,1538	psi/ft	$(fDPTurb2Loss*dout*7.48*(0.002228*QoutLoss)^2)/(144*Pi()^2*(DPID2/12)^5)$
DPFricLamTurb1Loss	1065,6	psi	$IF(ReDP1Loss<NReDPCr,(DPFricLam1Loss*(DPL1-WashoutDepth)/0.3048),(DPFricTurb1Loss*(DPL1-WashoutDepth)/0.3048))$
DPFricLamTurb2Loss	757,1	psi	$IF(ReDP2Loss<NReDPCr,(DPFricLam2Loss*DPL2/0.3048),(DPFricTurb2*DPL2/0.3048))$
VelAnn1Loss	4,5134	ft/s	$(0.408*QoutLoss)/(AnnCsgOD1^2-AnnCsgID1^2)$
VelAnn2Loss	4,5622	ft/s	$(0.408*QoutLoss)/(AnnCsgOD2^2-AnnCsgID2^2)$
VelAnn3Loss	7,1854	ft/s	$(0.408*QoutLoss)/(AnnCsgOD3^2-AnnCsgID3^2)$
Ca1Loss	0,6491	unitless	$1-(1/(1+n))*T0/(T0+K*((2*(2*n+1))/(n*((AnnCsgOD1*0.5/12)-(AnnCsgID1*0.5/12))))*((0.002228*QoutLoss)/(Pi()*((AnnCsgOD1*0.5/12)^2-(AnnCsgID1*0.5/12)^2))))^n$
Ca2Loss	0,6508	unitless	$1-(1/(1+n))*T0/(T0+K*((2*(2*n+1))/(n*((AnnCsgOD2*0.5/12)-(AnnCsgID2*0.5/12))))*((0.002228*QoutLoss)/(Pi()*((AnnCsgOD2*0.5/12)^2-(AnnCsgID2*0.5/12)^2))))^n$
Ca3Loss	0,7380	unitless	$1-(1/(1+n))*T0/(T0+K*((2*(2*n+1))/(n*((AnnCsgOD3*0.5/12)-(AnnCsgID3*0.5/12))))*((0.002228*QoutLoss)/(Pi()*((AnnCsgOD3*0.5/12)^2-(AnnCsgID3*0.5/12)^2))))^n$
ReAnn1Loss	755,6	unitless	$(4*(2*n+1)/n)*(7.48*dout*VelAnn1Loss^(2-n)*(0.5*((AnnCsgOD1-AnnCsgID1)/12))^n)/((T0*(((AnnCsgOD1-AnnCsgID1)/12)*0.5/VelAnn1Loss)^n)+K*(2*(2*n+1)/(n*Ca1Loss))^n)$
ReAnn2Loss	768,4	unitless	$(4*(2*n+1)/n)*(7.48*dout*VelAnn2Loss^(2-n)*(0.5*((AnnCsgOD2-AnnCsgID2)/12))^n)/((T0*(((AnnCsgOD2-AnnCsgID2)/12)*0.5/VelAnn2Loss)^n)+K*(2*(2*n+1)/(n*Ca2Loss))^n)$
ReAnn3Loss	1448,7	unitless	$(4*(2*n+1)/n)*(7.48*dout*VelAnn3Loss^(2-n)*(0.5*((AnnCsgOD3-AnnCsgID3)/12))^n)/((R0*(((AnnCsgOD3-AnnCsgID3)/12)*0.5/VelAnn3Loss)^n)+K*(2*(2*n+1)/(n*Ca3Loss))^n)$
AnnFricLam1Loss	0,0396	psi/ft	$(4*K)/(14400*((AnnCsgOD1-AnnCsgID1)/12))*((T0/K)+(((16*(2*n+1))/(n*Ca1Loss*((AnnCsgOD1-AnnCsgID1)/12))))*((QoutLoss*0.002228)/(Pi()*((AnnCsgOD1/12)^2-(AnnCsgID1/12)^2))))^n$
AnnFricLam2Loss	0,0401	psi/ft	$(4*K)/(14400*((AnnCsgOD2-AnnCsgID2)/12))*((T0/K)+(((16*(2*n+1))/(n*Ca2Loss*((AnnCsgOD2-AnnCsgID2)/12))))*((QoutLoss*0.002228)/(Pi()*((AnnCsgOD2/12)^2-(AnnCsgID2/12)^2))))^n$
AnnFricLam3Loss	0,0923	psi/ft	$(4*K)/(14400*((AnnCsgOD3-AnnCsgID3)/12))*((T0/K)+(((16*(2*n+1))/(n*Ca3Loss*((AnnCsgOD3-AnnCsgID3)/12))))*((QoutLoss*0.002228)/(Pi()*((AnnCsgOD3/12)^2-(AnnCsgID3/12)^2))))^n$
fAnnTurb1Loss	0,0122	unitless	$y*(Ca1Loss*ReAnn1Loss)^{-z}$
fAnnTurb2Loss	0,0121	unitless	$y*(Ca2Loss*ReAnn2Loss)^{-z}$
fAnnTurb3Loss	0,0097	unitless	$y*(Ca3Loss*ReAnn3Loss)^{-z}$

Parameter:	Value:	Unit:	Discovery Web Formula:
AnnFricTurb1Loss	0,0369	psi/ft	$(fAnnTurb1Loss * 7.48 * dout * (0.002228 * QoutLoss)^2) / (144 * Pi()^2 * ((AnnCsgOD1 - AnnCsgID1) / 12) * ((AnnCsgOD1 / 12)^2 - (AnnCsgID1 / 12)^2)^2)$
AnnFricTurb2Loss	0,0378	psi/ft	$(fAnnTurb2Loss * 7.48 * dout * (0.002228 * QoutLoss)^2) / (144 * Pi()^2 * ((AnnCsgOD2 - AnnCsgID2) / 12) * ((AnnCsgOD2 / 12)^2 - (AnnCsgID2 / 12)^2)^2)$
AnnFricTurb3Loss	0,1316	psi/ft	$(fAnnTurb3Loss * 7.48 * dout * (0.002228 * QoutLoss)^2) / (144 * Pi()^2 * ((AnnCsgOD3 - AnnCsgID3) / 12) * ((AnnCsgOD3 / 12)^2 - (AnnCsgID3 / 12)^2)^2)$
AnnFricLamTurb1Loss	259,7	psi	$IF(QoutLoss > 0, IF(ReAnn1Loss < NReAnnCr, (AnnFricLam1Loss * (AnnCsgL1 - WashoutDepth) / 0.3048), (AnnFricTurb1Loss * (AnnCsgL1 - WashoutDepth) / 0.3048)), 0)$
AnnFricLamTurb2Loss	65,8	psi	$IF(QoutLoss > 0, IF(ReAnn2Loss < NReAnnCr, (AnnFricLam2Loss * AnnCsgL2 / 0.3048), (AnnFricTurb2 * AnnCsgL2 / 0.3048)), 0)$
AnnFricLamTurb3Loss	0,0	psi	

Output - Final			
Parameter:	Value:	Unit:	Discovery Web Formula:
WellDepth	4160	m	$InitialWellDepth + (ROP * TIME)$
FlowAChoke	0	lpm	$Qin + BackPPump$
CumLAnn	4160	m	$AnnCsgL1 + AnnCsgL2 + AnnCsgL3$
CumLDP	4160	m	$DPL1 + DPL2$
ChokeID	1,20	(0-1)	$ChokeOD - (ChokeOD * ChokeOpen)$
ChokeArea	2,54	in2	$3.14 / 4 * (ChokeOD - ChokeID)^2$
BitNozTFA	0,66	inch2	$(BitNozID / 32)^2 * 3.14 / 4 * BitNoz$
BitNozPloss	54,62	bar	$(din * (QoutLoss / 0.26417)^2 / 2959.41 / 0.95^2 / BitNozTFA^2) / 100$
SumAnnFric	35,87	bar	$(AnnFricLamTurb1Loss + AnnFricLamTurb2Loss + AnnFricLamTurb1) / 14.5038$
SumEqFric	29,60	bar	$IF(Qin > 0, ((Motor + MWD + SurfEq)), 0)$
SumDPFric	170	bar	$IF(QoutLoss > 0, (DPFricLamTurb1 + DPFricLamTurb1Loss + DPFricLamTurb2Loss), DPFricLamTurb1) / 14.5038$
ChokePress	0	bar	$(din * FlowAChoke^2 / (2959.41 * 0.95^2) / ChokeArea^2) / 100$
PumpPress	294	bar	$SumAnnFric + BitNozPloss + SumEqFric + SumDPFric + ChokePress$
ECDCalc	1,697	sg	$((dout / 8.33) * CumLAnn * 0.0981) + SumAnnFric + ChokePress$
BHP	692.5	bar	$ECDCalc * 0.0981 * CumLAnn$
Sensor1Target	166,8	bar	$IF(ReAnn1 < NReAnnCr, (AnnFricLam1 * Sensor1Depth) / (14.50378 * 0.3048), (AnnFricTurb1 * Sensor1Depth / (14.50378 * 0.3048))) + ((dout / 8.33) * 0.0981 * Sensor1Depth)$
Sensor2Target	333,5	bar	$IF(ReAnn1 < NReAnnCr, (AnnFricLam1 * Sensor2Depth) / (14.50378 * 0.3048), (AnnFricTurb1 * Sensor2Depth / (14.50378 * 0.3048))) + ((dout / 8.33) * 0.0981 * Sensor2Depth)$
Sensor3Target	500,3	bar	$IF(ReAnn1 < NReAnnCr, (AnnFricLam1 * Sensor3Depth) / (14.50378 * 0.3048), (AnnFricTurb1 * Sensor3Depth / (14.50378 * 0.3048))) + ((dout / 8.33) * 0.0981 * Sensor3Depth)$
Sensor1Total	166,8	bar	$IF(ReAnn1 < NReAnnCr, (AnnFricLam1 * Sensor1Depth) / (14.50378 * 0.3048), (AnnFricTurb1 * Sensor1Depth / (14.50378 * 0.3048))) + ((dout / 8.33) * 0.0981 * Sensor1Depth)$
Sensor2Total	333,5	bar	$Sensor2 + Sensor2Loss + ((dout / 8.33) * 0.0981 * Sensor2Depth)$
Sensor3Total	500,3	bar	$Sensor3 + Sensor3Loss + ((dout / 8.33) * 0.0981 * Sensor3Depth)$

2.3. Robertson-Stiff Frictional Model

Static Input:		
Parameter:	Value:	Unit:
BackPPump	0,00	lpm
VcutTransp	1,02	m/s
ChokeOD	3,00	inch
ChokeOpen	1,00	0-1
AnnCsgL1	3500,00	m
AnnCsgL2	500,00	m
AnnCsgID1	5,00	inch
AnnCsgID2	5,00	inch
AnnCsgID3	6,50	inch
DPL2	200,00	m
DPID1	4,27	inch
DPID2	2,50	inch
BitNoz	6,00	
BitNozID	12,00	
Motor	13,80	bar
MWD	13,80	bar
SurfEq	2,00	bar
dcuttings	2,50	sg
PackOffAnnL1	0,00	(0-1) %
PackOffAnnL2	0,00	(0-1) %
PackOffAnnL3	0,00	(0-1) %
CutCons	0,01	(0-1) %
InitialWellDepth	4000	m

Variable Input:		
Parameter:	Value:	Unit:
Qin	2000	lpm
din	1,6	sg
ROP	40,0	m/h
TIME	4	h

Output			
Parameter:	Value:	Unit:	Discovery Web Formula:
d	13,33	ppg	8.33*din
Q	528,34	gpm	0.26417*Qin
C	52,01		
B	0,3130		
A	3054,246		
dout	13,40	ppg	((1-CutCons)*din+dcuttings*CutCons)*8.33
AnnCsgOD1	8,53	inch	8.53*(1-PackOffAnnL1)
AnnCsgOD2	8,50	inch	8.50*(1-PackOffAnnL2)
AnnCsgOD3	8,50	inch	8.50*(1-PackOffAnnL3)
DPV1	11,823	ft/s	0.408*Q/(DPID1^2)
DPV2	34,490	ft/s	0.408*Q/DPID2^2
ReDP1	8251,17	unitless	89100*DPV1^(2-B)*d/A*(0.0416*DPID1/(3+1/B))^B
ReDP2	42475	unitless	89100*DPV2^(2-B)*d/A*(0.0416*DPID2/(3+1/B))^B
NReLamCr	3041	unitless	3470-1370*B
NReDPTurbCr	3841		4270-1370*B
DPFricLam1	0,03524	psi/ft	8.33/10000*2^(2+B)*(A/478.789033)*((3+1/B)*((0.2*60*DPV1+C/6*DPID1)/DPID1^(1/B+1)))^B
DPFricLam2	0,09402	psi/ft	8.33/10000*2^(2+B)*(A/478.789033)*((3+1/B)*((0.2*60*DPV2+C/6*DPID2)/DPID2^(1/B+1)))^B

Parameter:	Value:	Unit:	Discovery Web Formula:
a1	0,06851		(LOG(B)+3.93)/50
b2	0,32206		(1.75-LOG(B))/7
fDPTurb1	0,00375	unitless	a1/ReDP1^b2
fDPTurb2	0,00221	unitless	a1/ReDP2^b2
DPFricTurb1	0,0634466	psi/ft	(fDPTurb1*d*DPV1^2)/(25.81*DPID1)
DPFricTurb2	0,5440832	psi/ft	(fDPTurb2*d*DPV2^2)/(25.81*DPID2)
DPL1	3960	m	(AnnCsgL1+AnnCsgL2-DPL2)+(ROP*TIME)
DPFricLamTurb1	824	psi	IF(ReDP1<NReLamCr,(DPFricLam1*DPL1/0.3048),IF(ReDP1>NReDPTurbCr,(DPFricTurb1*DPL1/0.3048),0))
DPFricLamTurb2	357	psi	IF(ReDP2<NReLamCr,(DPFricLam2*DPL2/0.3048),IF(ReDP2>NReDPTurbCr,(DPFricTurb2*DPL2/0.3048),0))
VelAnn1	4,5134	ft/s	(0.408*Q)/(AnnCsgOD1^2-AnnCsgID1^2)
VelAnn2	4,5622	ft/s	(0.408*Q)/(AnnCsgOD2^2-AnnCsgID2^2)
VelAnn3	7,1854	ft/s	(0.408*Q)/(AnnCsgOD3^2-AnnCsgID3^2)
ReAnn1	1602,26	unitless	109000*VelAnn1^(2-B)*dout/A*(0.0208*(AnnCsgOD1-AnnCsgID1)/(2+1/B))^B
ReAnn2	1627,24	unitless	109000*VelAnn2^(2-B)*dout/A*(0.0208*(AnnCsgOD2-AnnCsgID2)/(2+1/B))^B
ReAnn3	2938,84	unitless	109000*VelAnn3^(2-B)*dout/A*(0.0208*(AnnCsgOD3-AnnCsgID3)/(2+1/B))^B
AnnFricLam1	0,040871	psi/ft	8.33/10000*4^(1+B)*(A/478.789033)*((2+1/B)*((0.2*60*VelAnn1+C/8*(AnnCsgOD1-AnnCsgID1))/(AnnCsgOD1-AnnCsgID1)^(1/B+1)))^B
AnnFricLam2	0,041397	psi/ft	8.33/10000*4^(1+B)*(A/478.789033)*((2+1/B)*((0.2*60*VelAnn2+C/8*(AnnCsgOD2-AnnCsgID2))/(AnnCsgOD2-AnnCsgID2)^(1/B+1)))^B
AnnFricLam3	0,093258	psi/ft	8.33/10000*4^(1+B)*(A/478.789033)*((2+1/B)*((0.2*60*VelAnn3+C/8*(AnnCsgOD3-AnnCsgID3))/(AnnCsgOD3-AnnCsgID3)^(1/B+1)))^B
NReAnnTurbCr	3841,14		4270-1370*B
fAnnTurb1	0,00636	unitless	a1/ReAnn1^b2
fAnnTurb2	0,00633	unitless	a1/ReAnn2^b2
fAnnTurb3	0,00523	unitless	a1/ReAnn3^b2
AnnFricTurb1	0,01906	psi/ft	(fAnnTurb1*dout*VelAnn1^2)/(25.81*(AnnCsgOD1-AnnCsgID1))
AnnFricTurb2	0,01955	psi/ft	(fAnnTurb2*dout*VelAnn2^2)/(25.81*(AnnCsgOD2-AnnCsgID2))
AnnFricTurb3	0,07015	psi/ft	(fAnnTurb3*dout*VelAnn3^2)/(25.81*(AnnCsgOD3-AnnCsgID3))
AnnCsgL3	160,00	m	ROP*TIME
xint3	-0,128		(ReAnn3-NReLamCr)/(NReDPTurbCr-NReLamCr)
AnnFricLamTurb1	469	psi	IF(ReAnn1<=NReLamCr,(AnnFricLam1*AnnCsgL1/0.3048),IF(ReAnn1>=NReAnnTurbCr,(AnnFricTurb1*AnnCsgL1/0.3048),0))
AnnFricLamTurb2	68	psi	IF(ReAnn2<=NReLamCr,(AnnFricLam2*AnnCsgL2/0.3048),IF(ReAnn2>=NReAnnTurbCr,(AnnFricTurb2*AnnCsgL2/0.3048),0))
AnnFricLamTurb3	49	psi	IF(ReAnn3<=NReLamCr,(AnnFricLam3*AnnCsgL3/0.3048),IF(ReAnn3>=NReAnnTurbCr,(AnnFricTurb3*AnnCsgL3/0.3048),(((1-xint3)*(AnnFricLam3*AnnCsgL3/0.3048))+((AnnFricTurb3*AnnCsgL3/0.3048)*xint3))))
WellDepth	4160,00	m	InitialWellDepth+(ROP*TIME)
FlowAChoke	0	lpm	Qin+BackPPump
CumLAnn	4160,00	m	AnnCsgL1+AnnCsgL2+AnnCsgL3
CumLDP	4160,00	m	DPL1+DPL2
ChokeID	1,20	(0-1)	ChokeOD-(ChokeOD*ChokeOpen)
ChokeArea	2,54	in2	3.14/4*(ChokeOD-ChokeID)^2

<i>Parameter:</i>	<i>Value:</i>	<i>Unit:</i>	<i>Discovery Web Formula:</i>
BitNozTFA	0,66	inch2	$(\text{BitNozID}/32)^2 * 3.14/4 * \text{BitNoz}$
BitNozPloss	54,62	bar	$(\text{din} * \text{Qin}^2 / 2959.41 / 0.95^2 / \text{BitNozTFA}^2) / 100$
SumAnnFric	40,42	bar	$\text{IF}(\text{Qin} > 0, ((\text{AnnFricLamTurb1} + \text{AnnFricLamTurb2} + \text{AnnFricLamTurb3}) / 14.5038), 0)$
SumEqFric	29,60	bar	$\text{IF}(\text{Qin} > 0, ((\text{Motor} + \text{MWD} + \text{SurfEq}), 0)$
SumDPFric	81,45	bar	$(\text{DPFricLamTurb1} + \text{DPFricLamTurb2}) / 14.5038$
ChokePress	0	bar	$((\text{dout} / 8.33) * \text{FlowAChoke}^2 / (2959.41 * 0.95^2) / \text{ChokeArea}^2) / 100$
PumpPress	209,81	bar	$\text{SumAnnFric} + \text{BitNozPloss} + \text{SumEqFric} + \text{SumDPFric} + \text{ChokePress}$
ECDCalc	1,7077	sg	$((\text{dout} / 8.33) * \text{CumLAnn} * 0.0981) + \text{SumAnnFric} + \text{ChokePress} / (\text{CumLAnn} * 0.0981)$
BHP	696.9	bar	$\text{ECDCalc} * 0.0981 * \text{CumLAnn}$

3. Log input data

This is an example of what a manipulated log that is implemented into Discovery Web looks like. The following example is taken from the connection scenario.

```
TIME,BLOCKCOMP,MWIN,FLOWIN,FRAC_EQMD,POR_EQMD,CumTime
yyyy-MM-dd"THH:mm:ss.fffzzz,m,sg,L/min,sg,sg,h
2014-02-28T08:02:00.000+01:00,28.98,1.60,2000.00,1.75,1.50,0
2014-02-28T08:03:00.000+01:00,28.13,1.60,2000.00,1.75,1.50,0.01667
2014-02-28T08:04:00.000+01:00,26.88,1.60,2000.00,1.75,1.50,0.03333
2014-02-28T08:05:00.000+01:00,26.22,1.60,2000.00,1.75,1.50,0.04999
2014-02-28T08:06:00.000+01:00,25.25,1.60,2000.00,1.75,1.50,0.06665
2014-02-28T08:07:00.000+01:00,24.62,1.60,2000.00,1.75,1.50,0.08331
2014-02-28T08:08:00.000+01:00,23.83,1.60,2000.00,1.75,1.50,0.09997
2014-02-28T08:09:00.000+01:00,23.48,1.60,2000.00,1.75,1.50,0.11663
2014-02-28T08:10:00.000+01:00,22.74,1.60,2000.00,1.75,1.50,0.13329
2014-02-28T08:11:00.000+01:00,22.19,1.60,2000.00,1.75,1.50,0.14995
2014-02-28T08:12:00.000+01:00,21.24,1.60,2000.00,1.75,1.50,0.16661
2014-02-28T08:13:00.000+01:00,20.19,1.60,2000.00,1.75,1.50,0.18327
2014-02-28T08:14:00.000+01:00,18.92,1.60,2000.00,1.75,1.50,0.19993
2014-02-28T08:15:00.000+01:00,18.10,1.60,2000.00,1.75,1.50,0.21659
2014-02-28T08:16:00.000+01:00,17.26,1.60,2000.00,1.75,1.50,0.23325
2014-02-28T08:17:00.000+01:00,16.05,1.60,2000.00,1.75,1.50,0.24991
2014-02-28T08:18:00.000+01:00,15.18,1.60,2000.00,1.75,1.50,0.26657
2014-02-28T08:19:00.000+01:00,14.31,1.60,2000.00,1.75,1.50,0.28323
2014-02-28T08:20:00.000+01:00,12.86,1.60,2000.00,1.75,1.50,0.29989
2014-02-28T08:21:00.000+01:00,12.22,1.60,2000.00,1.75,1.50,0.31655
2014-02-28T08:22:00.000+01:00,11.57,1.60,2000.00,1.75,1.50,0.33321
2014-02-28T08:23:00.000+01:00,11.12,1.60,2000.00,1.75,1.50,0.34987
2014-02-28T08:24:00.000+01:00,10.36,1.60,2000.00,1.75,1.50,0.36653
2014-02-28T08:25:00.000+01:00,9.27,1.60,2000.00,1.75,1.50,0.38319
2014-02-28T08:26:00.000+01:00,7.76,1.60,2000.00,1.75,1.50,0.39985
2014-02-28T08:27:00.000+01:00,6.58,1.60,2000.00,1.75,1.50,0.41651
2014-02-28T08:28:00.000+01:00,5.27,1.60,2000.00,1.75,1.50,0.43317
2014-02-28T08:29:00.000+01:00,4.03,1.60,2000.00,1.75,1.50,0.44983
2014-02-28T08:30:00.000+01:00,2.81,1.60,2000.00,1.75,1.50,0.46649
2014-02-28T08:31:00.000+01:00,1.87,1.60,2000.00,1.75,1.50,0.48315
2014-02-28T08:32:00.000+01:00,1.47,1.60,2000.00,1.75,1.50,0.49981
2014-02-28T08:33:00.000+01:00,0.85,1.60,0.00,1.75,1.50,0.51647
2014-02-28T08:34:00.000+01:00,4.44,1.60,0.00,1.75,1.50,0.53313
2014-02-28T08:35:00.000+01:00,4.21,1.60,0.00,1.75,1.50,0.54979
2014-02-28T08:36:00.000+01:00,8.46,1.60,0.00,1.75,1.50,0.56645
2014-02-28T08:37:00.000+01:00,31.90,1.60,0.00,1.75,1.50,0.58311
2014-02-28T08:38:00.000+01:00,32.46,1.60,833.33,1.75,1.50,0.59977
2014-02-28T08:39:00.000+01:00,31.12,1.60,1000.00,1.75,1.50,0.61643
2014-02-28T08:40:00.000+01:00,31.12,1.60,2000.00,1.75,1.50,0.63309
2014-02-28T08:41:00.000+01:00,31.12,1.60,2000.00,1.75,1.50,0.64975
```